To the Graduate Council:

I am submitting herewith a dissertation written by Geraldine Mahany Eaton entitled "Sorption/Desorption of Sulfur Dioxide by Cellulosic Fibers." I have examined the final copy of this dissertation for form and content and recommend that it be accepted in partial fulfillment of the requirements for the degree of Doctor of Philosophy, with a major in Human Ecology.

Bhuvenesh C. Goswami
Major Professor

We have read this dissertation and recommend its acceptance:

M. H. Liebhafsky

D. Eastwood

Byrone L. Vigo

Larry C. Wadsworth

Kermit E. Duncan

Accepted for the Council:

Vice Provost
and Dean of The Graduate School

SORPTION/DESORPTION OF SULFUR DIOXIDE BY CELLULOSIC FIBERS

A Dissertation

Presented for the

Doctor of Philosophy

Degree

The University of Tennessee, Knoxville

Geraldine Mahany Eaton

December 1986

Copyright © Geraldine Mahany Eaton, 1986
All rights reserved

DEDICATED TO:

The late Dr. C. N. Bogner, Dean Emeritus
School of Education and Allied Professions,
Miami University,
Oxford, Ohio

. . . for getting me started down the right path.

ACKNOWLEDGMENTS

Sincere appreciation is extended to the many individuals and institutions who have contributed to the completion of this work, including:

Dr. B. C. Goswami, committee chairman and now friend, for his expertise and encouragement throughout the course of this study. His guidance has been an invaluable aid for professional development;

Dr. T. L. Vigo, committee member, for his interest in and financial support of the project. His constructive criticism and editorial expertise have been greatly appreciated;

Dr. K. E. Duckett, committee member, for his time and help along the way and for stimulating discussions of scientific matters not always related to this work;

Dr. L. C. Wadsworth, committee member, for arranging for the loan of the SO_2 analyzer and for the $NH_3(\ell)$ treatment of the fibers used in this study. His support during the manuscript preparation phase of this work was especially appreciated;

Dr. M. H. Lietzke, committee member, for his instruction in physical chemistry and for service above and beyond the call of duty throughout the course of the study;

Dr. D. B. Eastwood, committee member, for his time and willingness to contribute and for broadening my perspective;

Dr. Billie Collier, Ohio University, for laying the groundwork for the present study while serving as a post-doctoral research associate at the University of Tennessee;

Dr. Wayne Davis, environmental engineering, for loan of the SO_2 analyzer used in the study and for advice concerning the design of the exposure apparatus;

Mr. Bobby McGill, polymer engineering, for SEM and x-ray spectroscopy assistance;

Dr. Arlene Garrison and Mr. Paul Flowers, chemistry, for FTIR evaluations;

Dr. J. Wightman, Virginia Tech University, for ESCA evaluations;

Quantichrome Corporation for mercury porosimetry;

American Enka, Enka, NC, and StarLab, Knxoville, TN, for supplying the fibers used;

Cotton, Inc., Raleigh, NC, for $NH_3(\ell)$ treating the cotton fibers;

U.S. Department of Agriculture, A.R.S.; Department of Textiles, Merchandising & Design; and the American Association of Textile Chemists and Colorists for financial support;

My husband, Walter Eaton, not only for emotional and financial support, but also for many of the graphic illustrations contained herein and for his electronics troubleshooting. Without him the project could not have been completed;

My daughter, Katherine Ann Eaton, for helping to put my priorities in order and for providing inspiration when I needed it most;

And my parents, Mr. and Mrs. John B. Mahany, for their unfailing love and for fostering in me the will to achieve.

ABSTRACT

The purpose of this study was to determine the mechanism and degree of SO_2 sorption by native cellulose (ethanol extracted cotton), modified cellulose (mercerized cotton and liquid ammonia treated cotton), and regenerated cellulose (viscose rayon) under dynamic environmental conditions. The effects of fiber fine structure, moisture content, and temperature on SO_2 sorption were examined as well.

An exposure chamber was developed which would simulate ambient conditions. Fiber samples were dried or conditioned to 69 ± 1% RH and exposed to 3 ppm SO_2 for 5 hours at 170 cc/min. Following exposure to SO_2 the samples were exposed to a stream of dry air at the same flow rate for 4 hours. The concentration of gas exiting the chamber was monitored and compared with the known concentration of gas introduced into the chamber to evaluate the amount of gas sorbed.

For the dried fiber exposures, mercerized cotton sorbed more SO_2 at each temperature than any other fiber. Dried viscose rayon sorbed the least SO_2 at each temperature. Conditioned fiber samples sorbed more SO_2 than dried fiber samples. The rates of SO_2 desorption were similar for all samples.

Several instrumental techniques were used to evaluate the presence of sulfur remaining in the fibers following desorption. X-ray spectroscopy showed small sulfur peaks on exposed extracted cotton, mercerized cotton, and $NH_3(\ell)$ treated cotton. ESCA and FTIR were unable to confirm the presence of residual sulfur in the samples. Total sulfur analysis showed only similar trace amounts of sulfur in unexposed and exposed cotton.

Fiber fine structure, moisture content, and temperature were all found to affect the rate and magnitude of SO_2 sorption. Sulfur dioxide sorption increased with decreasing molecular order, increased with the addition of fiber moisture, and decreased with increasing temperature.

The mechanism of SO_2 sorption by cellulose is thought to be physical sorption with van der Waals forces forming the basis for attraction. Sorption by both dried and conditioned fibers is reversible. All of the SO_2 was desorbed following exposure of the samples to a stream of dry air.

TABLE OF CONTENTS

CHAPTER		PAGE
I.	INTRODUCTION	1
	Objectives	2
	Assumptions	3
	Limitations	3
II.	REVIEW OF LITERATURE	4
	Indoor Air Pollution	4
	Sulfur Dioxide	6
	Textile Degradation	9
	Sorption of Gases by Polymers	16
	Reactions Related to Polymer Degradation and Gas Sorption	21
	Deposition Velocity and Resistance	24
	Properties of Cotton, Modified Cellulosics, and Viscose Rayon	25
III.	EXPERIMENTAL	34
	Materials	34
	Fibers	34
	Sample Preparation	35
	Exposure Chamber Development	36
	Exposure of Fibers to Sulfur Dioxide	39
	Change in Fiber Moisture Content on Exposure to Air	41
	Analytical Methods for Fiber Characterization	41
IV.	RESULTS AND DISCUSSION	45
	Fiber Characterization	45
	Change in Total Fiber Moisture on Exposure to Dry Air	59
	Sorption of Sulfur Dioxide by Dried Fibers	65
	Desorption of Sulfur Dioxide by Dried Fibers	84
	Comparison of Sorption/Desorption by Conditioned and Dried Fibers	91
	Post Exposure Analysis	100
IV.	SUMMARY, CONCLUSIONS, AND RECOMMENDATIONS	114
	Summary	114
	Conclusions	115
	Recommendations	116

PAGE

LITERATURE CITED 119

APPENDICES 126

A. X-RAY DIFFRACTOGRAMS 127
B. MERCURY POROSIMETRY DATA 139
C. ESCA OUTPUT 148

VITA 171

LIST OF TABLES

TABLE		PAGE
1.	Unit Cell Dimensions of Three Cellulose Lattice Configurations	30
2.	Percent Crystallinity for Cellulose Fibers as Reported in the Literature	46
3.	Accessibility and Crystallinity in Cellulose Fibers	54
4.	Fiber Surface Area and Pore Radius Determined by Mercury Porosimetry	54
5.	Percent Moisure Regain and Percent Moisture Content for Cellulose Fibers	60
6.	Initial Rate of SO_2 Removal by the System Using Dried Fibers	69
7.	Time to Minimum Concentration Reaching the Analyzer for Dried Fibers	71
8.	Secondary Rate of SO_2 Sorption by Dried Fibers	73
9.	Time Constants for SO_2 Sorption for Dried Fibers	76
10.	SO_2 Sorption by Dried Fibers	78
11.	Initial Rates of SO_2 Desorption by Dried Fibers	86
12.	Secondary Rates of Desorption by Dried Fibers	89
13.	Initial Rates of SO_2 Removal by Conditioned vs. Dried Fibers at 25°C	92
14.	Secondary Rates of SO_2 Sorption by Conditioned vs. Dried Fibers at 25°C	94
15.	Time to Minimum SO_2 Concentration Within the Exposure Chamber for Conditioned vs. Dried Fibers at 25°C	96
16.	Comparison of SO_2 Sorption by Conditioned vs. Dried Fibers at 25°C	98

TABLE PAGE

17. Initial Rates of SO_2 Desorption by Conditioned vs. Dried Fibers at 25°C 101

18. Secondary Rates of SO_2 Desorption by Conditioned vs. Dried Fibers at 25°C 103

LIST OF FIGURES

FIGURE		PAGE
1.	Cotton Fiber Internal Structure	26
2.	Structure of the Cellulose Polymer	28
3.	Unit Cell Structures for Cellulose I, II, and III	29
4.	Schematic of Exposure Apparatus	37
5.	Fiber Sample Mounted in Exposure Flask	40
6.	X-Ray Diffraction Patterns for Four Types of Cellulosic Fibers	48
7.	X-Ray Diffractogram of Unexposed Extracted Cotton	49
8.	X-Ray Diffractogram of Unexposed Mercerized Cotton	50
9.	X-Ray Diffractogram of Unexposed $NH_3(\ell)$ Treated Cotton	51
10.	X-Ray Diffractogram of Unexposed Viscose Rayon	52
11.	Surface Porosity of Cellulose Fibers by Mixed Hexanes Evaporation	56
12.	Surface Porosity of Cellulose Fibers by Cyclohexane Evaporation	57
13.	Surface Porosity of Cellulose Fibers by n-Hexane Evaporation	58
14.	Fiber Moisture Loss for Extracted Cotton at Four Temperatures	61
15.	Fiber Moisture Loss for Mercerized Cotton at Four Temperatures	62
16.	Fiber Moisture Loss for $NH_3(\ell)$ Treated Cotton at Four Temperatures	63
17.	Fiber Moisture Loss for Viscose Rayon at Four Temperatures	64

FIGURE PAGE

18. Chart Recorder Output Showing Initial and Secondary Sorption Slopes 67

19. Time to Minimum Concentration Reaching the Analyzer 72

20. Secondary Rate of SO_2 Sorption by Dried Fibers 74

21. SO_2 Sorption by Dried Fibers at Four Temperature Levels 79

22. Diffractogram of $NH_3(\ell)$ Treated Cotton Exposed to SO_2 at 25°C 82

23. Diffractogram of $NH_3(\ell)$ Treated Cotton Exposed to SO_2 at 50°C 83

24. Chart Recorder Output Showing Initial and Secondary Desorption Slopes 85

25. Initial Rates of Desorption 88

26. Secondary Desorption Rates 90

27. Initial Rates of SO_2 Removal by Conditioned vs. Dried Fibers at 25°C 93

28. Secondary Rates of SO_2 Sorption by Conditioned vs. Dried Fibers at 25°C 95

29. Comparison of SO_2 Sorption by Conditioned vs. Dried Fibers at 25°C 99

30. Initial Rates of SO_2 Desorption by Conditioned vs. Dried Fibers at 25°C 102

31. Secondary Rates of SO_2 Desorption by Conditioned vs. Dry Fibers at 25°C 104

32. Surface of Extracted Cotton Before and After Exposure to 3 ppm SO_2 at 25°C 106

33. Surface of Viscose Rayon Before and After Exposure to 3 ppm SO_2 at 25°C 107

34. X-Ray Spectrum for Extracted Cotton Exposed to 3 ppm SO_2 108

FIGURE PAGE

35. X-Ray Spectrum for Mercerized Cotton Exposed to 3 ppm SO_2 109

36. X-Ray Spectrum for $NH_3(\ell)$ Treated Cotton Exposed to 3 ppm SO_2 110

37. FTIR Spectra of Exposed and Unexposed Extracted Cotton 112

38. X-Ray Spectra of Exposed and Unexposed Mercerized Cotton 113

A-1. X-Ray Diffractogram of Dried Extracted Cotton Exposed to 3 ppm SO_2 at 25°C 128

A-2. X-Ray Diffractogram of Dried Mercerized Cotton Exposed to 3 ppm SO_2 at 25°C 129

A-3. X-Ray Diffractogram of Dried $NH_3(\ell)$ Treated Cotton Exposed to 3 ppm SO_2 at 25°C 130

A-4. X-Ray Diffractogram of Dried Viscose Rayon Exposed to 3 ppm SO_2 at 25°C 131

A-5. X-Ray Diffractogram of Dried Extracted Cotton Exposed to 3 ppm SO_2 at 50°C 132

A-6. X-Ray Diffractogram of Dried Mercerized Cotton Exposed to 3 ppm SO_2 at 50°C 133

A-7. X-Ray Diffractogram of Dried $NH_3(\ell)$ Treated Cotton Exposed to 3 ppm SO_2 at 50°C 134

A-8. X-Ray Diffractogram of Dried Viscose Rayon Exposed to 3 ppm SO_2 at 50°C 135

A-9. X-Ray Diffractogram of Conditioned Extracted Cotton Exposed to 3 ppm SO_2 at 25°C 136

A-10. X-Ray Diffractogram of Conditioned Mercerized Cotton Exposed to 3 ppm SO_2 at 25°C 137

A-11. X-Ray Diffractogram of Conditioned $NH_3(\ell)$ Treated Cotton Exposed to 3 ppm SO_2 at 25°C 138

CHAPTER I

INTRODUCTION

Because energy costs increased dramatically during the late 1970s and early 1980s, people were encouraged to insulate their homes better in order to save both energy and money. Unfortunately, as the air exchange with the outdoor air was reduced, pollutants accumulated inside, resulting in a decline in indoor air quality (1).

Airborne pollutants may enter buildings from the outside or be generated indoors. The types and amounts of pollutants coming inside from outdoors vary with the locale and weather. These may include any of the five primary pollutants: sulfur oxides (SO_x), nitrogen oxides (NO_x), hydrocarbons, carbon monoxide (CO), and particulates (2). Furthermore, secondary pollutants, such as peroxyacyl nitrate (PAN), may also enter enclosed structures from outdoors. Pollutants may be generated indoors by aerosol sprays (particulates), insulation (formaldehyde), tobacco smoke (CO), gas ranges (CO, NO_x, particulate sulfur), gas, oil, wood, or coal heaters (CO, NO_x, SO_x), and rock and cement (radon) (2, 3, 4, 5).

Many of these pollutants are known to cause damage to textiles. The degradative effect of ozone (O_3) on cotton was first studied by Bogaty (6) as early as 1952. The damaging effects of the other pollutants on textiles are also well documented. They include: soiling of fabric, loss of strength, dye fading by NO_2 and/or O_3, and discoloration of white fabrics on exposure to NO_2 (7). Chanlett (2) states

that sulfur dioxide (SO_2) represents the major degradative threat to textiles. Therefore, much of the work done to date relates to the damaging effects of SO_2 on textiles.

While there have been a number of studies investigating the degradative effects of pollutant gases on textiles, the data are not in complete agreement. The modes and mechanisms of degradation have not been conclusively demonstrated. One area of research that has recently been investigated is the sorption of gaseous pollutants by textile materials and polymer films. Rate studies centering mainly on the sorption of SO_2 by wool have been carried out by several researchers. Sulfur dioxide sorption by cotton, rayon, and nylon have also been examined. The results of these studies raise the possibility that textiles used for interior furnishing might beneficially act as sinks for pollutant gases inside just as vegetation, soil, and water act as pollution sinks outdoors (8).

The mechanism of SO_2 sorption by wool is thought to relate to the high acid combining potential of the wool fiber (9). The extent and mechanism of SO_2 sorption by other fibers, more commonly used for interior furnishings, must be ascertained and the influencing parameters identified before practical use of textiles can be made for the control of indoor air pollution.

Objectives

The overall objectives of the present study have been to:

1. determine the mechanism and degree of SO_2 sorption by native cotton, two types of treated cotton, and viscose rayon,
2. determine the effect of fiber fine structure on SO_2 sorption, and
3. determine the effect of fiber moisture content on SO_2 sorption.

Assumptions

The following assumptions have been made in the study:

1. the exposure apparatus designed for the study adequately simulates ambient exposure conditions,
2. mercerized and $NH_3(\ell)$ treated fibers are representative of commercially treated fibers, and
3. data from all of the techniques are valid and reproducible.

Limitations

The following limitations of the present study have been identified:

1. only five temperature levels, two humidities, and one gas concentration were used in the study,
2. there were a limited number of replications,
3. samples consisted of combed fibers; no yarns or fabrics were evaluated, and
4. all sorption measurements were carried out in the presence of light.

CHAPTER II

REVIEW OF LITERATURE

Indoor Air Pollution

Traditionally the Clean Air Act (10) has been interpreted as referring only to the outdoor environment. Indoor air pollution, however, may represent more of a threat to human well-being than pollution from outdoors. The seriousness of the situation has only recently begun to be recognized in the technical and popular literature.

Indoor air pollution can lead to problems such as cancer, allergies, and lung disease. Evidence is plentiful which demonstrates that nonsmokers who reside with smokers are at higher risk of developing lung cancer and impaired lung functions than are the general population. Furthermore, uranium miners are at greater risk of developing lung cancer from inhaled radon gas (11). Estimates are that 5-10% of all homes in this country may contain unsafe levels of radon. Various monitoring agencies have noted 28-60% of all tested homes have abnormally high levels of the gas (12).

Many early studies viewed indoor air pollution as a direct result of outdoor pollutant levels. More recent evidence shows that many potentially harmful pollutants are generated indoors. This coupled with the fact that most Americans spend approximately 70% of their lives indoors points out the potential problem.

A study of residential dwellings in Rotterdam, Netherlands, found indoor levels of SO_2 to average 20% of the outdoor concentration. The

SO_2 level was greatest in homes with gas heat. Interestingly, newer homes were found to have lower SO_2 levels than older homes. The researchers theorized that the gas was absorbed by the walls and ceilings and that surfaces in the older homes had become saturated (13).

Another study found that coal heated homes had levels of SO_2 and CO which were 4-8 times higher than other homes. The pollutant levels were found to be highest during stoking. Presumably, leaky furnaces were responsible (14).

A complicating factor in the attempt to control indoor air pollution is that modern buildings are designed to be more air tight than older buildings in an attempt to conserve energy. One estimate is that older homes go through 0.8-1.5 air changes per hour as compared to only 0.5-1.0 air changes per hour for newer homes (5). Another estimate is that many energy efficient homes undergo only 0.2 air changes per hour (3). Thus, pollutants remain trapped indoors for longer periods in newer buildings.

It is generally agreed that there are three procedures which can aid the maintenance of indoor air quality (4, 11). These include:

1. maintenance of adequate air exchange through ventilation.
2. filtration for air purification, and
3. reduction of the sources of air pollution.

Air purification (number 2 above) becomes quite important due to the need to reduce ventilation for energy conservation. Also, in areas with heavy outdoor air pollution, ventilation may not solve the problem (4).

Adsorption of pollutants is one possible method for air purification. This technique involves the deposition of the pollutant on the surface of a material. Textiles may be able to play a major role in the adsorption of pollutants from interior environments.

Sulfur Dioxide

Sulfur dioxide is a colorless, nonflammable, nonexplosive gas which has a strong, irritating odor in concentrations above 3.0 ppm. Taste sensations are apparent at as little as 0.3-1.0 ppm (15). Sulfur dioxide and its reaction products have received much attention with regard to their role as pollutants because of the very apparent damage they do.

There are many natural sources of sulfur pollutants, but man-made sources have generated far more interest. Stationary combustion of fossil fuels for power generation provides the bulk of the man-made emissions. Roughly 95% of all sulfur emissions are in the form of SO_2 (16). Approximately 73% of all SO_2 generated in this country comes from power plant emissions. It is formed by the oxidation of iron pyrite (FeS_2) in coal and by organic sulfur compounds in both coal and oil, the amount varying with the type of fuel used (2). Some other man-made emission sources include: petroleum refining, chemical manufacture, metals works, cement manufacture, and pulping. Indoor sources of sulfur pollutants originate mainly from coal, oil, and gas used for heating and cooking.

Upon release to the atmosphere, sulfur compounds undergo a variety of reactions. Hydrogen sulfide (H_2S) emissions are oxidized by atomic oxygen, molecular oxygen (O_2), and ozone (O_3) to SO_2. These reactions proceed slowly even when aerosol particulates provide a surface for catalysis. The reaction rate increases in humid atmospheres due to the water solubility of the reactants and products (16). The SO_2 gas reacts photochemically or catalytically with airborne substances to form a variety of products including SO_3, sulfuric acid (H_2SO_4), and sulfates. Two commonly mentioned pathways for H_2SO_4 formation include:

$$SO_2 + \tfrac{1}{2}O_2 + M \rightarrow SO_3 + M \quad \text{then} \quad SO_3 + H_2O \rightarrow H_2SO_4$$

$$SO_2 + H_2O \rightarrow H_2SO_3 \quad \text{then} \quad H_2SO_3 + \tfrac{1}{2}O_2 \rightarrow H_2SO_4$$

The M represents a third species which as an energy absorber prevents the reverse reaction. Particulates and oxides of nitrogen are known to catalyze this reaction. In fact, the reaction of SO_2 and NO_2 formed the basis of the lead chamber process for the manufacture of sulfuric acid (H_2SO_4) as demonstrated by the following reaction:

$$NO_2 + SO_2 + H_2O \rightarrow H_2SO_4 + NO$$

Conversion rates of 98.99% and sulfur yields of 92-96% are possible when utilizing this process (17). Sulfonic acids are a small component of sulfur polluted air. They result from the oxidation of organic sulfur compounds produced by natural and man-made sources (18). A variety of sulfates are formed in the presence of NH_3, NaCl, and metal oxides.

The atmospheric residence time of sulfur compounds varies, with sulfates said to persist for 2-7 days (19). Sulfate aerosols in conjunction with other components of polluted air have been responsible for adverse human health effects. However, the role of sulfur compounds in increased mortality during pollution episodes has been questioned. One researcher claims that the data indicate that suspended particulate levels likely have a greater detrimental effect (20). Still, most believe that airborne sulfur compounds have a deleterious effect on human health, though admittedly it is difficult to separate out the effects of particulates and humidity. Increased rates of respiratory problems are usually observed during periods of high sulfur concentration. Bronchoconstriction, increased frequency of asthma attacks, and decreased ventilatory function have been documented (15, 21). Little is known of the effects of chronic exposure to SO_2, and exposure to concentrations below 20 ppm is said to cause acute effects only.

Sulfur pollutants react with many surfaces causing varying degrees of damage. Vegetation is damaged when sulfur compounds deposit on the plant surfaces and are absorbed to react chemically (16). Acid precipitation strips protective waxes from some plants, damages root systems, increases the uptake of toxic metals, and inhibits transpiration, photosynthesis, and germination. It also depletes the soils of nutrients, notably calcium, magnesium, sodium, and potassium. Ironically the deposited sulfates cause some plants to thrive, masking long-term damage. Both West Germany and the U.S. have noted

damage to forests resulting from acid rain (22, 23). No measures currently known are expected to save the beech forests in West Germany (22).

Limestone and marble are both essentially calcium carbonate ($CaCO_3$). The sulfates in combination with water in acid rain react with $CaCO_3$ to form soluble calcium sulfate ($CaSO_4$) which simply washes off the structure (24). Buildings and statuary in areas with high levels of sulfur pollution have become stripped of detail.

Metal corrosion is accelerated in areas of high sulfur concentration. The corrosion rates in urban areas range from 1.5 to 5 times the rural rates depending on the acid concentration and the type of metal (15). Paint drying time is greatly increased by elevated levels of sulfur compounds in the atmosphere. As little as 1-2 ppm of SO_2 causes a 50-100% increase in paint drying time. Concentrations of 10 ppm increase the drying time to 2-3 days and cause the paint to have a less durable surface when dry (15).

Textile products show varying degrees of degradation by sulfuric acid aerosols. Nylon, rayon, silk spandex, azlon, cotton, and flax are all soluble in varying concentrations of H_2SO_4 and are thus subject to strength losses resulting in part from hydrolysis by the absorbed acid.

Textile Degradation

A variety of studies have examined the degradative effect of SO_2 on textile fibers (25, 26, 27, 28, 29, 30). Even though the test

conditions have differed, most have found varying degrees of degradation to acetate, acrylic, cotton, and nylon fibers. In one study the strength of modacrylic was found to increase slightly after exposure to 2 ppm SO_2 for 30 days (26). Fye et al. (25) found that after a 90 day exposure to 2 ppm SO_2 only nylon underwent degradation (as measured by a reduction in breaking strength). In the same study cotton, polyester, rayon, and polyester/cotton blend fabrics did not show reduced strength, in fact, the strength of the rayon increased somewhat. From their results, the researchers concluded that sulfuric acid aerosol was not formed in the test chamber. If acid had been formed, they reasoned, the cellulosic fibers would have been degraded. The presumption was that the mode of degradation for all fibers tested (except nylon) occurred by acid hydrolysis of the polymer chain. The researchers could not explain why the rayon increased in strength. Furthermore, they reasoned that because the nylon was degraded in the absence of acid formation, some other mechanism must be involved for that polymer.

Later research by Zeronian (29) tends to disallow that the mode of degradation by SO_2 occurs by acid hydrolysis alone. In several studies, cotton, viscose rayon, high wet modulus (HWM) rayon, and poly(hexamethylene adipamide) (nylon 66) were exposed to very low concentrations of SO_2. In the study examining the cellulosic fabrics, samples were exposed to light from a xenon arc lamp and air; light, air, and 0.1 ppm SO_2; or light, air, SO_2, and intermittent water spray. For the sake of comparison, unexposed samples were

hydrolyzed in dilute H_2SO_4. The nylon exposure studies were essentially the same with the exception that the SO_2 concentration used was 0.2 ppm.

The cellulosic fabrics showed a reduction in breaking load (evidence of degradation) following each type of exposure as well as following acid hydrolysis. Degradation of the cellulosics was further determined by measurement of copper number (a test of the reducing power of aldehyde groups in degraded cellulose), carboxyl content, and fluidity. It was found that the copper number was less for the acid hydrolyzed specimens than for the exposed samples degraded to the same breaking strength. The acid hydrolyzed samples showed a smaller decrease in carboxyl content than the exposed samples. In fact, the acid hydrolyzed cotton had no decrease in carboxyl content. The variation in the results of acid hydrolysis and exposure to SO_2 points out that while hydrolysis by absorbed acid may play a role in the degradation of cellulosic fibers by SO_2, there are clearly other factors involved. Photochemically induced reactions seem to play a role.

It has been suggested that acetal bonds adjacent to the oxidized glucose unit can be activated by carboxyl and aldehyde groups. The result is an increased susceptibility to acid hydrolysis. Zeronian (29) postulates that in the viscose rayon samples examined, the hydrolysis does occur at the acetal bonds and that the carboxyl rich segment of the polymer is washed out after chain scission. This would explain the drop in carboxyl content for the acid hydrolyzed viscose rayon samples.

In a related test, Zeronian (29) found that cotton treated with a durable press resin increased in strength somewhat after exposure to light, air, and 0.1 ppm SO_2. He concluded that the resin treatment retarded degradation possibly by shielding the fiber polymer or by the formation of resin-quenched free radicals. Alternately, resin cross-links may have been cleaved on exposure to the test conditions.

While the exposure studies on nylon 66 involved essentially the same treatment described for the examination of cellulosic fibers (with the exception of the SO_2 concentration mentioned above), the physical and chemical tests employed were different. Titration was used to determine amine and carboxyl end groups. Additionally, scanning electron microscopy (SEM) and differential thermal analysis (DTA) were employed to determine other effects of the gas on the fiber (28, 30).

The SEM analysis showed that the surface of the unexposed fibers was smooth. After a 168 hour exposure to light, air, and intermittent spraying, surface pitting was noted, accompanied by a 40% strength reduction. Samples exposed to light, air, spray, and 0.2 ppm SO_2 for the same period showed the development of surface cavities and a strength loss of 80%. Doubling the exposure time for samples exposed only to light, air, and spray resulted in surface cavities similar to those noted on the samples exposed to SO_2 for 168 hours. The strength loss was 70% which was also comparable to that noted for the SO_2 exposed samples (28).

The surface of fibers hydrolyzed in H_2SO_4 to a 70% strength loss was smooth to rough with no apparent pitting. That the effect of acid

hydrolysis differed from the effect of light exposure led to the conclusion that SO_2 accelerates the degradation of nylon 66 by light, but does not change the mode. The nonuniformity of the pitting was presumed to result from the nonuniform dispersion of the delustrant particles. The photo-oxidation of nylon 66 is known to be accelerated by some forms of titanium dioxide (TiO_2) (30).

The mechanical properties of the nylon 66 samples were altered by exposure to SO_2. The reduction in breaking strength was accompanied by a loss in breaking extension. In fact, as the exposure conditions were intensified, the stress-strain curve approached that of a brittle plastic (30).

The end-group titration indicated a decrease in amine end-groups and an increase in carboxyl end-groups for samples exposed with and without SO_2. The intrinsic viscosity of the samples dropped as well, indicating the occurrence of chain scission (30).

The chemical properties of the acid hydrolyzed samples differed from those of the exposed samples mentioned above. The relative viscosity decreased to a much greater extent for hydrolyzed samples. The relative viscosity of light, air, and spray exposed samples was twice the relative viscosity of acid hydrolyzed samples. The number of carboxyl end-groups increased more for the acid hydrolyzed samples and the number of amine end-groups increased after an initial fall (30).

Zeronian et al. (30) concluded that the damage to nylon 66 by SO_2 cannot be explained totally by the formation of acid aerosols and

resulting hydrolysis of the polymer chain. The amount of acid formed is small (estimated at 1% per hour at 50% relative humidity) and very little of it is sorbed by the nylon. Thus, only a minimum amount of the degradation can be attributed to acid hydrolysis.

The DTA analysis revealed that after exposure to light, air, spray, and SO_2 the curves, in the melting region, resemble those of nylon which has been melted, cooled, and reheated. The researchers suggest that an explanation for this phenomenon lies in the difference between the mode of attack by light and the mode of attack by acid. Because of the decreasing intensity of light as it penetrates the fiber, photochemical degradation will occur mainly at the fiber surface. Crystalline and amorphous regions may both be attacked. Acid hydrolysis on the other hand, can occur throughout the fiber with the amorphous regions being attacked preferentially due to their greater accessibility.

Hrdlovic et al. (31) prepared isotactic polystyrene films with four different degrees of crystallinity. They plotted degradation vs. time for exposure of the films to SO_2, oxygen (O_2), and ultraviolet light (UV). It was found that degradation was least for the amorphous film and greatest for the most crystalline film. The chain scission as evidenced by film degradation, is proposed to be greatest in the most crystalline film as a result of the structure of the crystallites. In a crystalline region, the polymer chains are folded back upon each other. The fold regions of the polymer chains are under more strain than the chain segments in the amorphous regions. The strain causes

the fold regions to be more susceptible to chain scission, thus accounting for the greater degradation of the more highly crystalline films (i.e., those films with more numerous regions of folded chains).

A variety of polymer films were exposed by Jellinek et al. (32, 33, 34) to UV, O_2, and SO_2. The effects of the exposure were ascertained via infrared (IR) spectroscopy and viscosity measurements. Polyethylene underwent no change upon exposure to SO_2 and air. when the exposure conditions included UV, O_2, and SO_2, nearly complete cross-linking occurred. Under the same test conditions, polypropylene was also found to undergo extensive cross-linking. Apparently this reaction can occur due to the fact that some unsaturation is present in such polymers. The researchers suggest that the polymer degradation noted may actually result from polymer interaction with ozone (O_3) formed when SO_2 reacts with light and O_2 (33).

Poly(methyl methacrylate) showed some chain scission when exposed to UV, O_2, and SO_2. The isotactic polymer was degraded as indicated by a drop in its relative viscosity. The relative viscosity of the former decreased by 55% while the latter decreased by 29%. The same trend was noted for polystyrene. The decrease in relative viscosity of the atactic polymer after exposure to UV, O_2, and SO_2 was 17%. The isotactic counterpart showed a viscosity decrease of 55% (34). No mechanism was postulated.

Of the other polymers tested by Jellinek et al., only polyvinylformal and the elastomers (unsaturated polymers) showed marked degradation. The polyvinylformal underwent cross-linking.

After exposure to UV, O_2, and air, the relative viscosity dropped 27%, indicating chain scission. Of the elastomers, polyisoprene and polybutadiene underwent cross-linking and butyl rubber underwent some chain scission. Poly(vinyl chloride) showed no major changes but apparently lost some chlorine in the presence of SO_2. The effect of SO_2 on the other polymers tested was minor (34).

Thus degradation of many polymers upon exposure to varying concentrations of SO_2 has been demonstrated. The results of the various studies indicate that it is unlikely that acid hydrolysis is the primary mode of degradation. From these data it seems far more likely that SO_2 intensifies the degradative effects of photo-oxidation. No specific mechanisms have been determined.

Sorption of Gases by Polymers

A review of relevant work concerning sorption equilibria and kinetics of polymer films and textile materials has been compiled. Early work on the sorption and diffusion of gases in polymer films sought to elucidate polymer morphology and to assess the suitability of polymeric substrates for environmental research.

Walters et al. (8) summarized the work leading to the dual sorption model for the interaction of gases and polymer films. It has been shown that the sorption of gases by rubbery polyethylene conforms to Henry's law at or below pressures of 1 atm. Furthermore, when the solubility constants were calculated from the amount sorbed, they were found to be proportional to the degree of amorphous

structure in the polymeric material in question (13). Glassy polymers, on the other hand, required a more complex sorption model. The simple solubility relationship was inadequate to describe the observed results. Meares (35) postulated that microvoids, essentially frozen in the polymer at temperatures below its glass transition temperature (T_g), were responsible for any sorption differences. Sorption of gas by glassy polymers is said to follow the dual sorption model where the gas is adsorbed in the microvoids following Langmuir's isotherm with the total sorption process expressed by:

$$C = C_D + C_H$$

$$= k_D P + \frac{C_H' b P}{a + bP}$$

where: C = concentration of gas in polymer

C_D = concentration of dissolved gas

C_H = concentration of gas in holes

k_D = solubility constant for dissolved gas

P = pressure

C_H' = saturation concentration of gas in holes

b = hole affinity constant (the equilibrium between sorption and desorption in the holes.

This dual sorption model has been verified for a variety of polymer-gas combinations (36, 37, 38). The values of C_H' and k_D have been calculated for several polymers (39). For polyethylene above its T_g, SO_2 is sorbed via simple dissolution, whereas for polycarbonate and a

polyamide (nylon 11) below their T_g's, the dual sorption model is required.

Environmental researchers have carried out quantitative studies to determine the amount of SO_2 sorbed by materials for air sampling lines. In one such study, the two polymer materials examined were polytetrafluoroethylene (Teflon®) and poly(vinyl chloride) (Tygon®) tubings (40).

The Teflon® showed no adsorption or desorption of the SO_2 when exposed to low concentrations [12-114 parts per hundred million (pphm)] at a flow rate of 28.3 L/min. Teflon® was not tested at a lower flow rate as the presumption was that sorption would not be evidenced.

Tygon® sorbed almost completely all of the SO_2 to which it was exposed at both a low flow rate (1.4 L/min) and a higher flow rate (28.3 L/min). There was eventual cessation of SO_2 sorption by Tygon® with no accompanying desorption. The implication is that Tygon® chemically sorbs the SO_2 at certain sites. The sites eventually become filled, temporarily preventing further sorption. However, desorption has been shown to occur over a period of months, accompanied by subsequent SO_2 sorption (59).

Several researchers have studied sorption of SO_2 by wool fibers (40, 41, 42, 43). In related studies, Walsh et al. and Crawshaw found that sorption of SO_2 by wool was affected by pH. Sorption was retarded at low pH conditions, but not enhanced at high pH. This observation agrees with the observation that sorption of SO_2 by water

decreases as the pH is lowered (41, 43). In a different study, Gregory recorded no sorption of SO_2 below pH 3.6 (9). The researchers also found that wool has an extremely high capacity for SO_2 removal. The wool continued to sorb SO_2 after exposure of the carpet samples to the equivalent of 27 years at 30 $\mu g/m^3$, even though its sorption rate was reduced by a factor of three (43). The wool carpet pile sorbed more SO_2 than either jute or latex foam carpet backing in spite of the fact that the backings contained more mass. Presumably the greater surface area of the carpet pile and the greater acid combining capacity of the wool were responsible for this behavior. The facility of SO_2 sorption by wool is commonly attributed to its high acid combining potential.

An earlier study by Spedding (42) in 1971, examined a variety of flooring materials including wool carpet. In this study, wool carpet was found to sorb only a small amount of SO_2. Its SO_2 uptake was found to be similar to that of nylon carpet. Interestingly, the sorption was reduced by acid, basic, disperse, and direct dyes; all of which have different binding mechanisms. Textile finishes and other chemicals may also have an effect on the SO_2 sorption process.

Gregory (9) found wool to sorb far more SO_2 than nylon. In fact, nylon sorbed almost none of the SO_2 to which it was exposed, while wool sorbed 55% of the 0.2 ppm SO_2 passed over the substrate at 2 L/min for 30 minutes. In a 60 minute exposure the wool sorbed 60% of the SO_2.

Cotton and viscose rayon were examined by Gregory in addition to wool and nylon. Both fibers demonstrated initial removal rates higher than wool but approached saturation far more quickly. Nylon evidenced the least capacity for sorption becoming saturated in less than 25 minutes.

Several factors were found to affect the rate of SO_2 removal by wool, nylon, cotton, and rayon. Higher fiber moisture content increased the sorption rate significantly. Sorption proceeded twice as fast for wool fibers containing 15.5% moisture than for those containing 5.5% moisture. Gregory postulated that the initial removal of SO_2 was the result of solution of the gas in the fiber held moisture. For rayon it was concluded the solution in the fiber held moisture is probably the only removal mechanism at work because the SO_2 was completely removed from the fiber by drying it. For cotton and wool, SO_2 removal was greater than that attributed solely to solution of the gas by moisture held in the fiber. Chemical reaction of SO_2 with cotton and wool is probable. The initially higher rate of sorption by cotton and higher total sorption by wool indicate that the reaction sites are more accessible in cotton, but more numerous in wool (9).

Pretreatment with SO_2 of all fibers in Gregory's study led to a decrease in the rate of gas sorption. He concluded that a lowering of the pH of the moisture held within the fibers would account for such an occurrence. Preexposing the fibers to nitrogen dioxide (NO_2) also retarded sorption of SO_2 presumably due to the lowered pH of the fibers or partial saturation of the adsorption sites by NO_2.

The concentration of SO_2 introduced affected the rate of sorption by the fibers. The removal of SO_2 from the gas stream was found to increase with increasing SO_2 concentration. Thus, the rate and extent of SO_2 sorption by the fibers tested was found to vary with fiber type, pH of the surrounding moisture, and concentration of the gas introduced (9).

Reactions Related to Polymer Degradation and Gas Sorption

In the fiber study mentioned above, Gregory concluded that SO_2 sorption by nylon and rayon consists mainly of solution of the gas in fiber held moisture. This conclusion is based on two findings: (a) the original sorptive capacity was restored after drying the fibers thus indicating that the sorbed SO_2 was driven off with the water, and (b) the pH of the surrounding moisture dropped rapidly as would be expected if the mechanism for sorption was primarily solution of the gas in moisture.

Gregory could offer no explanation why cotton demonstrated greater and more permanent sorptive capacity than rayon. He surmised that the difference must lie in the fiber morphology. Cellulosics do not have the acid combining capacity of wool. Anionic dyes are attracted to these fibers only by ion-dipole forces at strongly hydrated sites (i.e., water held via hydrogen bonding to a hydroxyl group or to an ether oxygen) (9). The crystalline regions of the fiber have been found relatively inaccessible to dye molecules. This led Gregory

to the conclusion that morphology differences must account for the dissimilarity in the SO_2 sorption characteristics of rayon and cotton.

Gregory explained the sorption of SO_2 by fibers as the dissolution of SO_2 in the retained moisture of the fibers, followed by its reaction of the dissociated species of sulfurous acid (H_2SO_3) with certain chemical constituents of the fibrous polymer (9). Depending on the pH, the following species may be available for reaction with and incorporation into the polymer chain: H^+, HSO_3^-, SO_3^{2-}, and H_2SO_3. These species are generated by the following reaction sequence involving the solution of SO_2 and the dissociation of H_2SO_3.

Solution of SO_2 in water:

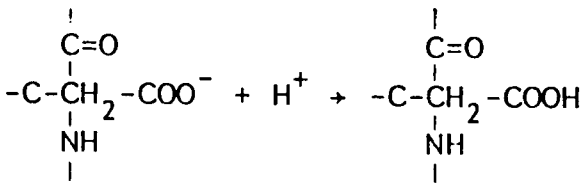
$$SO_2 + H_2O \rightarrow H_2SO_3$$

Dissociation of H_2SO_3:

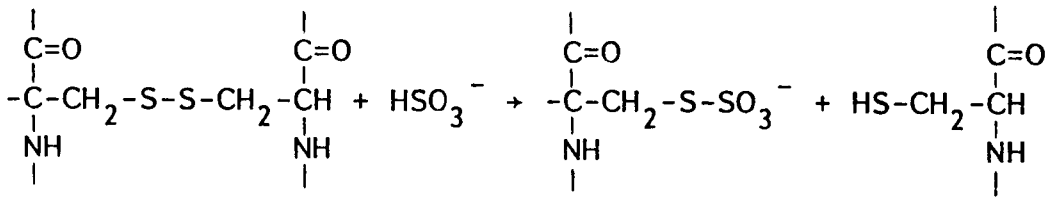
$$H_2SO_3 \rightarrow H^+ + HSO_3^-$$

$$HSO_3^- \rightarrow H^+ + SO_3^{2-}$$

At a low pH, the wool protein (keratin) has ionized carboxyl and amino groups available for reaction with the dissociated species listed above. Ionizable carboxyl groups may be found as end-groups or on side chains. The reaction between aspartic acid and a dissociated proton from H_2SO_3 represents a typical reaction (9).



Bisulfite ions (HSO_3^-) are known to disrupt cystine linkages as follows (9):



Several studies by Jellinek (32, 33, 34) and co-workers represent another attempt to understand the mechanism of SO_2 sorption by polymeric materials. They propose the following reaction series for the interaction of SO_2 with saturated hydrocarbons (RH) (33).

$$SO_2 + h\nu \rightarrow SO_2^*$$
$$SO_2^* + RH \rightarrow RSO_2H \text{ (sulfinic acid)}$$
$$SO_2^* + RH \rightarrow SO_2 + RH$$
$$SO_2^* + SO_2 \rightarrow SO_2 + SO_2$$
$$SO_2^* \rightarrow SO_2$$

The proposed reaction series for the reaction of SO_2 with unsaturated hydrocarbons (B) is as follows (33):

$$SO_2 + h\nu \rightarrow SO_2^*$$
$$SO_2^* \rightarrow SO_2$$
$$SO_2^* + B \rightarrow SO_2 + B$$
$$SO_2^* + B \rightarrow BSO_2$$

Presumably, in each case, the excited SO_2 (SO_2^*) is deactivated by an energy absorbing species.

Deposition Velocity and Resistance

Several researchers have evaluated their data in terms of the deposition velocity (v_g) of SO_2. Chamberlain defines v_g in two ways (44, 45).

$$v_g = \frac{\text{rate of deposition per cm}^2 \text{ per sec}}{\text{volumetric concentration per cm}^3}$$

or

$$= \frac{\text{amount deposited per cm}^2}{\text{time integral of volumetric concentration (dosage per cm}^3\text{)}}$$

The concept of deposition velocity has been useful for those attempting to describe the transfer of a gas between an atmosphere and a surface. There are, however, some problems associated with its use. In studies in which the v_g has been calculated for the exposure of carpet samples to SO_2, different values were obtained depending on whether the floor surface area or the fiber surface area was considered in the calculations. In cases where the total fiber surface area is used, v_g is smaller, typically by about a factor of three. In line with Spedding's conclusions concerning the deposition of SO_2 onto barley leaves, it is probable that not all the fibers are exposed to the same conditions of gas flow (46). Further, deposition velocity is controlled by the design of the exposure chamber, the gas flow rate, and offers no insight into the differentiation between transfer of the substance in the gas phase and sorption onto the surface (47, 48).

The inverse of the deposition velocity is defined as the resistance to sorption. It depends on the affinity of the surface in question toward the gas and is generally considered to be more a useful descriptor of the sorption phenomenon. Resistance is expressed as follows:

$$r = r_s + r_a + r_b = \frac{1}{v_g}$$

where r_s = surface resistance

r_a = aerodynamic resistance

r_b = laminar layer resistance

To distinguish between gas phase and surface resistance, researchers have determined the v_g for sodium carbonate, a perfect sink for SO_2 (46, 47). In such cases, $r_s = 0$ and $1/v_g = r_a + r_b$, so theoretically the resistance for a perfect sink could be subtracted from the total resistance for exposed surfaces to yield accurate values for r_s.

Properties of Cotton, Modified Cellulosics, and Viscose Rayon

Cotton

The cotton fiber consists of a single cell which grows from the cotton seed (49). The mature fiber resembles a flattened ribbon and is characterized by convolutions along its length. The cross-section has been described as being either bean or kidney shaped. It is composed of four distinct sections: cuticle, primary wall, secondary wall, and lumen. Examination of the secondary wall reveals daily growth rings made up of fibrils as shown in Figure 1. The cotton

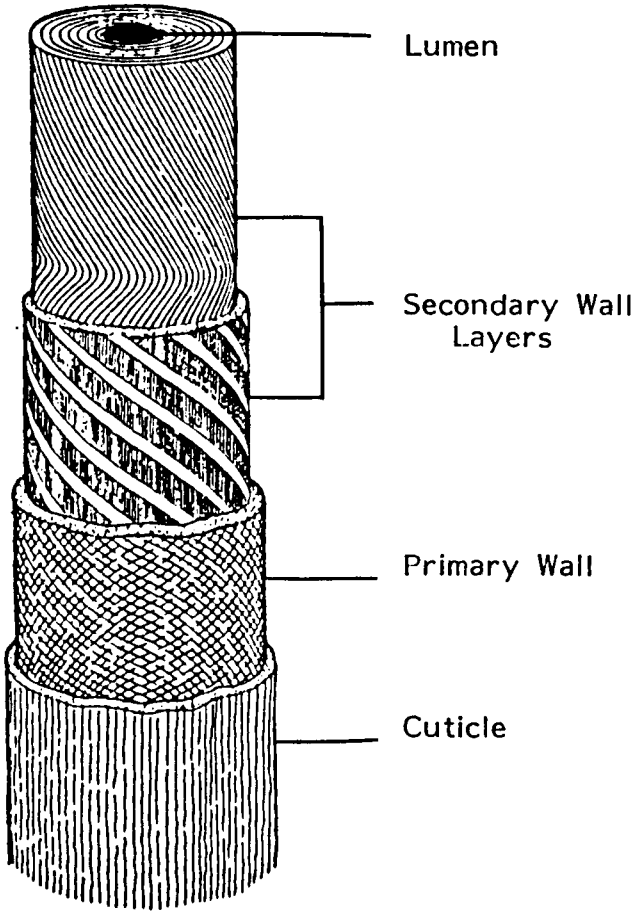


Figure 1. Cotton fiber internal structure. Adapted from J. G. Cook, Handbook of Textile Fibers, I. Natural Fibers, Merrow Pub. Co. Ltd., England, 1968, 42.

fiber is approximately 90% cellulose by weight. At 1.52-1.56 g/cm^3 cotton is one of the most dense fibers.

The cellulose polymer in cotton (Figure 2) is generally reported to have a degree of polymerization (DP) of 10,000. Cotton is an extremely crystalline fiber. The degree of crystallinity is typically reported at about 67%, but some have suggested that it may go as high as 100% (51).

Each anhydroglucose unit in the cellulose polymer has three hydroxyl groups (one each on carbons 2, 3, and 6). The hydroxyl groups are the reactive groups on the polymer chain. Inter- and intramolecular hydrogen bonding are very prevalent in cotton. Hydrogen bonding is responsible for many of the properties of cotton including crystallinity, strength, and high moisture regain. The crystalline lattice of native cotton is noted in the literature as Cellulose I (Cell I) as shown in Figure 3. Unit cell dimensions for Cell I, II, and III are presented in Table 1.

Mercerized Cotton

Mercerization of cotton usually involves treating the fibers with a 13% or greater (w/w) aqueous solution of sodium hydroxide (NaOH). Frequently this treatment is used to increase the fiber luster, but tensile strength and dyeability are increased as well. Mercerization shrinks the cotton fibers unless the process is carried out under tension.

Mercerization yields little or no polymer degradation but there is a marked decrease in crystallinity accompanied by a change in the

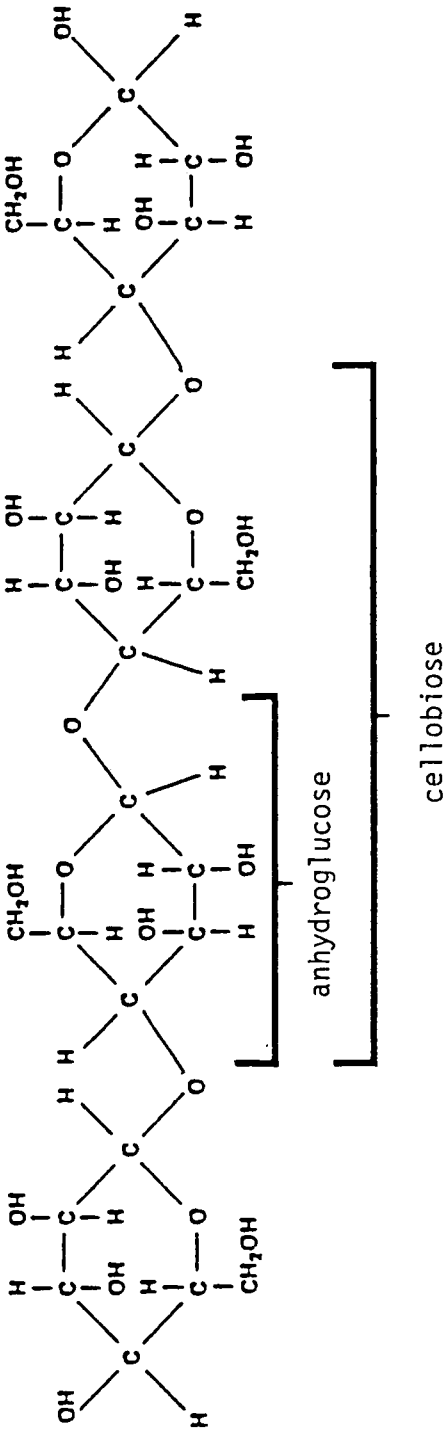


Figure 2. Structure of the cellulose polymer.

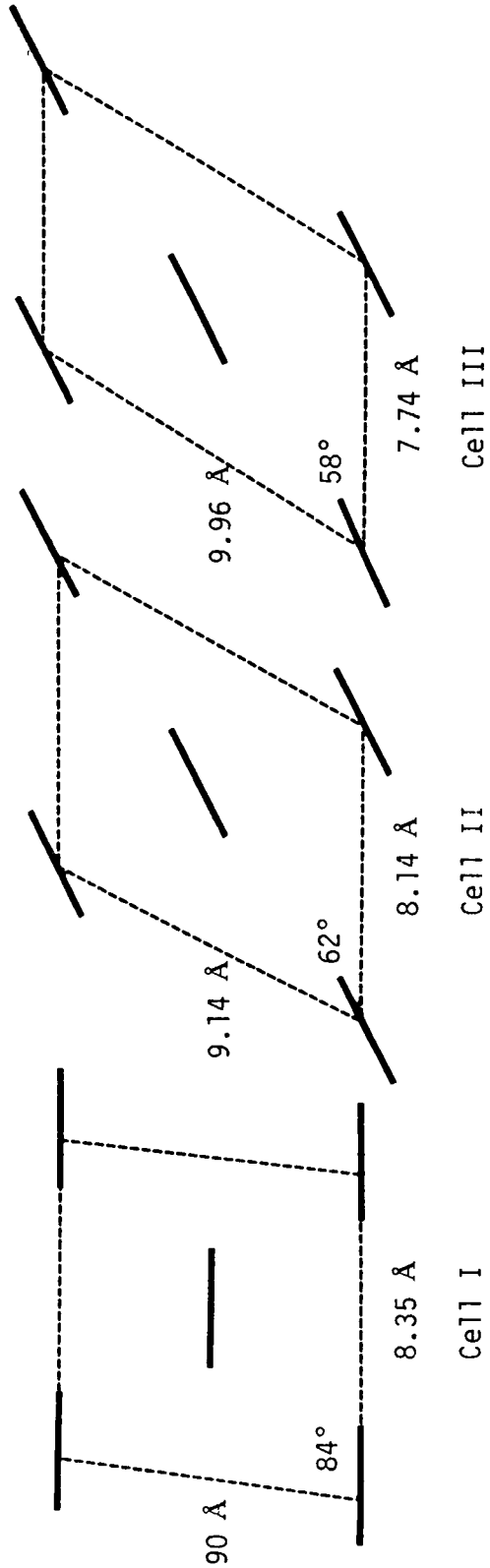


Figure 3. Unit cell structures for cellulose I, II, and III.

Table 1. Unit cell dimensions of three cellulose lattice configurations.

Lattice type	a	b	c	β
Cell I	8.35 Å	10.30 Å	7.90 Å	84°
Cell II	8.14 Å	10.30 Å	9.14 Å	62°
Cell III	7.74 Å	10.30 Å	9.96 Å	58°

orientation of the crystallites (52). Rousselle and Nelson (53) measured the crystallinity of cotton treated in 20% NaOH to be 43%. The increase in noncrystalline regions over native cellulose means that the fiber is more accessible. This accounts for its greater moisture regain, reactivity, and dyeability.

In mercerization, the NaOH enters the fiber and disrupts the hydrogen bonded network replacing many of the hydrogens in the hydroxyl groups with sodium, thereby forming soda cellulose. During the treatment the fiber swells, loses many of its convolutions, and takes on a more circular cross-section. The sodium ions are then removed and new hydrogen bonds formed by treating the fibers in dilute acid. The fiber retains the more circular cross-section with fewer convolutions, resulting in increased fiber luster.

It is commonly stated that the crystalline lattice of mercerized cotton changes from Cell I to Cell II (Figure 3). X-ray diffraction studies by Rousselle et al. (54) indicate that this is essentially true. They found 81.4% of the crystalline regions to be Cell II and 18.6% of the crystalline regions to be Cell I in the sample they studied. The

actual degree of conversion to Cell II will depend on the experimental conditions. The conversion to Cell II is irreversible even though Cell I is the form in which native cellulose exists.

Liquid Ammonia Treated Cotton

Like NaOH, liquid ammonia ($NH_3(\ell)$) is also known to swell cotton fibers. Treatment is quite simple and involves immersing the fibers in $NH_3(\ell)$ for a period of time, then removing the ammonia via evaporation or quenching in water. The effects of $NH_3(\ell)$ treatment on cotton are similar in many ways to the effects of NaOH mercerization. Liquid ammonia treated fibers have been shown to exhibit increased tenacity, elongation, toughness, moisture regain, and accessibility, accompanied by decreased stiffness and crystallinity (55).

In one study the total crystallinity of cotton fibers in which the $NH_3(\ell)$ was allowed to evaporate fell to 37%. The crystallinity of the water-quenched fibers fell to 39% (53). Accompanying the reduction in crystallinity is a reduction in crystallite size (54). As with mercerized fibers, the increase in noncrystalline areas accounts for the increased regain and accessibility.

The reaction of $NH_3(\ell)$ with cellulose is thought to occur in both the crystalline and noncrystalline regions (56). The $NH_3(\ell)$ enters the fiber and swells it by breaking the existing hydrogen bonds and forming a new hydrogen bonded complex with the ammonia. Upon removal of the ammonia new hydrogen bonds are formed among the rearranged polymer chains. The resulting fibers have more circular cross-sections and fewer convolutions. Water quenched fibers tend to have

more convolutions, and therefore less luster, than those fibers in which the $NH_3(\ell)$ was evaporated. Neither treatment swells the fiber to the same extent as NaOH nor produces the same degree of luster. The method of removing the ammonia from the fiber determines which crystalline lattice will result. Cell III (Figure 3) is formed when cotton fibers are treated with $NH_3(\ell)$. The degree of lattice conversion from Cell I to Cell III depends on the treatment parameters. Upon quenching the fibers with water, Cell I is almost completely regenerated (53, 54, 56, 57). In one study 90% of the remaining crystalline regions were found to be Cell I, while only 10% were Cell III when the fiber had been water quenched (53).

Evaporative removal of $NH_3(\ell)$ leads to a mixed crystalline lattice of mainly Cell III with some Cell I (53, 54, 56, 57). The relative percentages of Cell I and Cell III were measured in one study to be 27% and 73%, respectively (53). However, Roldan (58) states that the change from Cell I to Cell III is not permanent and rehydration will result in the regeneration of Cell I.

Viscose Rayon

Viscose rayon is produced by forming a soluble unstable cellulose derivative from woodpulp or cotton linters, then regenerating the cellulose in fiber form (59). The standard process for viscose manufacture is as follows:

1. purified woodpulp is pressed into sheets,
2. sheets are steeped in 18% NaOH to form soda cellulose,
3. soda cellulose sheets are shredded then aged,

4. soda cellulose is reacted with carbon disulfide (CS_2) to form a soluble cellulose derivative: sodium cellulose xanthate (SCX),
5. SCX is dissolved in dilute NaOH to form the viscose solution,
6. viscose solution is filtered, then aged to obtain the correct DP for spinning, and
7. viscose solution is spun into an acid bath for regeneration of cellulose.

Rayon is essentially pure cellulose and as such is similar in many ways to cotton. However, the properties of rayon are controlled by the production parameters.

The degree of polymerization (DP) of rayon is typically 200-700. It is approximately one third crystalline with the degree of crystallite orientation being largely dependent on the amount of fiber drawing. The tenacity of rayon is significantly lower than cotton due to the much lower DP and crystallinity. The decreased order causes rayon to be more accessible and to have a higher moisture regain than cotton. In the manufacturing process the crystalline lattice is changed from Cell I to Cell II. This is an irreversible change.

Viscose fibers are available in both filament and staple forms. The cross-section is extremely irregular, resulting in a high surface area. There are both skin and core layers, the percentage of each depending on the processing parameters.

CHAPTER III

EXPERIMENTAL

The purpose of the present study was to undertake a systematic examination of the SO_2 sorption characteristics of four types of cellulosic fibers. This chapter outlines the experimental design and analytical methods used.

Materials

Native cotton silver obtained from StarLab in Knoxville, Tennessee, and unfinished rayon staple (DP = 225) obtained from American Enka were used in this study. Gases used were 3 ppm certified standard SO_2 in dry air obtained from Matheson and zero grade anhydrous air from Air Products. Fisher laboratory grade NaOH beads were used to prepare the mercerization bath and Fisher laboratory grade ethyl alcohol was used for cotton extraction. Fisher laboratory grade mixed hexanes, Fisher laboratory grade cyclohexane, and Spectrum 99+% mol n-hexane were used for the fiber porosity measurements.

Fibers

Four fiber types (all cellulosic and having the identical polymer repeat unit, Figure 1, p. 26) were chosen for this study. They include native cellulose (ethanol extracted cotton), modified cellulose (NaOH mercerized cotton and liquid ammonia [$NH_3(\ell)$] treated cotton),

and regenerated cellulose (viscose rayon). While chemically the same, these four fiber types differ greatly morphologically. Specifically, they differ in their crystalline lattice structure, accessibility, degree of order and crystallite orientation, and degree of polymerization.

Sample Preparation

The cotton sliver was extracted in a Soxhlet extractor for four hours with ethanol to remove the natural waxes. A portion of the extracted cotton was retained for use in that condition while some was mercerized with NaOH and some with $NH_3(\ell)$.

Mercerization was carried out by immersing short lengths of stabilized sliver in an 18% solution of NaOH for 15 minutes at room temperature. The fibers were then rinsed thoroughly in distilled water, neutralized in 3% acetic acid, rinsed again in distilled water, and left to air dry.

The liquid ammonia treatment, carried out by Cotton, Inc., involved immersing the stabilized sliver sections in liquid anhydrous ammonia for 30 seconds. The fibers were removed from the $NH_3(\ell)$ and left to air dry.

The viscose rayon staple fibers were parallelized using a Suter fiber sorter in order to minimize error by removing tangles which would retard diffusion of SO_2 throughout the sample. Small bundles of relatively parallel fibers were obtained by combing them twice in the device.

Exposure Chamber Development

In order to examine the sorptive behavior of cellulosic fibers under the dynamic conditions typically encountered within buildings it was necessary first to design and construct an exposure system which would simulate ambient conditions and provide adequate control over variables such as time, temperature, humidity, gas concentration, gas flow rate, and exposure to light.

Extensive research has been conducted on the sorption of many gases by a variety of surfaces. Some of these studies have specifically addressed the problem of which materials are acceptable for air sampling instruments. The results can be generalized to include the suitability of these materials for exposure chambers used in pollutant research.

Work by environmental researchers (41, 60, 61, 62) indicates that borosilicate glass and polytetrafluoroethylene (Teflon®) are generally inert to all gases except certain fluorides. Wohlers et al. (41, 62) found no adsorption or desorption of SO_2 or a SO_2/CO mixture by borosilicate glass or Teflon® conduit at lengths up to 30.5 meters. In their work on the effects of air pollutants on plants, Rogers et al. (63) used glass and Teflon® chamber interiors. They state that such materials will minimize the loss of gas to surface reactions and adsorption.

For the reasons given above, the exposure chamber (Figure 4) was constructed entirely of Pyrex® and Teflon®. The exposure line includes a ball rotameter (C) to measure gas flow because velocity of

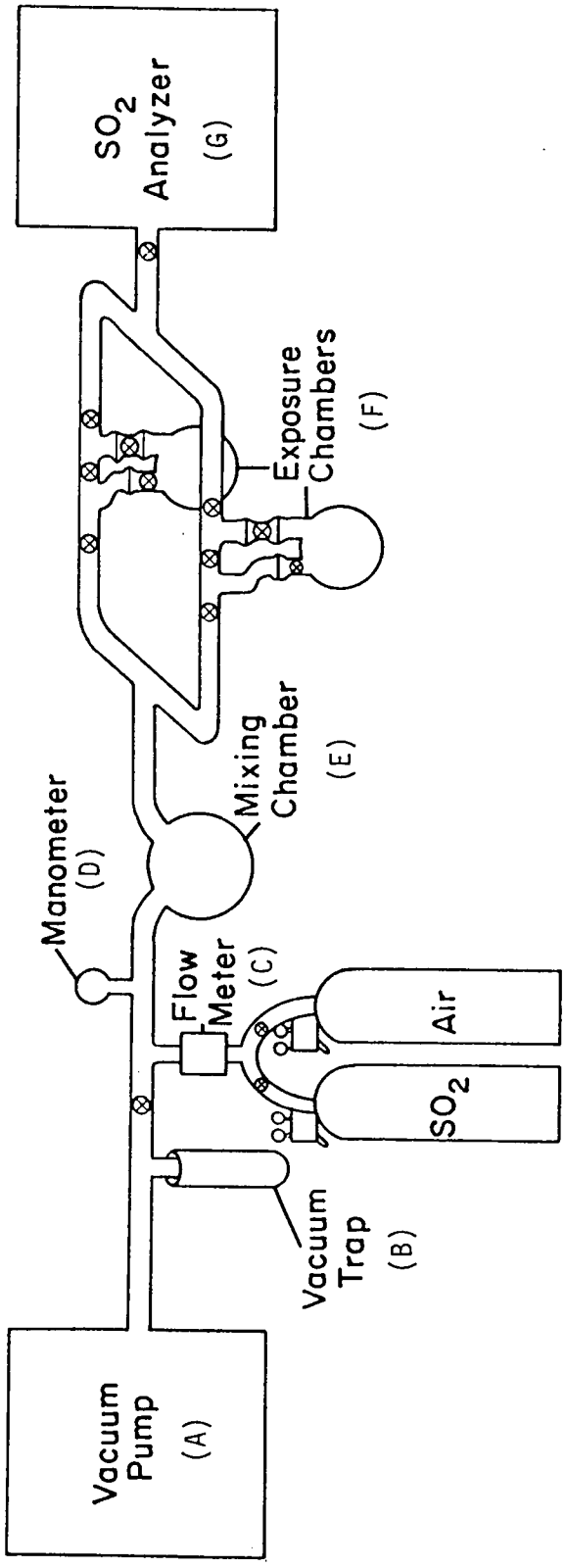


Figure 4. Schematic of exposure apparatus.

the gas stream has been shown to influence sorption characteristics of substrates. Additionally, it was important to quantify the amount of gas introduced into the chamber during the exposure period. The manometer (D) records the pressure within the chamber because changes in pressure will affect rates of sorption. The spherical mixing chamber (E), submerged in a water bath in order to maintain constant temperature, provides for complete mixing when two or more gases are being used simultaneously.

Two separate samples can be exposed during each run in 500 ml round bottomed flasks (F) submerged in a constant temperature bath. Teflon® high vacuum stopcocks direct the flow of gas within the chamber. The exposure line is equipped with a vacuum pump (A) so that the line can be thoroughly evacuated before exposing dried samples. Finally, for this study a Beckman model 906A SO_2 analyzer (G) has been used to measure the concentration of gas exiting the chamber.

The SO_2 analyzer operates via coulometric titration and utilizes a carbon paste reference electrode, platinum anode, and platinum cathode. In coulometric titration a reagent is generated by electrolysis. The reagent then reacts chemically with the substance under examination.

The analyzer used for the present study utilizes an iodine electrolyte for the generation of iodine at the anode and reduction of iodine at the cathode. When SO_2 enters the detector cell it reacts with the iodine as follows (6):

$$SO_2 + I_2 + 2H_2O \rightarrow SO_4^{2-} + 4H^+ + 2I^-$$

The reaction reduces the amount of iodine in solution and thereby causes the output at the cathode to be lower than the input at the anode. The current differential relates to the concentration of SO_2 in the air stream.

Exposure of Fibers to Sulfur Dioxide

Two-gram samples of opened sliver or combed rayon were weighed and suspended from glass hooks in the exposure flasks shown in Figure 5. Fibers were then conditioned or dried *in situ*. For the dried fiber runs the opened exposure flasks were placed in desiccators over phosphorous pentoxide (P_2O_5) for 24 hours. For the conditioned fiber runs the opened exposure flasks were placed in desiccators over a saturated solution of magnesium acetate for 24 hours and conditioned at 69 ± 1% R.H. and 20 ± 2°C. Preliminary work determined that fibers dried or conditioned in the manner described showed no perceptible weight change after 24 hours. However, it is acknowledged that for complete drying of fibers over P_2O_5 several weeks over the desiccant are typically required (51).

Following drying or conditioning of the fibers, the flasks were attached to the exposure line and exposed to 3 ppm SO_2 at 170 cc/min. for 5 hours. The concentration of SO_2 exiting the chamber was monitored on an Esterline Angus Speed Servo II chart recorder. The normalized amount of SO_2 exiting the chamber was compared to the known amount introduced into the chamber in order to calculate the quantity of gas sorbed by the substrate.

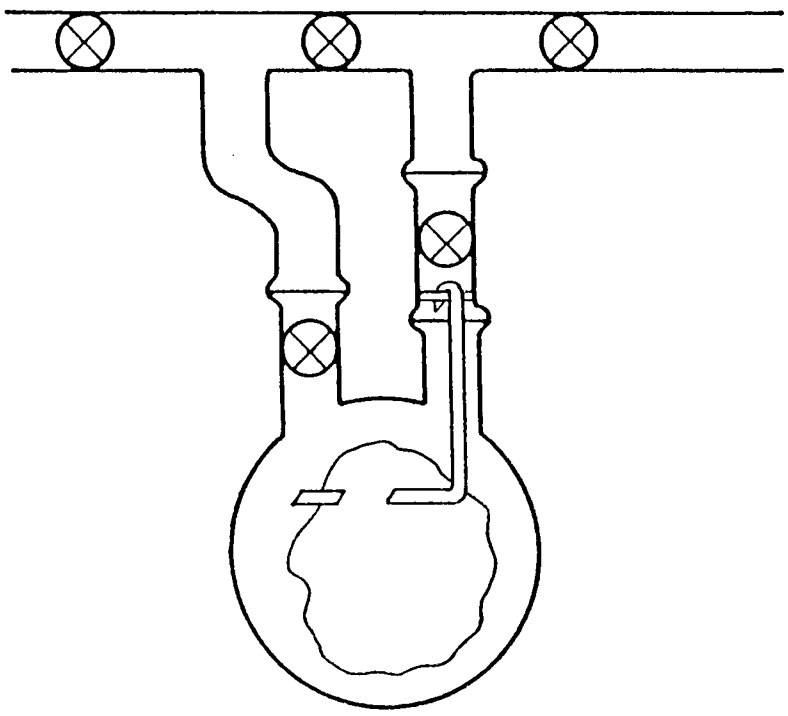


Figure 5. Fiber sample mounted in exposure flask.

Following the exposure period, the SO_2 was turned off and dry air was introduced into the chamber at 170 cc/min. for 4 hours in order to measure SO_2 desorption from the fibers. The concentration exiting the chamber was monitored continuously as described previously.

Blank runs were carried out under all exposure conditions. The blanks were reproducible indicating negligible SO_2 sorption by interior chamber surfaces.

Change in Fiber Moisture Content on Exposure to Air

Because it is possible that sorption of SO_2 by cellulose may be due to dissolution of the gas in fiber bound moisture, conditioned fibers were exposed to dry air at 170 cc/min. for 9 hours (equalling the total sorption/desorption exposure time) in order to observe the weight loss occurring during the exposure period. During these runs the exposure flasks were closed and removed from the line at intervals for weighing. Weight loss curves were established for each fiber type at four temperature levels.

Analytical Methods for Fiber Characterization

In an attempt to understand the phenomenon of SO_2 sorption by cellulosic fibers, several analytical techniques were employed. These are described below.

Moisture Regain and Moisture Content

Moisture regain and content were determined for each fiber type by a method adapted from AATCC 20A-1981. Fiber samples of approximately 1.5 grams each were conditioned for 24 hours at 65 ± 2% R.H. and 70 ± 2°F. The samples were weighed in previously weighed containers then dried either over P_2O_5 for 24 hours or in an oven at 110 ± 2°C with weighings at intervals.

Percent moisture regain and percent moisture content were calculated according to the following formulas:

$$\% \text{ Moisture Regain} = \frac{\text{conditioned weight-dried weight}}{\text{dried weight}} \times 100$$

$$\% \text{ Moisture Content} = \frac{\text{conditioned weight-dried weight}}{\text{conditioned weight}} \times 100$$

Values were compared for fibers dried over P_2O_5 and for oven dried fibers to determine the effectiveness of the drying method used in this study.

Scanning Electron Microscopy

Representative fibers were examined for gross surface changes following exposure to SO_2 using an AMR model 9000 scanning electron microscope. The fiber samples were glued to the sample holders and sputter-coated with gold. Photographs were taken at 500X, 1000X, and 2000X.

X-Ray Spectroscopy

An Ortec model 6200 x-ray spectroscope was used to detect trace amounts of sulfur remaining in the fibers following desorption of SO_2.

Sample holders were coated with carbon prior to gluing the fibers on them. The fibers were then sputter coated with carbon. The spectrogram was printed out on a chart recorder.

X-Ray Diffraction

X-ray diffraction techniques were utilized for the elucidation of the crystalline structure of the fiber samples. X-ray diffraction patterns of parallelized fibers taped onto holders were photographed using a Norelco Phillips x-ray diffractometer equipped with a copper target. A Rigaku Geiger Flex x-ray diffractometer equipped with a copper target and operated in the transmission mode was used to obtain diffractograms of randomized fiber samples taped onto holders. For each sample, 20 scans were obtained between 8° and 30°.

Fiber Porosity and Surface Area

Two methods were employed for the determination of relative porosity for each fiber type. First, fibers were evaluated using a Quantichrome series 2000 mercury pressure porosimeter. Data were obtained for total pore volume, percent pore volume, and surface area.

Additionally, in a technique adapted from Mikhail and Robens (64), combed fiber samples of approximately 10 mg each were dried for at least 100 hours over P_2O_5. The samples were weighed then immersed in hexane, and vibrated in an ultrasonic bath for one hour to remove trapped air from the pores. The samples were taken from the bath, shaken once to remove excess hexane, and suspended from a torsional balance. Weight readings were taken at intervals as the

hexane evaporated. The procedure was repeated for each fiber type using each of the following hydrocarbon solvents: mixed hexanes, cyclohexane, and n-hexane.

Surface Analysis

Selected fibers were evaluated by Fourier transform infrared spectroscopy (FTIR) and electron spectroscopy for chemical analysis (ESCA). A Digilab FTS-20E FTIR spectrophotometer with a TGS detector was used. Samples were taped to holders and scanned between 399.3 and 2000.2 wavenumbers. A Varian IEE 15 ESCA with a Mg anode was employed for ESCA measurements.

Total Sulfur Analysis

Samples of exposed and unexposed extracted cotton were sent to Galbraith Laboratories, Knoxville, Tennessee, for total sulfur analysis. Four-gram samples were evaluated using a Leco oxygen combustion analyzer equipped with an infrared detector.

CHAPTER IV

RESULTS AND DISCUSSION

The purpose of the present study was to determine the mechanism and degree of SO_2 sorption by four types of cellulosic fibers. Additionally, the contributing effects of fiber moisture content, fine structure, and temperature on SO_2 sorption were also examined.

Fiber Characterization

Four types of cellulosic fibers used for this study included: native cotton, NaOH mercerized cotton, $NH_3(\ell)$ treated cotton, and viscose rayon. These four types were chosen to provide similar chemical properties but differing physical properties. Chemically all four fiber types are comprised of the cellulose polymer (Figure 2, p. 28). Their physical properties however, vary greatly due to alterations in fine structure resulting from processing conditions.

Crystallinity

The effects of caustic mercerization and $NH_3(\ell)$ treatment on the disruption of crystallinity within cotton fibers have been well documented in the literature. Furthermore, the viscose process for rayon production produces fibers which are also less crystalline than cotton. X-ray diffraction studies confirm these facts for the fiber types used in the present study. For the sake of discussion, crystallinity values (and their methods of determination when available), as reported in the literature, are presented in Table 2. The method of crystallinity

Table 2. Percent crystallinity for cellulose fibers as reported in the literature.*

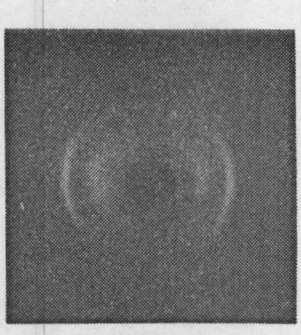
Fiber type	% Crystallinity	Technique for determination	Reference
Native cotton	67-100	x-ray diffraction	51
	70	-	66,67
	70	x-ray diffraction	68
	82-87	acid hydrolysis	69
	84	formic acid esterification	70
Mercerized cotton	43	x-ray diffraction	53
	50	-	67
	68	acid hydrolysis	69
	72	formic acid esterification	70
$NH_3(\ell)$ treated cotton	37	x-ray diffraction	53
Viscose rayon	33	-	51
	25-30	-	66
	40	-	67
	40	x-ray diffraction	68
	68	acid hydrolysis	69
	46	formic acid esterification	70

*Values are not absolute and should be viewed in terms of the technique for determination.

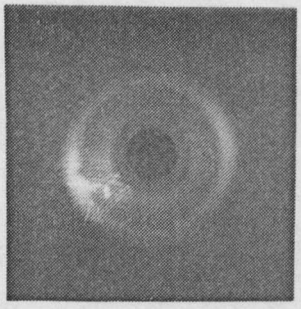
determination affects the value obtained. Chemical methods such as acid hydrolysis and formic acid esterification reach only the most accessible regions of the fiber and tend to yield higher crystallinity values than are obtained with x-ray diffraction.

X-ray diffraction patterns and diffractograms of unexposed fibers (Figures 6-10) indicate that the crystallinity of extracted cotton was substantially reduced following treatment by NaOH or $NH_3(\ell)$ and by regeneration to viscose rayon. Diffractogram patterns correspond well with those reported in the literature. Reduction in crystallinity for modified and regenerated fibers is observed in the diffraction patterns as broadening of the arcs. As crystallinity decreases the patterns become less defined and more diffused. The transition from Cell I to Cell II is observed as a shift of the $10\bar{1}$ reflection away and toward the 002 reflection (68). This shift is observable in the diffraction patterns of mercerized cotton and viscose rayon shown in Figure 2, p. 28.

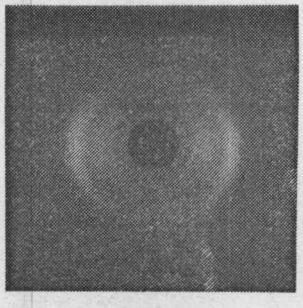
Crystallinity and crystallite orientation are measured from diffractograms by their peak widths. A narrow peak width as seen in the diffractogram for cotton (Figure 7) is indicative of a highly crystalline material. Wide peak widths seen in Figures 8-10 demonstrate the effect of mercerization, $NH_3(\ell)$ treatment, and regeneration on the ultimate degree of order. Diffractograms for fibers exposed to SO_2 are similar to those of the unexposed fibers and are contained in Appendix A.



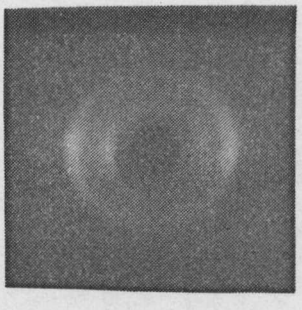
(a)
Extracted Cotton



(b)
Mercerized Cotton



(c)
$NH_3(\ell)$ Treated Cotton



(d)
Viscose Rayon

Figure 6. X-ray diffraction patterns for four types of cellulosic fibers.

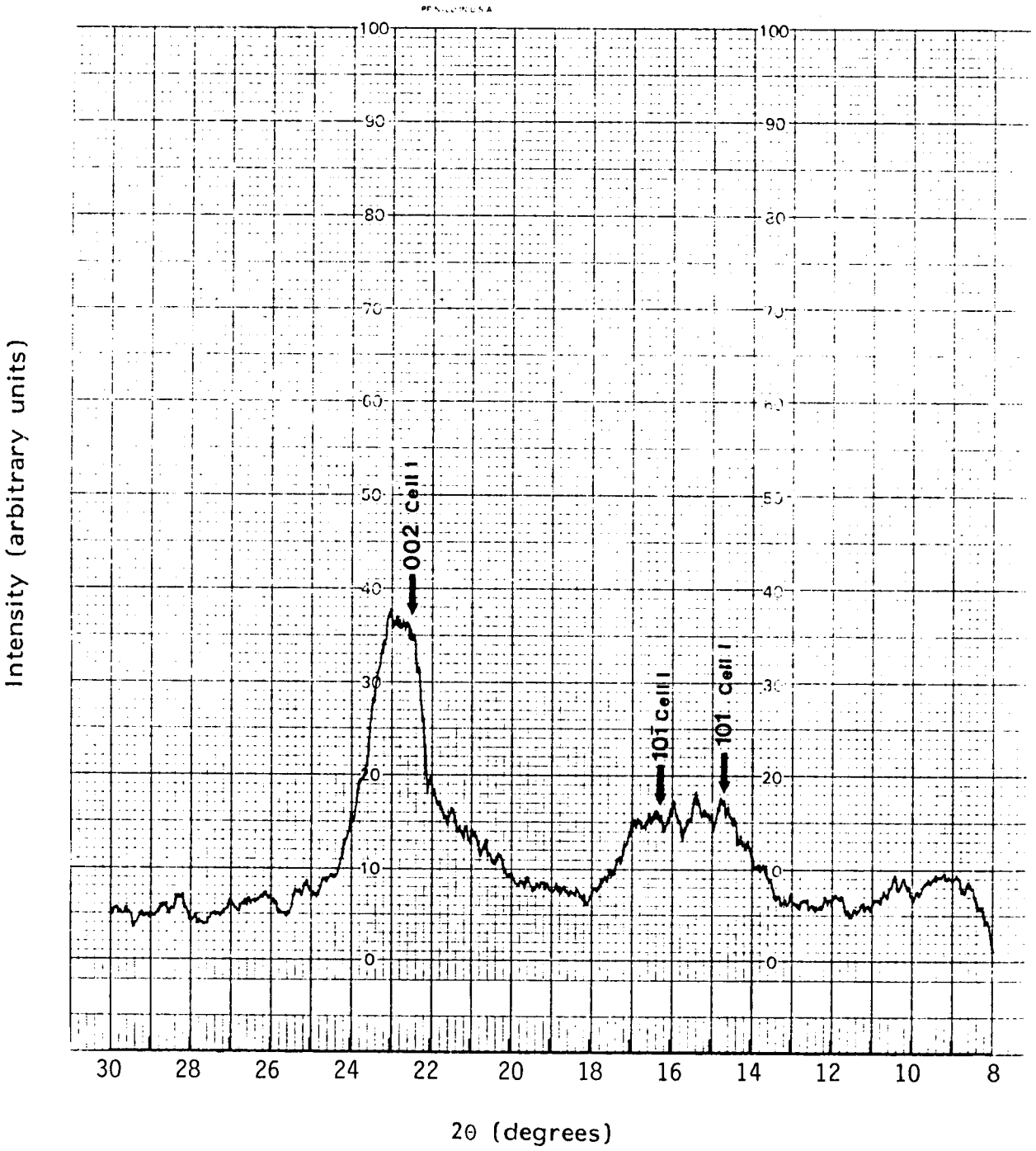


Figure 7. X-ray diffractogram of unexposed extracted cotton.

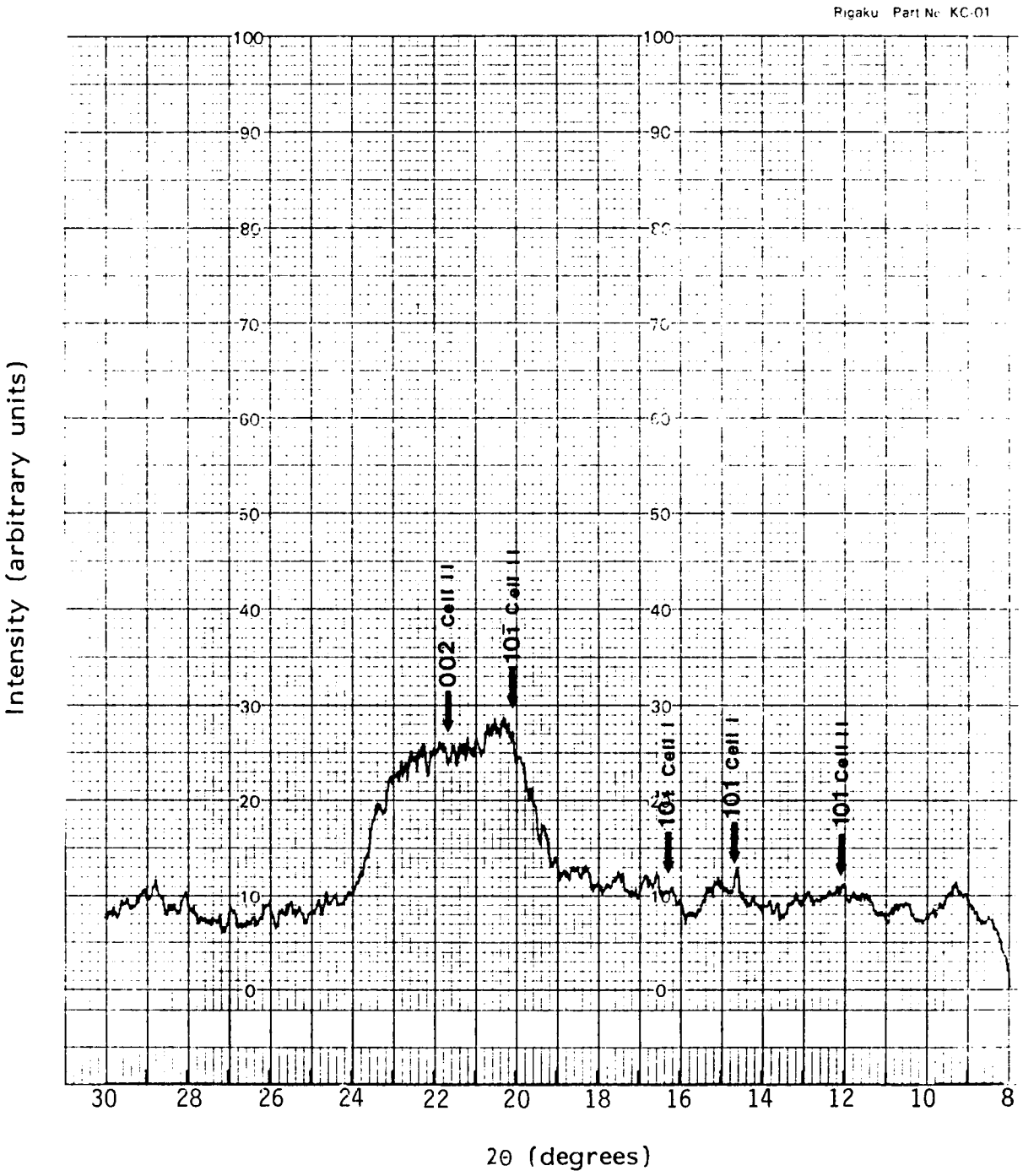


Figure 8. X-ray diffractogram of unexposed mercerized cotton.

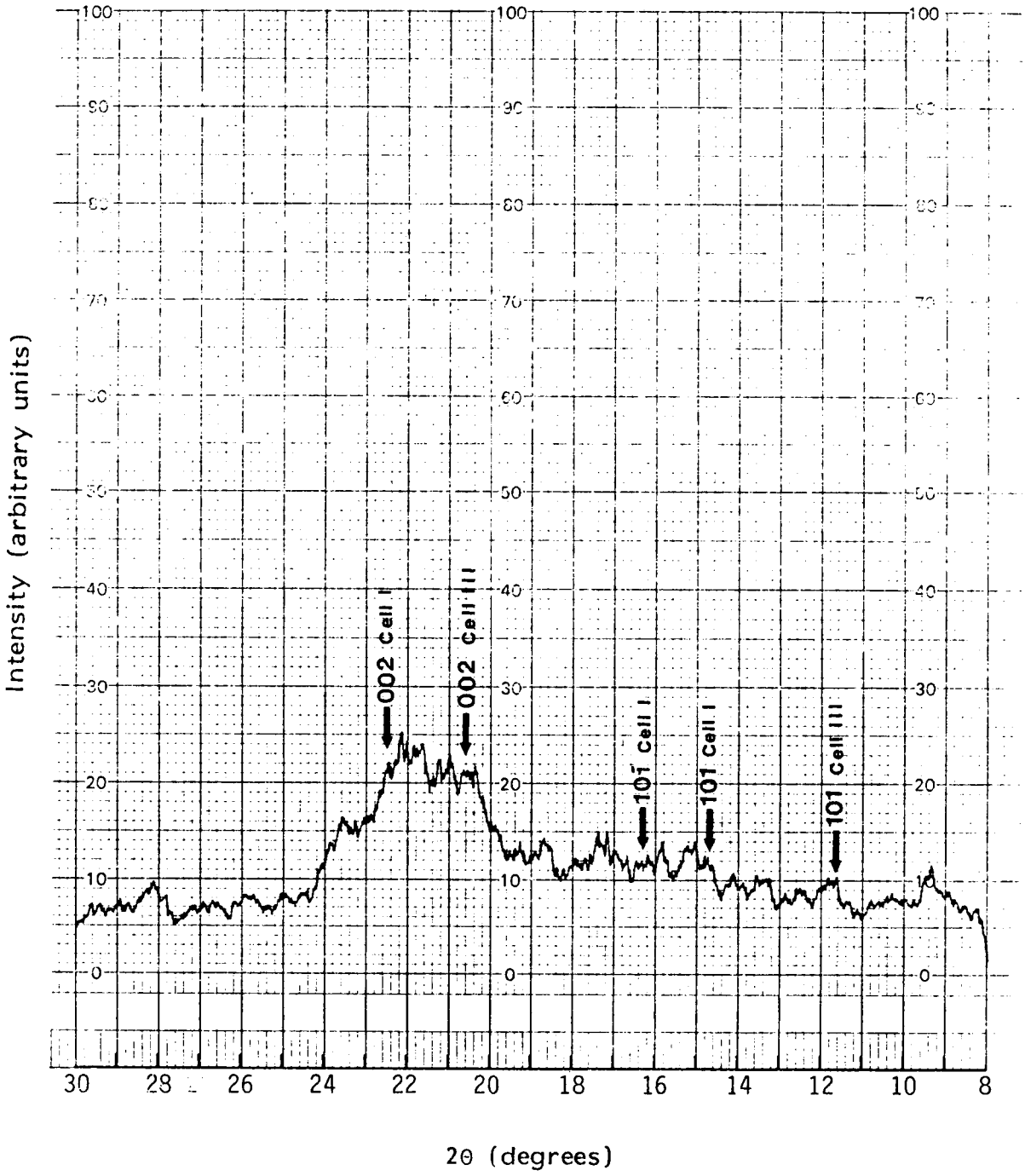


Figure 9. X-ray diffractogram of unexposed NH_3(ℓ) treated cotton.

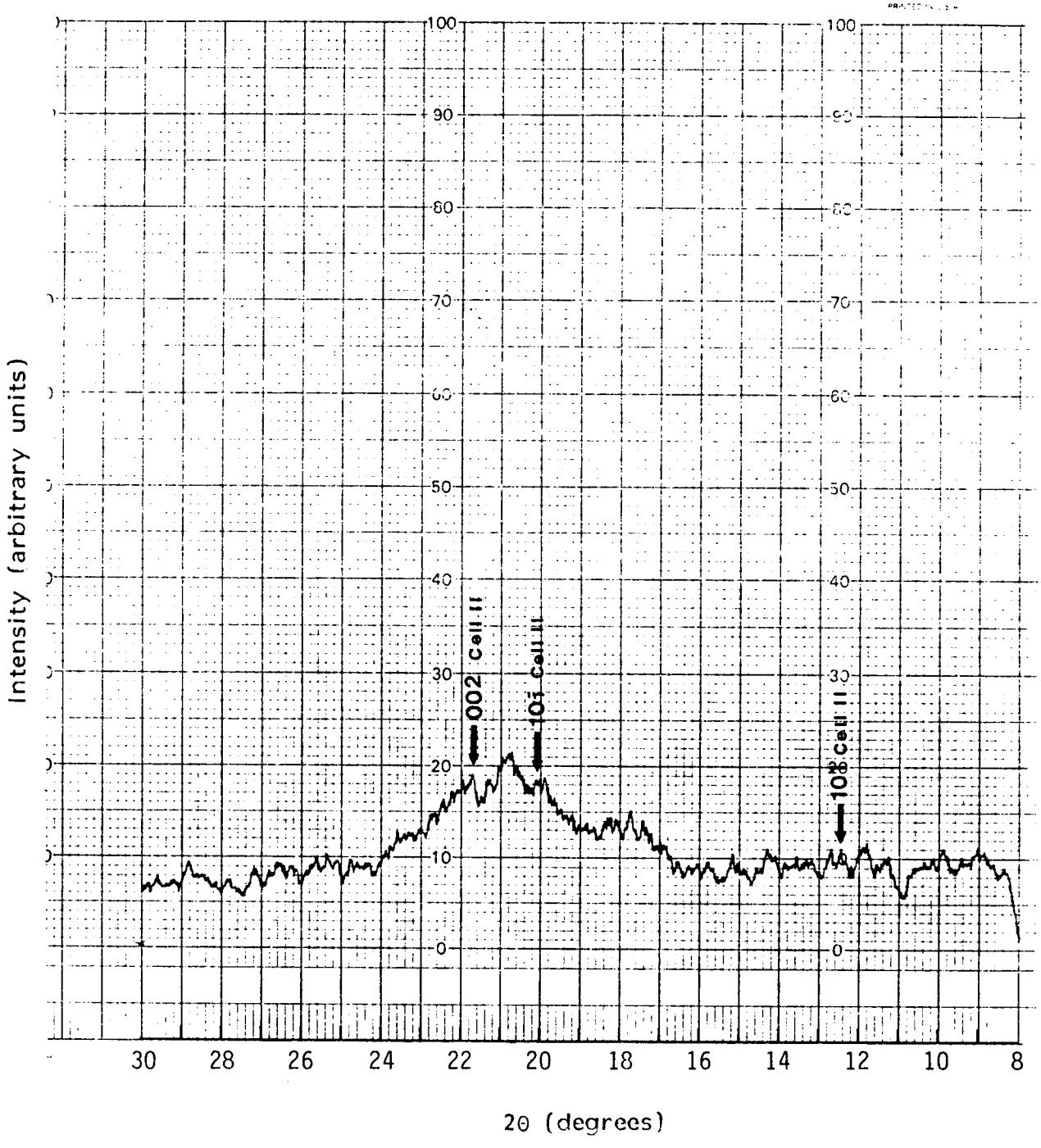


Figure 10. X-ray diffractogram of unexposed viscose rayon.

Diffractogram peak positions are labeled according to Rousselle et al. (54). It can be seen that mercerization resulted in almost complete conversion from Cell I to Cell II. Only a trace of the 101 peak of Cell I remains at $2\theta = 14.7°$, which is in complete agreement with the literature. Treatment with $NH_3(\ell)$ resulted in a mixed lattice of Cell I and Cell III that also agrees with the literature (54). The diffractogram for viscose rayon indicates the presence of only Cell II.

Accessibility increases as crystallinity is reduced. The relationship was demonstrated by Nickerson (70) from his work with formic acid esterification of cellulose. His findings are presented in Table 3. The relationship between crystallinity and accessibility is further illustrated by the improved dyeing characteristics of mercerized cotton. The increased proportion of noncrystalline regions allows for easier penetration of dye molecules. It is reasonable to expect that the reduction in crystallinity and corresponding increase in accessibility would allow for easier penetration of gas molecules into the fiber.

Porosity and Surface Area

Attempts were made to determine the relative fiber porosity and surface area because of the impact of these factors on the ease of diffusion. Porosity measurements were made by Quantichrome Corporation by the mercury porosimetry technique. Surface area and pore radius values are presented in Table 4. The data printouts are contained in Appendix B. The pore radius values are excessively high, given that the average diameter of a cotton fiber is 12-25 μm (72). A likely explanation is that the mercury pressure used (listed in Table 4) was

Table 3. Accessibility and crystallinity in cellulose fibers.*

Fiber	% Accessible	% Noncrystalline	% Crystalline
Native cotton	12.5	16	84
Mercerized cotton	20	28	72
Viscose rayon	39	54	46

Source: R. F. Nickerson, Accessibility of Cellulose by Formic Acid Esterification, Text. Res. J. 1951, 21, 200.

Table 4. Fiber surface area and pore radius determined by mercury porosimetry.

Fiber type	Surface area (m^2/g)	Pore radius (μm)	Max. mercury pressure (pascals)
Extracted cotton	0.4745	35.46	1.68×10^5
Mercerized cotton	0.3468	31.59	1.68×10^5
$NH_3(\ell)$ treated cotton	0.2794	26.48	1.67×10^5
Viscose rayon	0.1658	36.51	1.63×10^5

not sufficiently high to cause penetration into the pores. What is reported as pore radius may actually be the measurement of interfiber channels.

Hexane evaporation from fiber samples was carried out in an alternate attempt to determine fiber porosity. In theory, hexane (a nonwetting liquid on cotton) should evaporate rapidly from the fiber surface and more slowly from the pores. The inflection point of the plotted data (point where the slope of the line clearly begins to change) should indicate the relative porosity of the fiber types studied. Three different hexanes were used to control for the influence of molecular shape on the porosity determination. The data are plotted in Figures 11-13. Readings were made at 10 second intervals during the initial evaporation phase. Relative porosity rankings were determined by examining the midpoint of the turn in the curves.

Using mixed hexanes as the solvent, mercerized cotton was determined to be the most porous fiber followed by extracted cotton, $NH_3(\ell)$ treated cotton, and viscose rayon in descending order. With n-hexane and cyclohexane mercerized cotton was also demonstrated to be the most porous fiber. Viscose rayon was shown to be the second most porous, followed by $NH_3(\ell)$ treated cotton. Extracted cotton was the least porous as determined by the latter two solvents.

Since the isomeric composition of the mixed hexanes is unknown, it is difficult to evaluate the reasonableness of those results. However, the relative rankings obtained using n-hexane and cyclohexane are plausible if hexane evaporated slowly from the

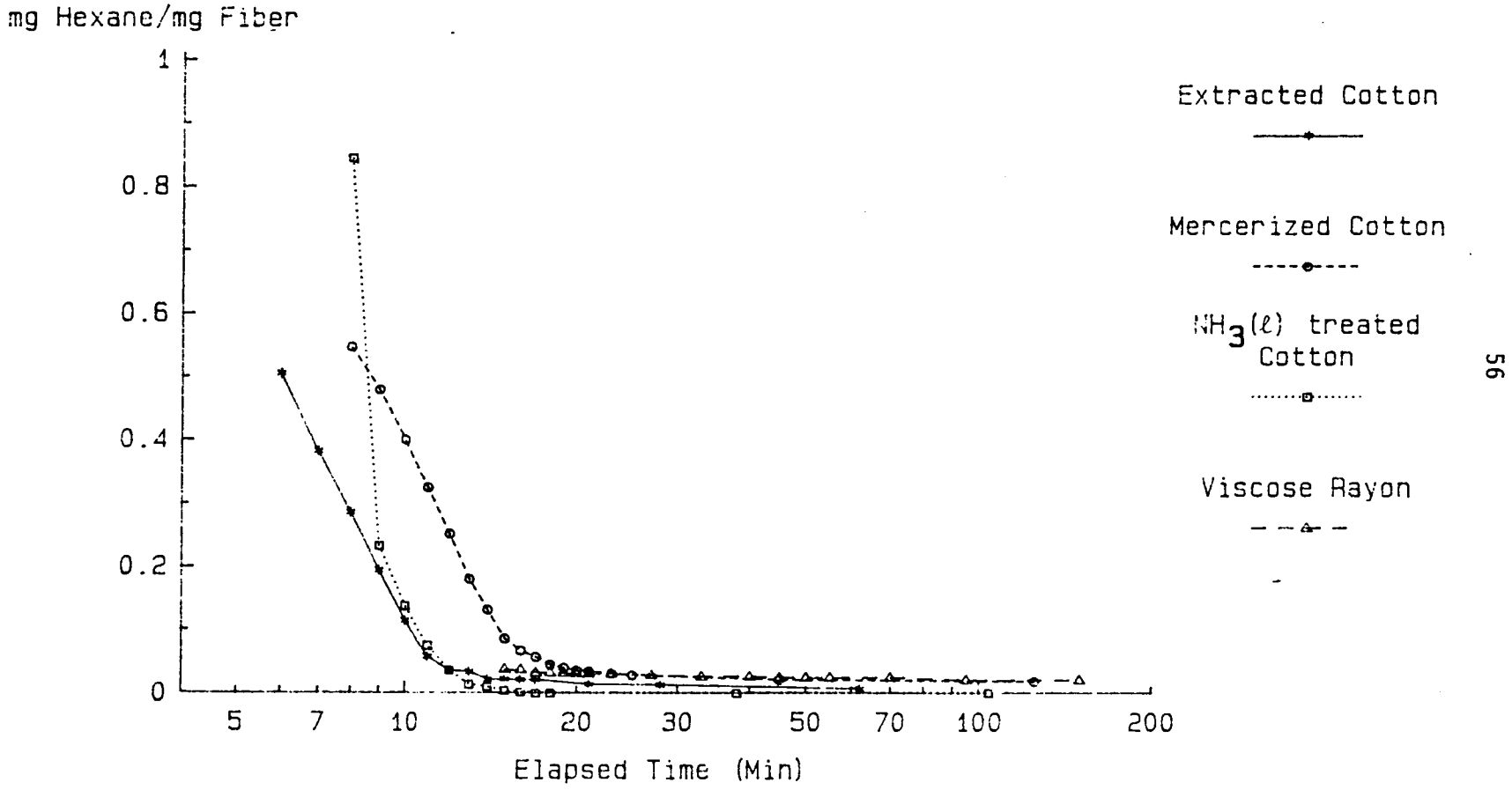


Figure 11. Surface porosity of cellulose fibers by mixed hexanes evaporation.

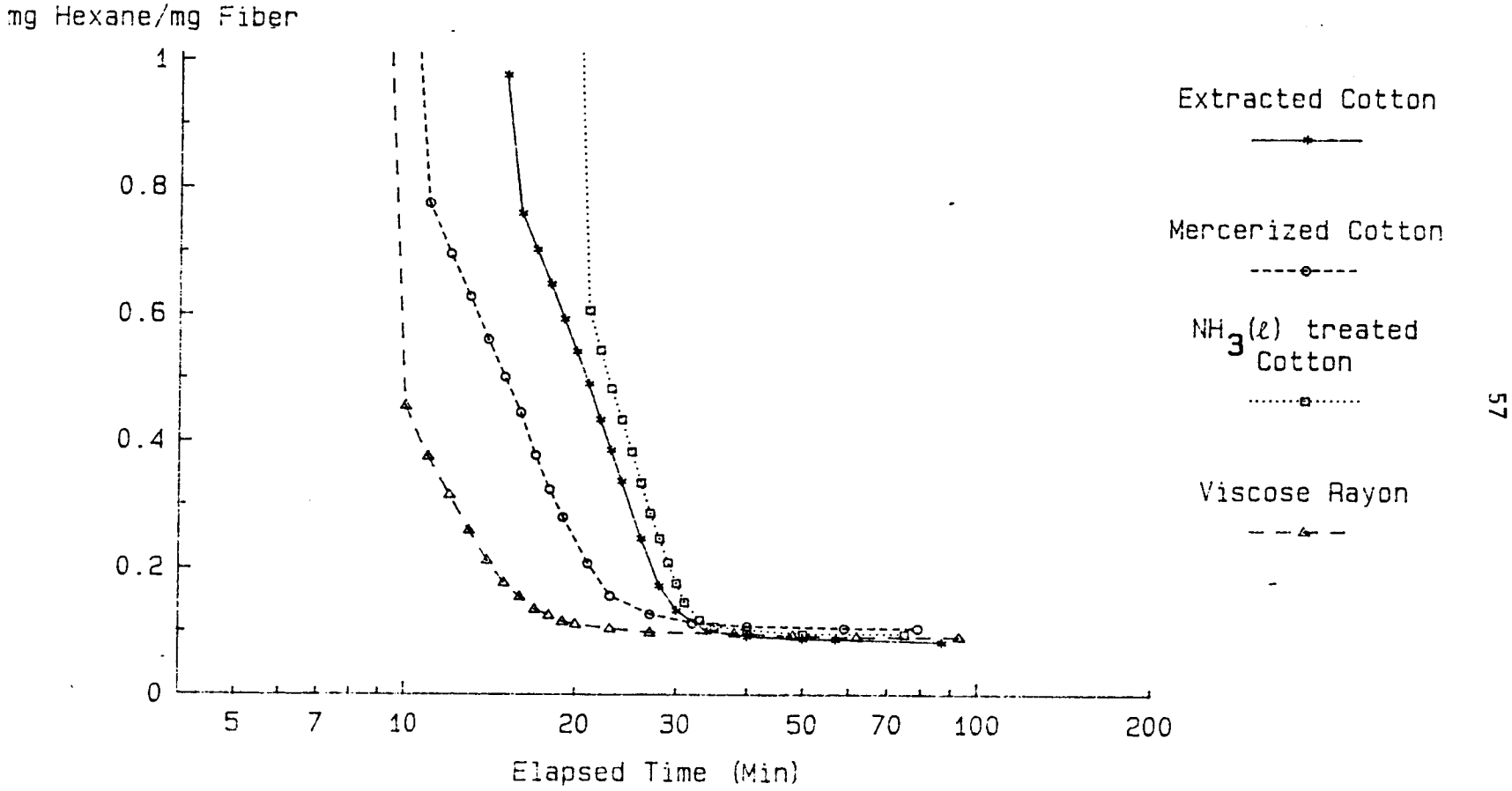


Figure 12. Surface porosity of cellulose fibers by cyclohexane evaporation.

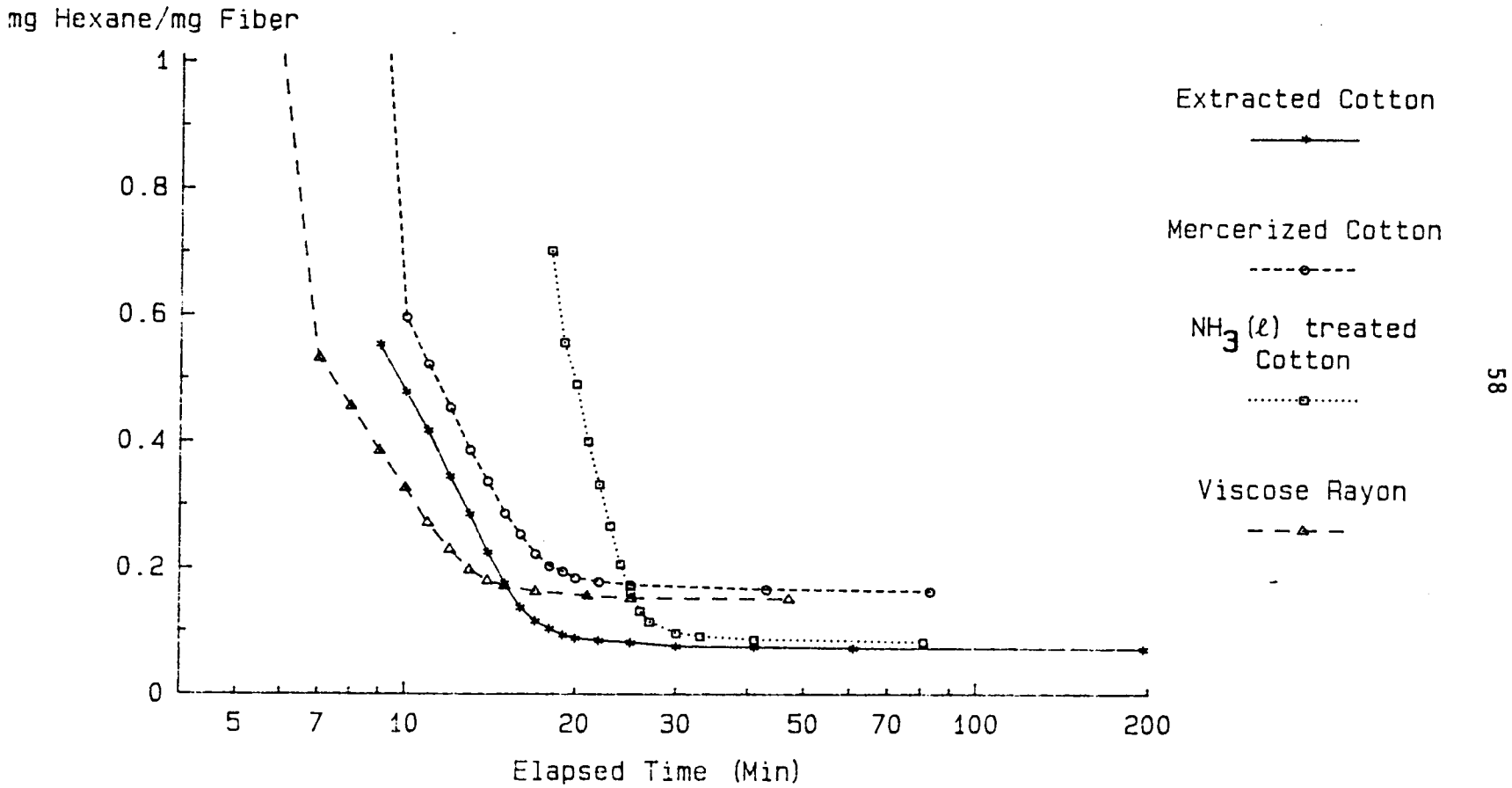


Figure 13. Surface porosity of cellulose fibers by n-hexane evaporation.

striation cavities of the viscose rayon in the same manner that it evaporated from the pores of the cottons. Both mercerized cotton and $NH_3(\ell)$ treated cotton are known to be more accessible than native cotton as given in Table 3. It is reasonable that the hexane would evaporate more slowly from the more accessible modified fibers.

Moisture Regain

Comparative moisture regain values (determined by oven drying versus drying over P_2O_5) are presented in Table 5. Fibers dried over P_2O_5 showed consistently lower values indicating that slightly more moisture was retained by fibers subsequent to drying. The ratio of regain values determined by each method is high, indicating that most of the moisture was successfully removed by the P_2O_5. However, the additional moisture in the P_2O_5 dried fibers must be considered when evaluating the SO_2 sorption results. Table 5 also presents the comparative moisture content values for the same fibers.

Change in Total Fiber Moisture on Exposure to Dry Air

For exposure of conditioned fibers to SO_2, samples, conditioned in flasks to 69 ± 1% relative humidity (RH), exposed to a dry stream of SO_2 followed by a stream of dry air. The dynamic interaction of the gas with conditioned fibers was determined by examining the percent weight loss incurred by fibers throughout the period of exposure. Percent weight lost was plotted against time for each fiber type (Figures 14-17).

Table 5. Percent moisture regain and percent moisture content for cellulose fibers.

Fiber type	Moisture regain			Moisture content		
	Oven Dried (OD)	P_2O_5 Dried (PD)	$\frac{PD}{OD} \times 100$	Oven Dried (OD)	P_2O_5 Dried (PD)	$\frac{PD}{OD} \times 100$
Extracted cotton	7.27	6.53	90	6.78	6.13	90
Mercerized cotton	9.85	8.67	88	8.97	7.98	89
$NH_3(\ell)$ treated cotton	8.66	8.11	94	7.97	7.50	94
Viscose rayon	10.38	10.07	97	9.40	9.15	97

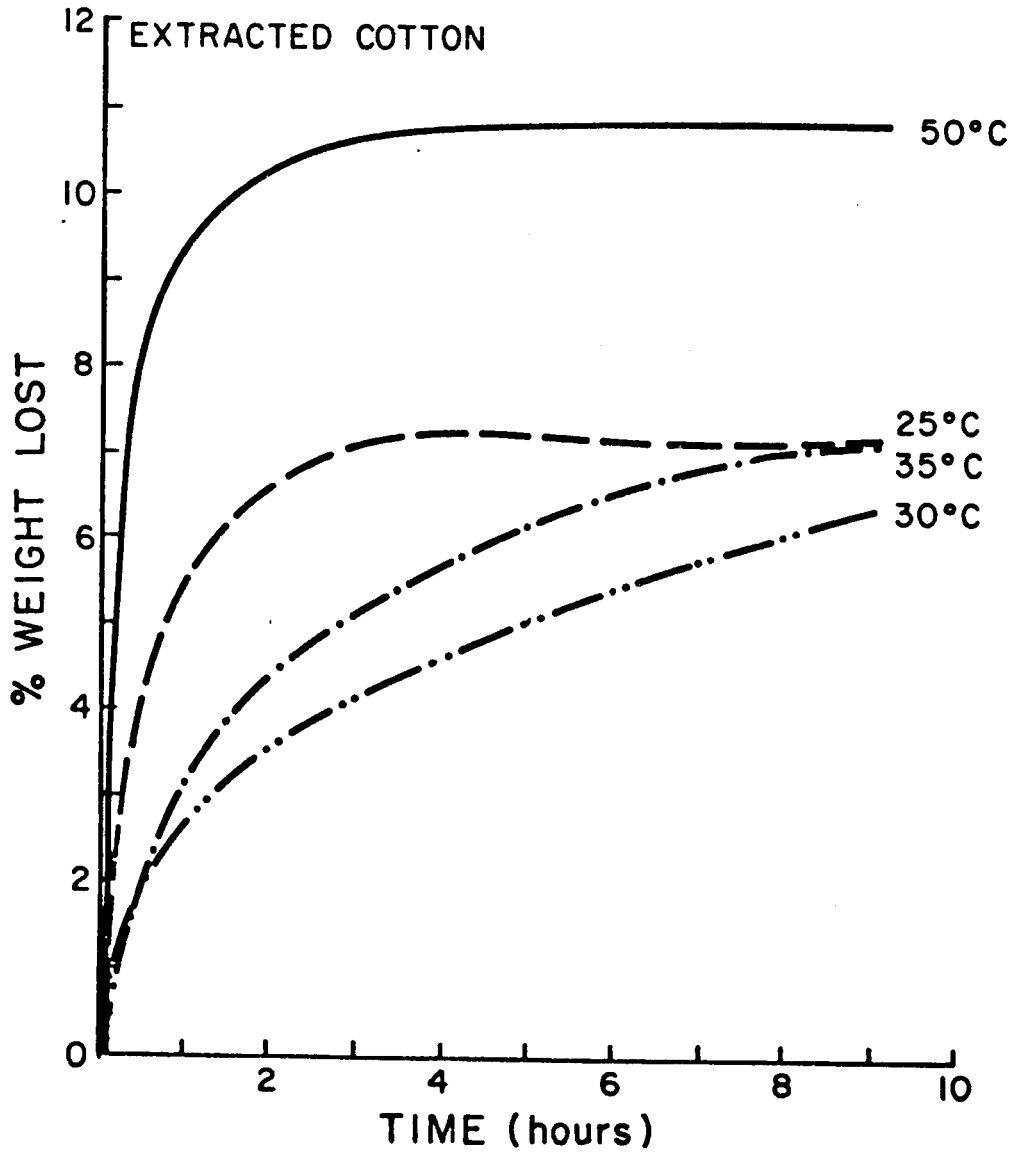


Figure 14. Fiber moisture loss for extracted cotton at four temperatures.

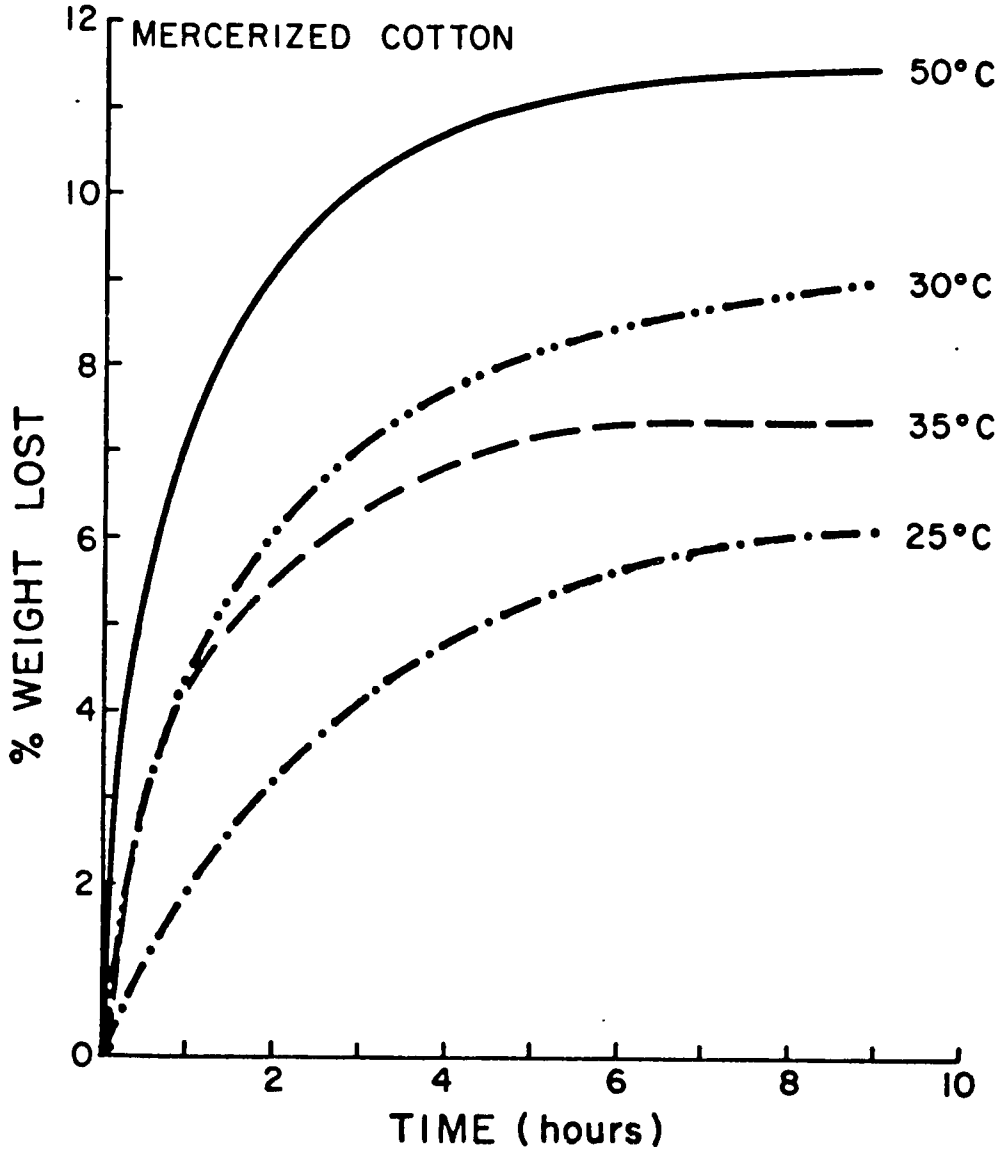


Figure 15. Fiber moisture loss for mercerized cotton at four temperatures.

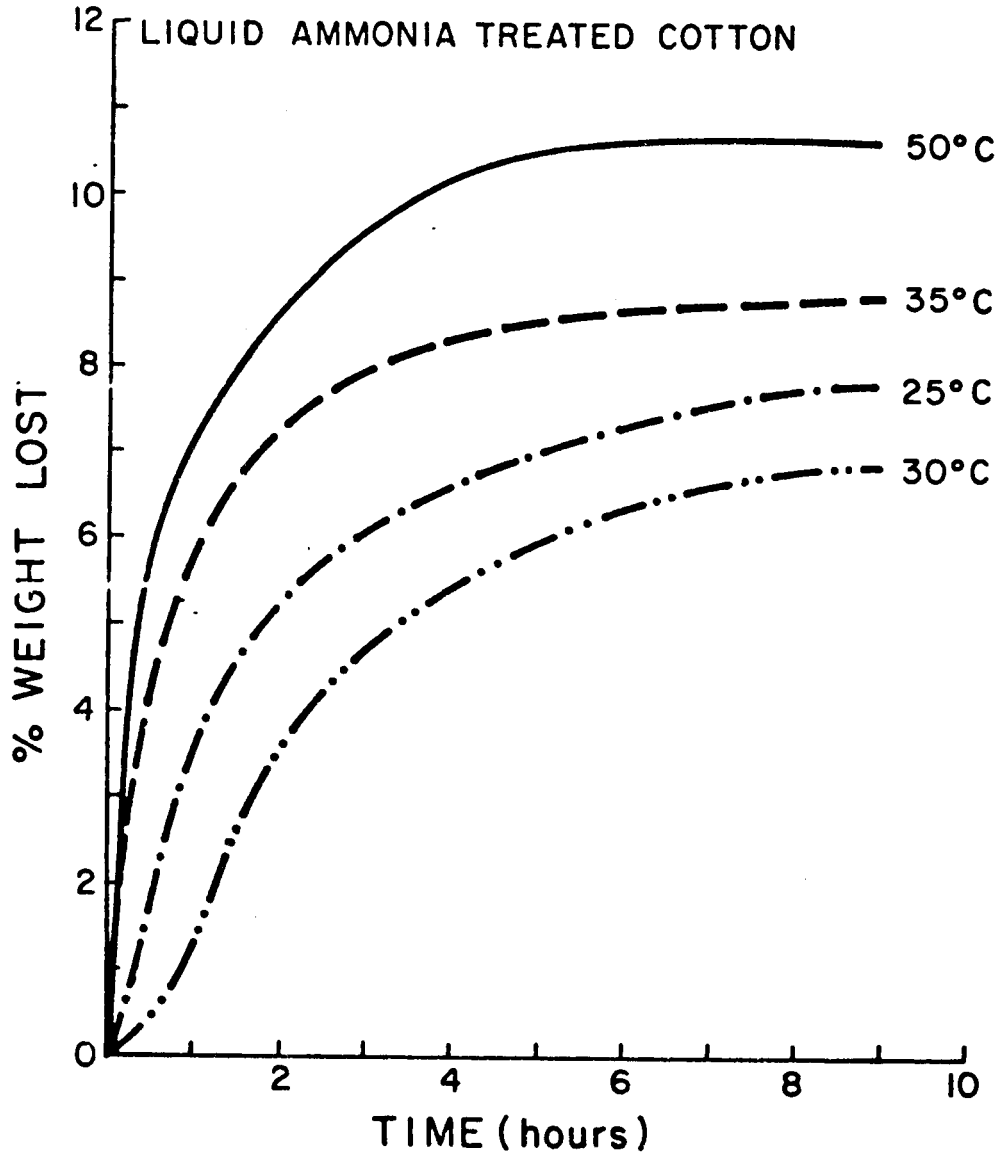


Figure 16. Fiber moisture loss for $NH_3(\ell)$ treated cotton at four temperatures.

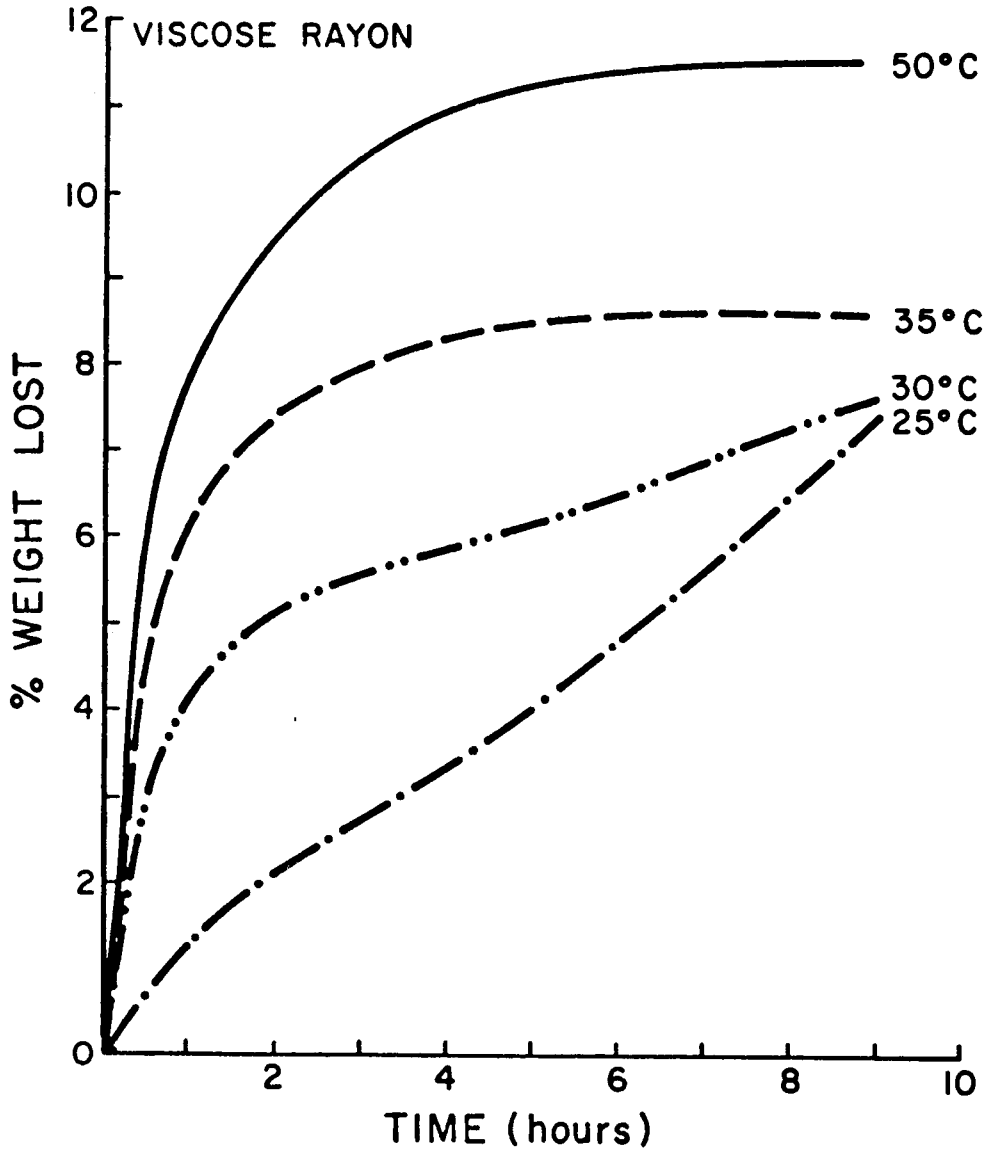


Figure 17. Fiber moisture loss for viscose rayon at four temperatures.

In general, it can be seen that weight loss for fibers run at 50°C was the greatest for all fiber types as would be expected. The elevated temperature would facilitate evaporation of moisture from the fibers and the gas stream would carry the water vapor away.

The temperature differential between 25°, 30°, and 35°C was not sufficient to demonstrate a clear cut temperature dependence for moisture loss. Apparently at those temperatures, increases in the root mean square velocities of the water vapor molecules (calculated at 6.4276×10^4 cm sec^{-1}, 6.4812×10^4 cm sec^{-1}, and 6.5345×10^4 cm sec^{-1}, respectively, for 25°, 30°, and 35°C) are not sufficiently different to produce discrete intervals of moisture loss. The root mean square velocity for water vapor molecules at 50°C was calculated at 6.6916×10^4 cm sec^{-1}, approximately 850 cm sec^{-1} greater than at 35°C.

With only one exception (viscose rayon at 25°C) the curves uniformly show that moisture loss occurs at a steadily decreasing rate. For viscose rayon at 25°C, it is possible that the low temperature in combination with the increased fraction of noncrystalline matter allowed for a more uniform rate of moisture desorption.

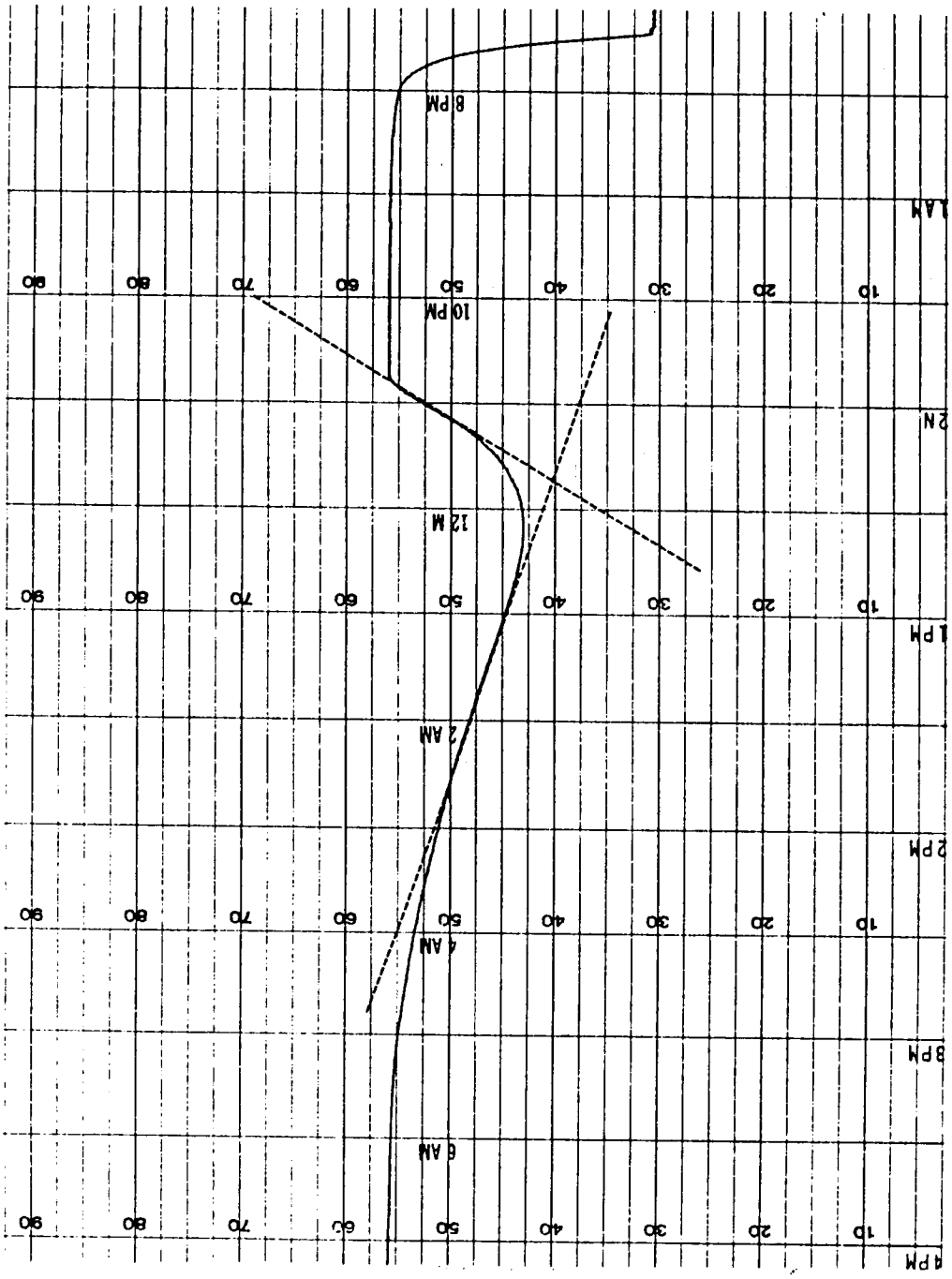
Sorption of Sulfur Dioxide by Dried Fibers

Fibers were exposed to 3 ppm SO_2 at two moisture content levels. Dried fibers were exposed at 25°, 30°, 35°, and 50°C, while fibers conditioned to 69 ± 1% R.H. were exposed at 25°C only.

The initial rate of SO_2 sorption was calculated from the slope of the line recorded when SO_2 concentration within the chamber began to decrease after opening the flasks and exposing the fibers to the 3 ppm gas stream. The secondary rate of sorption was calculated from the slope of the line recorded when the SO_2 concentration within the chamber began to increase. An example of primary and secondary sorption slopes is shown in Figure 18, which shows the chart recorder output for the sorption phase of a blank exposure at 50°C.

Prior to sample exposure, the line (minus exposure flasks) was flushed with dry air to remove residual moisture. Following that procedure, SO_2 was turned on and run through the line until the analyzer read 3 ppm SO_2. In Figure 18, 0 ppm is on the right at line 30.05. Three ppm SO_2 was reaching the analyzer when the chart recording reached line 56.00, moving from right to left. As the concentration of SO_2 within the chamber stabilized at 3 ppm, the closed exposure flasks were attached to the line. At the start of the exposure period the flasks were opened simultaneously. The SO_2 concentration within the chamber was initially reduced for both blank runs and sample runs as the result of dilution of the gas by the dried or conditioned air within the flasks. The slope of the line traced as the SO_2 concentration within the chamber fell was calculated and used to determine the initial rate of SO_2 removal from the system.

The SO_2 concentration within the chamber continued to fall for a period of time depending on the substrate within the flasks. The low point (minimum concentration reaching the analyzer) of the recorder


8 PM
10 PM
12 M
2 AM
4 AM
6 AM
8 PM
10 PM
12 M
2 PM
4 PM
6 PM

tracing was determined and time to that point calculated. The time required to achieve the minimum concentration reaching the analyzer varied with the fiber type and the exposure conditions as will be discussed below.

The fibers sorbed SO_2 at different rates. The secondary rate of sorption was calculated from the slope of the recorder tracing as the concentration of SO_2 within the chamber increased (Figure 18). Fibers that rapidly ceased SO_2 sorption demonstrated a steeper secondary slope.

For the blank run pictured in Figure 18, the SO_2 concentration within the chamber returned to 3 ppm in approximately 17 minutes. During some of the sorption runs involving fibers the SO_2 concentration within the chamber did not return to 3 ppm during the entire exposure period (5 hours); this indicated sustained sorption by the fibers. Blank exposure runs and fiber exposure runs were carried out in an identical fashion.

The initial rates of SO_2 removal are presented in Table 6. It can be seen that the values for the blanks are similar to those for all fiber types. In fact, at 30°C and 35°C, the initial rates of SO_2 removal are greater for the blanks than for any of the fiber types. It is probable that the initial decrease in SO_2 concentration within the chamber is mainly the result of dilution by the air within the exposure flasks. Each exposure flask contained a volume of 500 ml dry air. Because the 2 gram samples of dried cotton or rayon displaced only about 1.3 ml air, it is reasonable that the blank values should be similar to

Table 6. Initial rate of SO_2 removal by the system using dried fibers (ppm/min).[a]

Fiber type	Temperature (°C)			
	25	30	35	50
Blank	1.21	1.45	1.54	1.07
Extracted cotton	1.40[b]	1.24	1.27	1.31
Mercerized cotton	1.25	1.42	1.36	1.26
$NH_3(\ell)$ treated cotton	0.87	1.29	1.27[c]	1.12
Viscose rayon	0.53	1.45	1.54	1.00

[a]All values are the result of one experimental run unless otherwise indicated.

[b]Value is the average of four experimental runs.

[c]Value is the average of three experimental runs.

the values obtained with fibers only if dilution was the primary mechanism for the reduction of SO_2 concentration during this phase.

The time required to reach the minimum SO_2 concentration within the chamber is also indicative of the initial rate of sorption. Materials with little or no sorptive capacity will reach the minimum faster than those materials with greater sorptive capacity. The data are summarized in Table 7 and pictured in Figure 19. In general, the time required to reach the point of minimum concentration reaching the analyzer declined with increasing temperature. The decline was not however, uniform. Extracted cotton and viscose rayon showed similar, steady declines. Mercerized cotton and $NH_3(\ell)$ treated cotton, on the other hand, showed a very steep decline from 25°C to 35°C. The shapes of these curves are quite similar to those for total sorption which will be discussed below. The power regression line demonstrates the trend toward more rapid cessation of SO_2 sorption at higher temperatures despite the high degree of scatter for mercerized cotton and $NH_3(\ell)$ treated cotton.

The secondary rates of sorption are shown in Table 8 and Figure 20. A lower secondary rate indicates a longer sustained sorption of SO_2 by the fibers. A higher secondary rate indicates a steeper slope as the concentration of SO_2 within the chamber approaches 3 ppm and therefore indicates less sorption.

Curves were fit by the least squares technique. Each fiber type shows an increasing secondary sorption rate with increasing temperature; indicating prolonged sorption at lower temperatures.

Table 7. Time to minimum concentration reaching the analyzer for dried fibers (min).[a]

Fiber type	Temperature (°C)			
	25	30	35	50
Blank	3.03	2.60	2.40	2.60
Extracted cotton	3.24[b]	2.81	3.05	2.87
Mercerized cotton	6.50	3.00	3.75	3.50
$NH_3(\ell)$ treated cotton	7.00	3.04	2.77[c]	5.51
Viscose rayon	3.28	2.81	2.81	2.23

[a]All values are the result of one experimental run unless otherwise indicated.

[b]Value is the average of four experimental runs.

[c]Value is the average of three experimental runs.

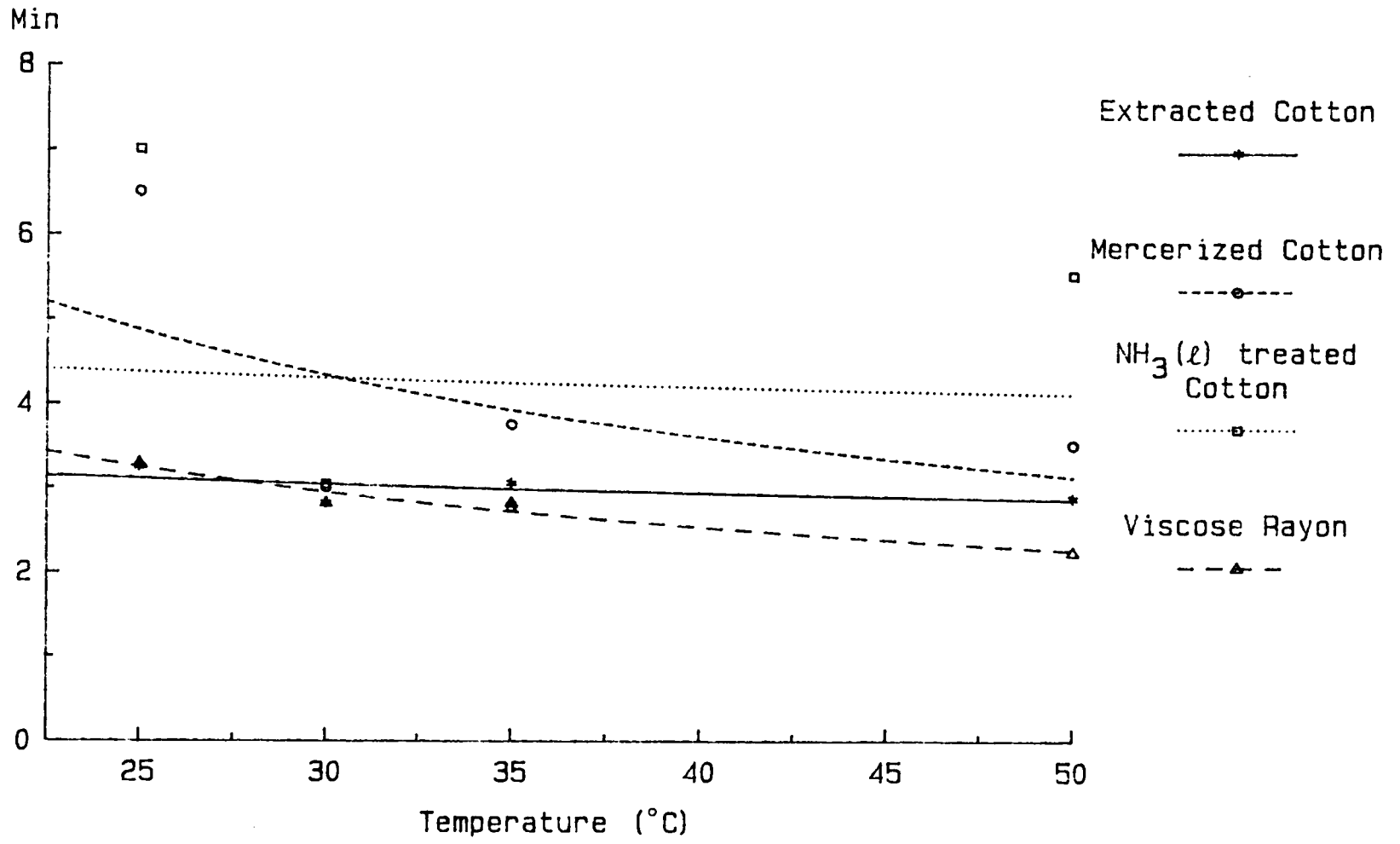


Figure 19. Time to minimum concentration reaching the analyzer.

Table 8. Secondary rate of SO_2 sorption by dried fibers (ppm/min).[a]

Fiber type	Temperature (°C)			
	25	30	35	50
Blank	0.25	0.29	0.25	0.21
Extracted cotton	0.11[b]	0.07	0.11	0.14
Mercerized cotton	0.03	0.06	0.06	0.09
$NH_3(\ell)$ treated cotton	0.05	0.08	0.15[c]	0.12
Viscose rayon	0.22	0.23	0.21	0.29

[a]All values are the result of one experimental run unless otherwise indicated.

[b]Value is the average of four experimental runs.

[c]Value is the average of three experimental runs.

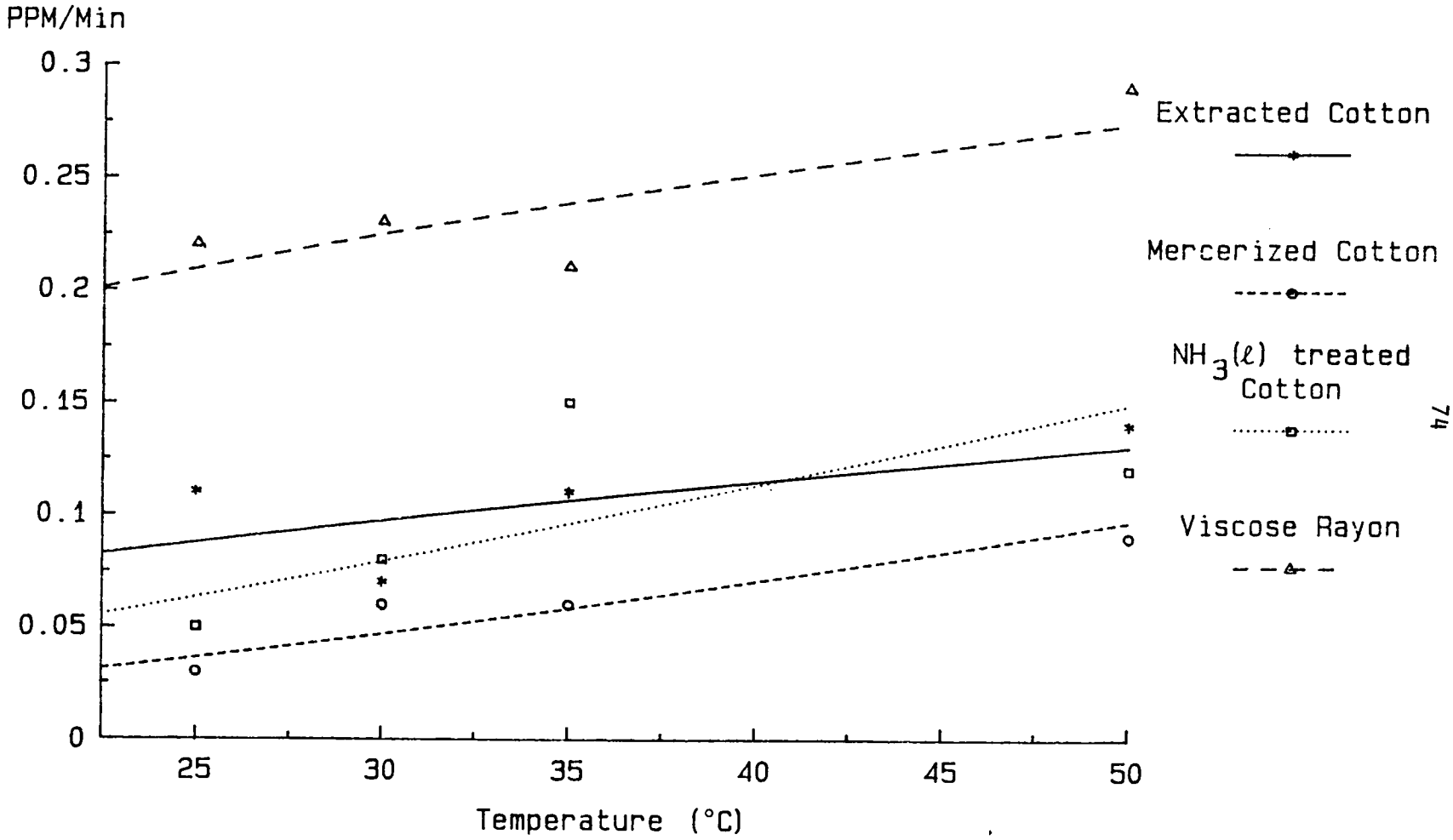


Figure 20. Secondary rate of SO_2 sorption by dried fibers.

With a SO_2 chamber concentration increase of only 0.03 ppm/min mercerized cotton at 25°C exhibited the most prolonged SO_2 sorption by a dried sample. The rate of increase in SO_2 chamber concentration was the greatest for viscose rayon at 50°C. For that run, the rate of SO_2 increase was 0.29 ppm/min. This value was higher than that for the blank run at the same temperature.

For further evaluation of the sorption phase, time constants, defined as the time required for the concentration of SO_2 within the chamber to drop from 90% to 50% of full scale, were computed. These are presented in Table 9. Interestingly, while no clear cut trend emerged, the time constants increased for extracted cotton, viscose rayon, and blanks at 50°C. This increase indicates that at 50°C the concentration of gas within the chamber decreased from 90% to 50% of 3 ppm more slowly than at the lower temperatures. In other words, sorption by the fibers occurred more slowly. This is a reasonable finding since all fibers sorbed less gas at 50°C than at the lower temperatures. For mercerized cotton and $NH_3(\ell)$ treated cotton, the time constants at 50°C did not show a great increase from 30°C and were substantially lower than at 25°C despite the fact that both fiber types sorbed the most gas at 25°C. The high time constant for these two fiber types at 25°C indicates that it took longer for the concentration of gas within the chamber to fall. It can be assumed that the opening up of the polymer network due to increased molecular motion allows the initial sorption to proceed more quickly for these two fiber types.

Table 9. Time constants* for SO_2 sorption for dried fibers (min).[a]

Fiber type	Temperature (°C)			
	25	30	35	50
Blank	1.15	0.83	0.93	1.73
Extracted cotton	1.02[b]	1.20	1.05	1.78
Mercerized cotton	1.59	0.95	0.87	1.05
$NH_3(\ell)$ treated cotton	1.59	0.83	1.24[c]	1.36
Viscose rayon	1.13	0.95	1.09	1.70

*90%-50% full scale.

[a]All values are the result of one experimental run unless otherwise indicated.

[b]Value is the average of four experimental runs.

[c]Value is the average of three experimental runs.

Total SO_2 sorbed by the fibers was calculated in terms of weight of SO_2 as a function of fiber weight (μg SO_2/g fiber) and is shown in Table 10. The value was determined by first calculating the normalized percent SO_2 sorbed. A planimeter was used to calculate the area over the sorption curve. This area minus the blank area was compared to the theoretical area had 100% of the gas been sorbed to calculate the percent SO_2 sorbed. By multiplying the percent gas sorbed by the total μg SO_2 introduced into the chamber during the five hour exposure run and dividing by the sample weight, it was possible to determine the μg SO_2 sorbed per gram of fiber. The data are plotted in Figure 21. Each fiber type shows a clearly decreasing trend in SO_2 sorption with increasing temperature. The maximum sorption was exhibited by mercerized cotton at 25°C. It sorbed 26.28 μg SO_2 per gram of fiber. The minimum SO_2 sorption was exhibited by viscose rayon at 50°C. In the experimental run that sample sorbed less SO_2 than could be accounted for by simple dilution as measured in the blank run. Overall, mercerized cotton demonstrated the highest capacity for SO_2 sorption while viscose rayon demonstrated the least capacity.

Two phenomena occur at higher temperatures making it reasonable to expect such a trend. First, at higher temperatures there is an increase in polymer segmental mobility. The polymer structure opens up as chain motion increases, causing accelerated diffusion of SO_2 both into and out of the fiber. Additionally, the energy of the molecules increases. Their more rapid movement inhibits the formation of strong attractions with the fiber molecules.

Table 10. SO_2 sorption by dried fibers (μg SO_2/g fiber).[a]

Fiber type	Temperature (°C)			
	25	30	35	50
Extracted cotton	9.23[b]	8.56	11.85	7.05
Mercerized cotton	26.28	16.19	15.15	13.29
$NH_3(\ell)$ treated cotton	18.89	10.49	5.16[c]	1.10
Viscose rayon	3.06	0.51	0.53	*

*Meaningful value not obtained.

[a]All values are the result of one experimental run unless otherwise indicated.

[b]Value is the average of four experimental runs.

[c]Value is the average of three experimental runs.

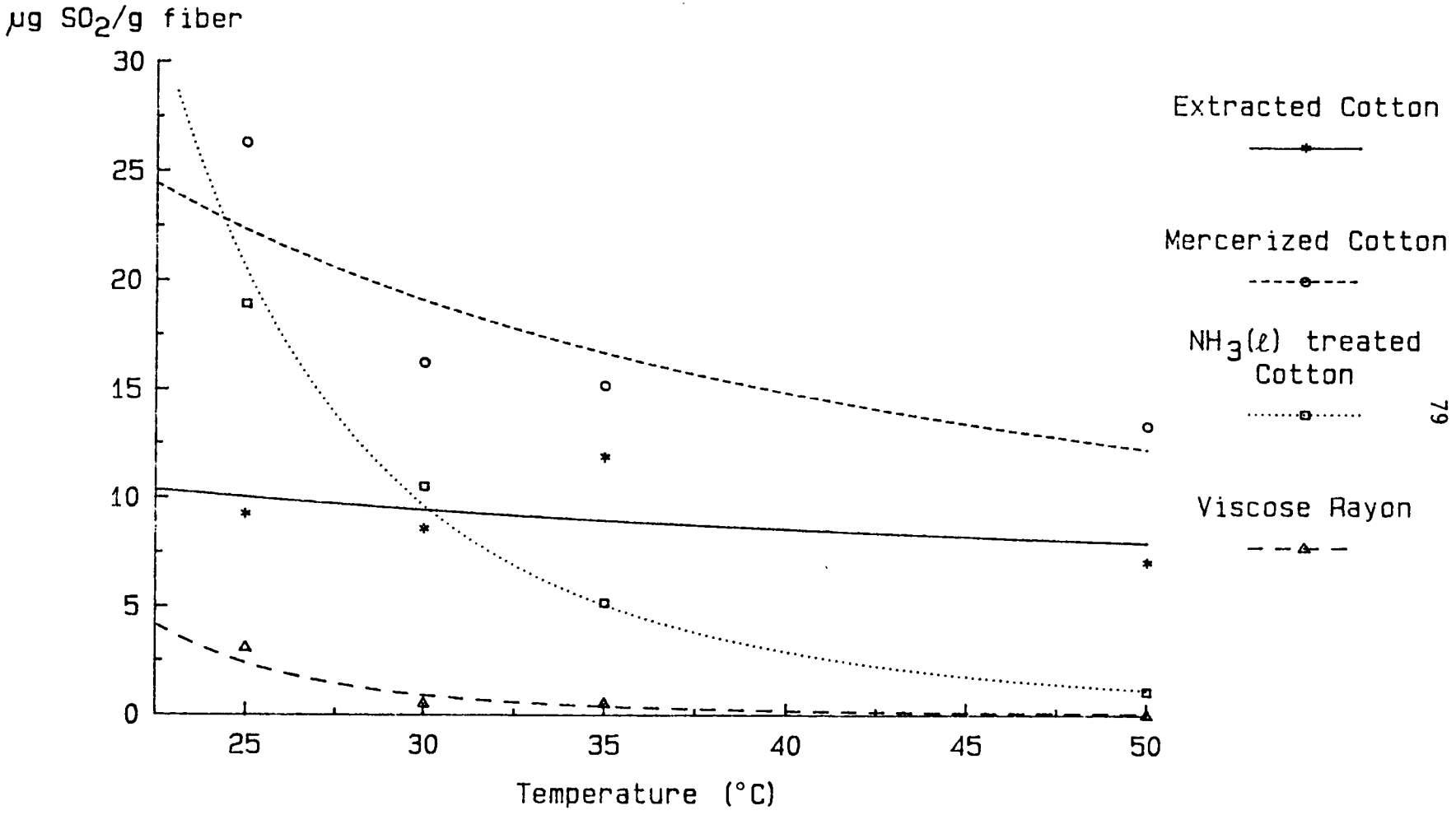


Figure 21. SO_2 sorption by dried fibers at four temperture levels.

As the SO_2 enters the exposure flasks, some of it diffuses to the fiber surface. As the exposure temperature is increased, the root mean square velocity of the SO_2 molecules increases. For this study, the values were calculated as 3.4066×10^4 cm sec^{-1} at 25°C, 3.435×10^4 cm sec^{-1} at 30°C, 3.4633×10^4 cm sec^{-1} at 35°C, and 3.5466×10^4 cm sec^{-1} at 50°C. Thus, the gas molecules diffuse slightly more quickly to the surface of the fibers at higher temperatures.

For sorption to occur, gas molecules must be sorbed at the surface and penetrate into the bulk of the fiber. Just as some fiber surfaces resist penetration by dye molecules, it is reasonable to assume that some fiber surfaces resist penetration by gas molecules. In this study rayon, with its more highly oriented and finer textured skin, may well have provided a barrier to the penetration of SO_2.

Fiber porosity plays a great role in sorption at the fiber surface. From the hexane evaporation data, mercerized cotton would seem to be the most porous fiber. This is consistent with the fact that mercerized cotton sorbed the most SO_2 at all temperatures.

Following sorption at the fiber surface, the gas is sorbed into the fiber. At this point it can be surmised that fiber morphology takes over as the controlling factor in the magnitude of the sorption observed. The schematic representation of the cotton fiber (Figure 1, p. 26) illustrates the fibrillar layers characteristic to cotton. Such an internal structure would conceivably provide more internal voids than the simple skin/core internal structure of rayon. This supposition is

supported by the sorption data. The three cottons sorbed more SO_2 at all temperature levels than the rayon did.

Mercerized cotton, $NH_3(\ell)$ treated cotton, and viscose rayon are all known to be substantially less crystalline than native cotton. As discussed previously, the reduction in crystallinity is accompanied by an increase in accessibility. The increased accessibility provides more accessible sorption sites for SO_2.

Qualitative examination of the x-ray diffraction data in Figures 7-10 (pp. 49-52) shows mercerized cotton to have the broadest diffraction peak and derivatively the lowest degree of order. The fact that mercerized cotton consistently sorbed the most SO_2 implies that lowering the degree of order within a fiber opens the internal structure making adsorption sites more available to the gas. If this is correct, powdered cellulose would exhibit an increased capacity for SO_2 sorption.

Liquid ammonia treated cotton is also less crystalline than native cotton. At 25°C and 30°C, $NH_3(\ell)$ treated cotton sorbed more SO_2 than native cotton, while at 35°C and 50°C it sorbed less. Diffractograms of $NH_3(\ell)$ treated cotton exposed at 25°C and 50°C (Figures 22-23) reveal an undetermined structural shift at $2\theta = 21.25°$ which may account for the steep decline in SO_2 sorptive capacity with increasing temperature. A more exhaustive examination of the x-ray data is called for in order to explain adequately this observation.

Viscose rayon was found to sorb far less SO_2 than native cotton despite the fact that it is more accessible. This finding is in complete

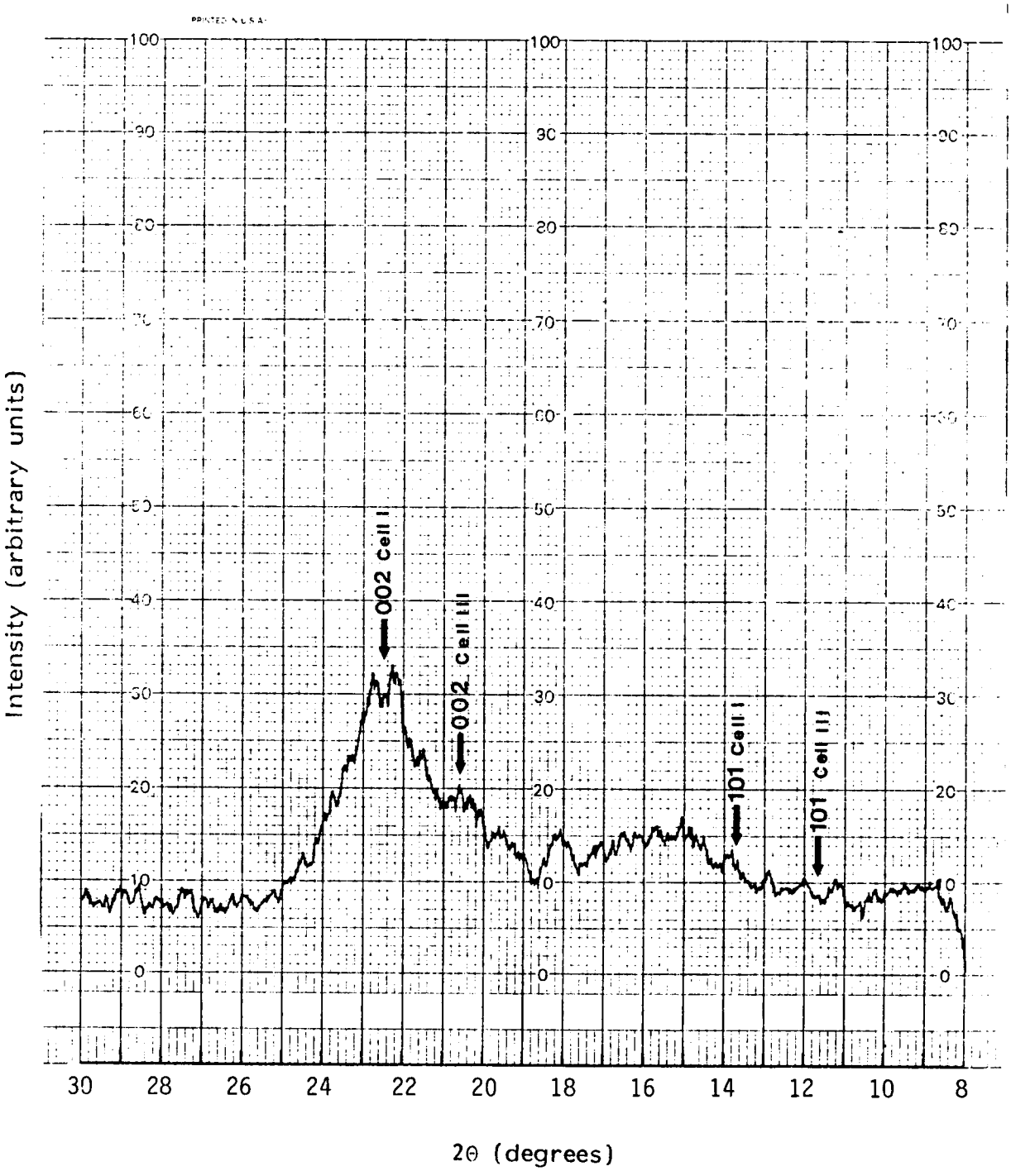


Figure 22. Diffractogram of $NH_3(\ell)$ treated cotton exposed to SO_2 at 25°C.

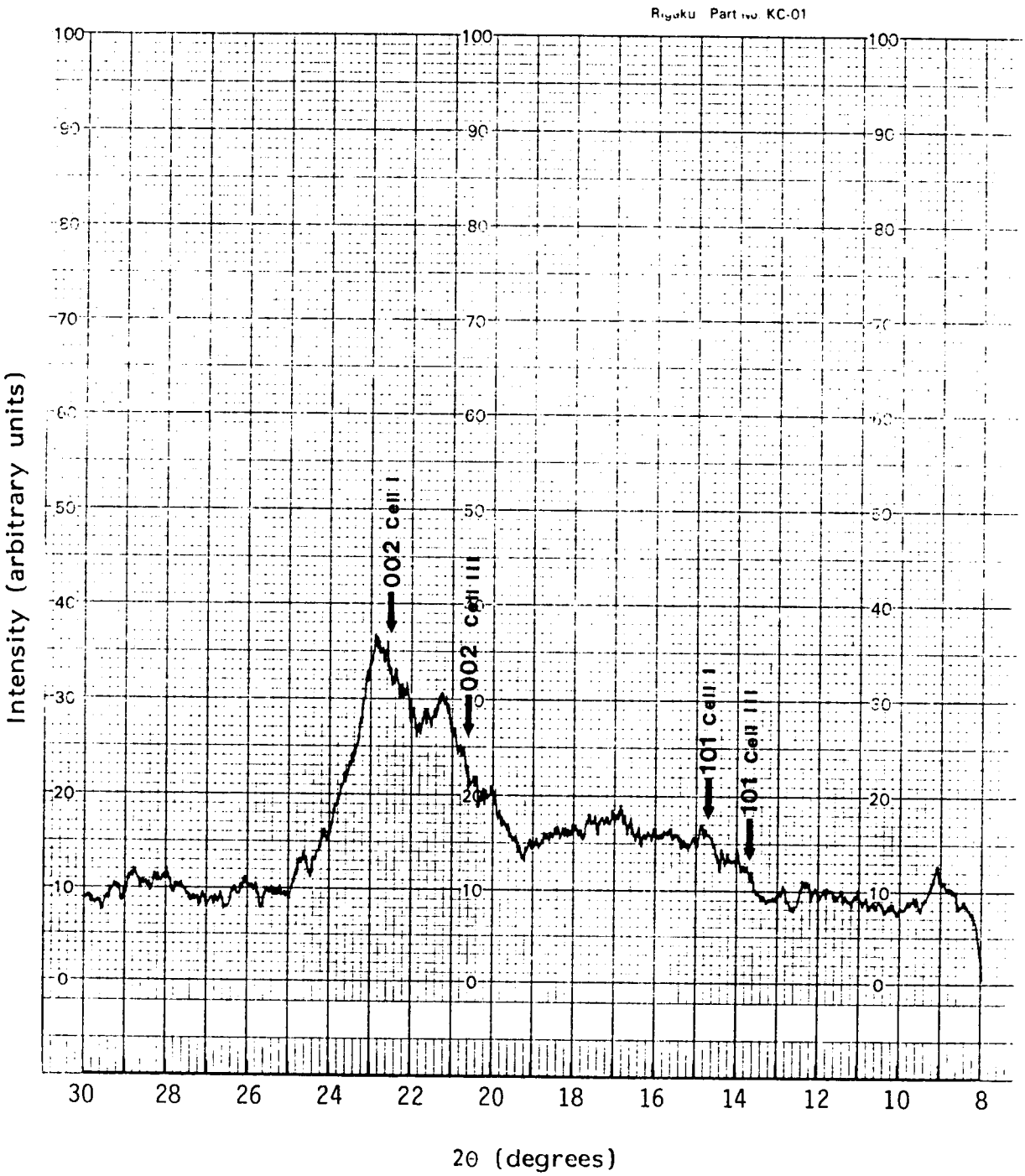


Figure 23. Diffractogram of $NH_3(\ell)$ treated cotton exposed to SO_2 at 50°C.

agreement with Gregory's (9) results. He found the initial rates of SO_2 sorption for cotton and viscose rayon to be comparable. However, rayon became saturated more quickly than cotton and exhibited less total sorption. The rayon skin/core effect may play an important role in this phenomenon. As described previously the skin is finer textured and more oriented than the core. It is possible that the skin limits diffusion of SO_2 into the bulk of the fiber.

Desorption of Sulfur Dioxide by Dried Fibers

Desorption data were evaluated in a similar manner to sorption data. Initial and secondary rates of desorption, calculated from the chart recordings, are shown in Figure 24.

Proceeding from right to left (on the chart shown in Figure 24), SO_2 concentration in the chamber decreases steadily when, following the exposure period, SO_2 is turned off and dry air is turned on. Flushing of the fibers with dry air continued for four hours during which time the concentration of SO_2 within the chamber approached 0 ppm.

The initial rate of desorption was calculated from the slope of the line tangent to the recorder tracing as the SO_2 concentration began to decrease. The secondary rate of desorption was calculated from the slope of the arbitrarily placed tangent to the final linear portion of the recorder tracing shown in Figure 24.

The initial rates of desorption are presented in Table 11. Curves were fit by the least squares technique. The data plots, shown in

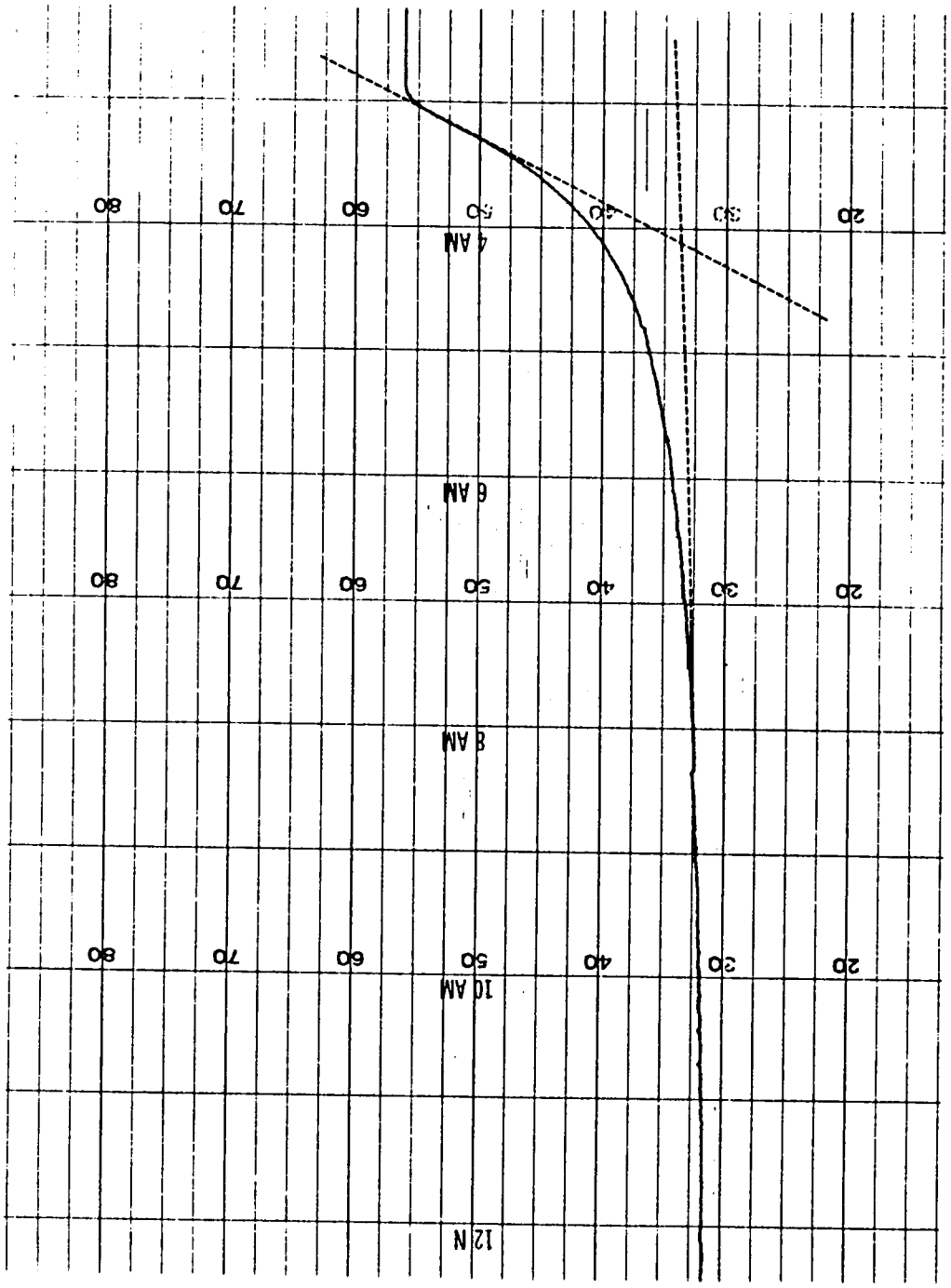


Figure 24. Chart recorder output showing initial and secondary desorption slopes.

Table 11. Initial rates of SO_2 desorption by dried fibers (ppm/min).[a]

Fiber type	Temperature (°C)			
	25	30	35	50
Extracted cotton	0.15[b]	0.14	0.17	0.20
Mercerized cotton	0.11	0.12	0.14	0.16
$NH_3(\ell)$ treated cotton	0.15	0.15	0.15[c]	0.18
Viscose rayon	0.17	0.13	0.15	0.21

[a]All values are the result of one experimental run unless otherwise indicated.

[b]Value is the average of four experimental runs.

[c]Value is the average of three experimental runs.

Figure 25, have very similar slopes with high correlation coefficients. There is virtually no difference in the initial rates of desorption for the four fiber types. This finding is somewhat surprising because the amounts of SO_2 sorbed varied greatly. It is probable that just as with the initial sorption rate, dilution is the primary factor. In the case of desorption, dilution of the SO_2 concentration within the chamber occurs by the introduction of dry air following the completion of the exposure period.

It should be noted that the rate of desorption increases with increasing temperature for every fiber type. This fact lends further support to the idea that increased molecular motion promotes greater diffusion into, and more importantly out of, the fiber bulk.

Secondary rates of desorption are tabulated in Table 12. It is difficult to infer a great deal from the plots of these data (Figure 26) because so little of the SO_2 remained on the fibers at the point of measurement. Additionally, instrumental sensitivity was not sufficient to detect accurately such small amounts of SO_2 in the gas stream.

A complicating factor in the analysis of the desorption phase relates to the dynamic nature of the sorption/desorption process. Because SO_2 was diffusing into and out of the fiber throughout the sorption phase, desorption was presumably occurring as well. Such desorption is impossible to quantify by the techniques used in the present study. Post exposure analysis (SEM, x-ray spectroscopy, ESCA, FTIR and total sulfur content) was utilized to determine whether the desorption rates were similar because some fiber types were holding

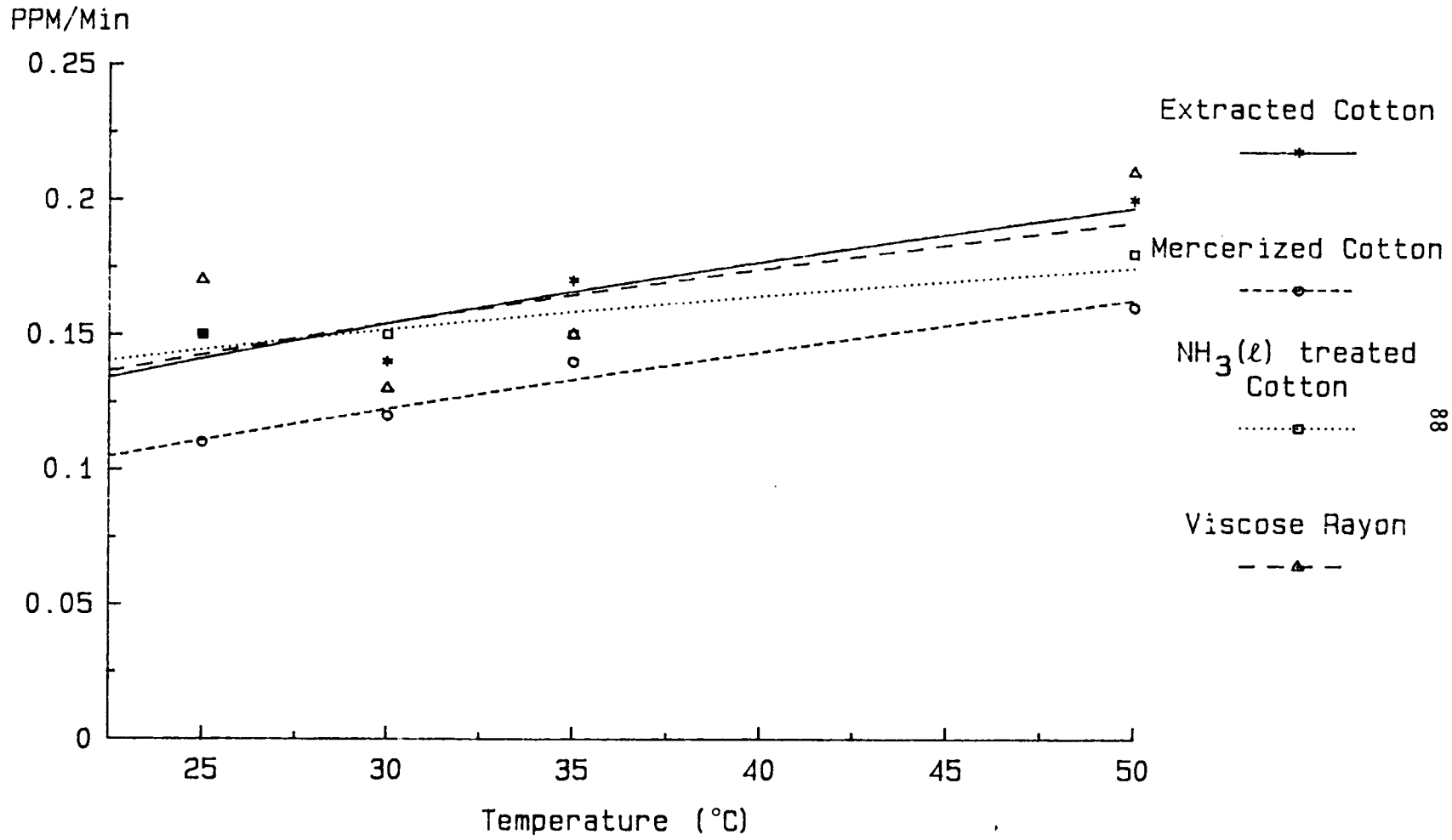


Figure 25. Initial rates of desorption.

Table 12. Secondary rates of desorption by dried fibers (ppm/min).[a]

Fiber type	Temperature (°C)			
	25	30	35	50
Extracted cotton	0.006[b]	0.003	0.001	0.001
Mercerized cotton	0.003	0.002	0.002	0.003
$NH_3(\ell)$ treated cotton	0.008	0.006	0.003[c]	0.004
Viscose rayon	0.006	0.001	0.004	0.004

[a]All values are the result of one experimental run unless otherwise indicated.

[b]Value is the average of four experimental runs.

[c]Value is the average of three experimental runs.

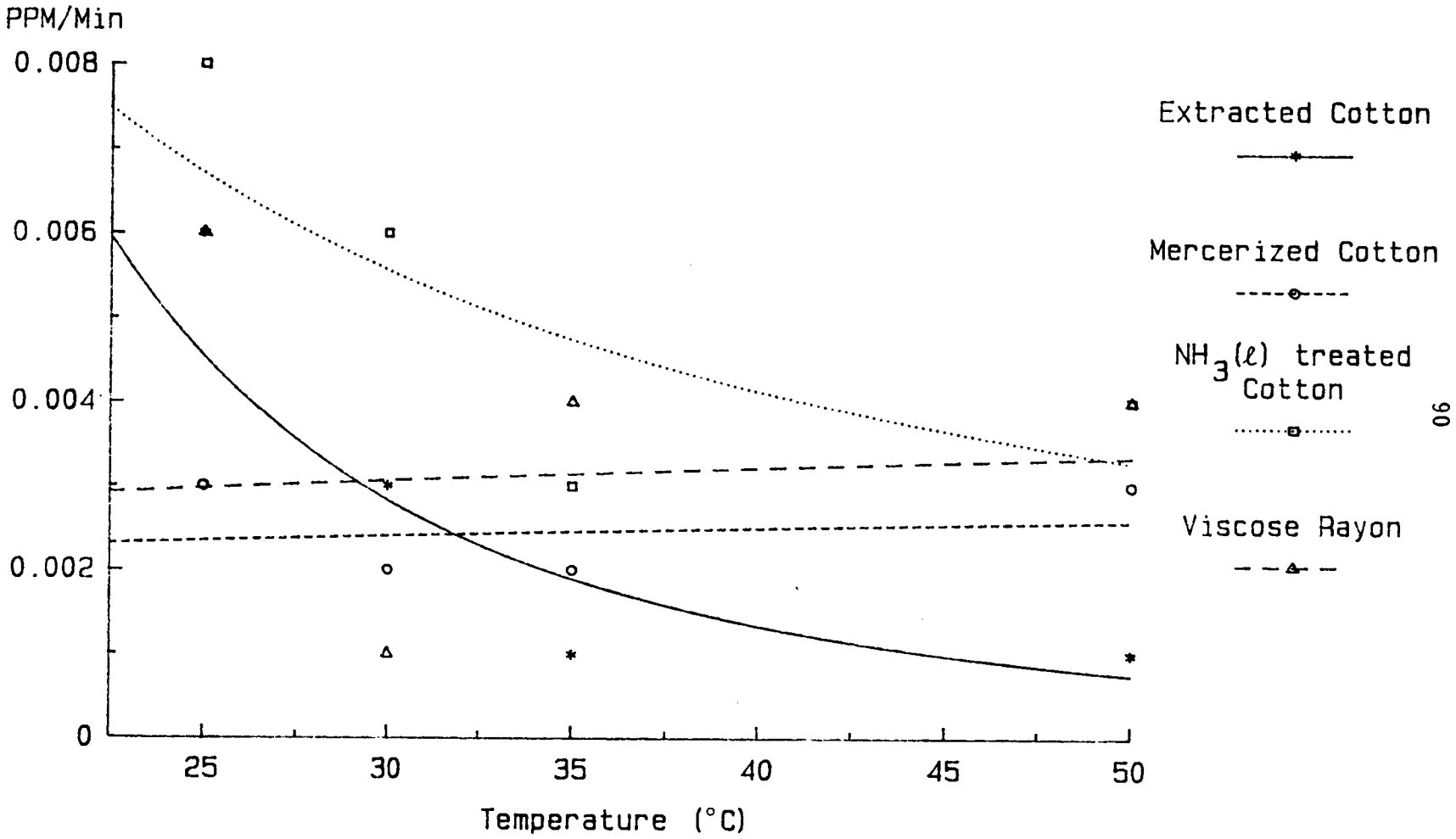


Figure 26. Secondary desorption rates.

SO_2 or because each fiber type was losing all of the SO_2 sorbed at the same rate.

Comparison of Sorption/Desorption by Conditioned and Dried Fibers

To evaluate the relative contribution of increased fiber moisture to the process of SO_2 sorption, fiber samples were conditioned to 69 ± 1% R.H. and exposed to 3 ppm SO_2 at 25°C. The results were compared with those of dried fibers also exposed at 25°C. The initial rates of SO_2 removal from the gas stream, shown in Table 13 and Figure 27, were higher for conditioned fibers of all types except extracted cotton. This fact does not preclude the previously discussed likelihood that dilution is the initial removal mechanism. Both the air (approximately 500 ml) and the fibers within the flasks were conditioned. For conditioned runs it is quite likely that the SO_2 initially interacts with the moisture in the conditioned air.

Secondary sorption rates for conditioned fibers showed a dramatic difference from the secondary sorption rates of the dried fibers as shown in Table 14 and Figure 28. The SO_2 concentration increase within the exposure chamber was far less for conditioned fibers, indicating that they continued to sorb SO_2 for a longer period of time.

The time required to reach the minimum SO_2 concentration within the chamber (Table 15) further illustrates the sustained sorption exhibited by the conditioned fibers. For each fiber type, it required a longer period of time for conditioned fibers to achieve the minimum

Table 13. Initial rates of SO_2[a] removal by conditioned vs. dried fibers at 25°C (ppm/min).

Fiber type	Conditioned	Dried
Extracted cotton	1.39[b]	1.40[c]
Mercerized cotton	1.76	1.26
$NH_3(\ell)$ treated cotton	1.58	0.87
Viscose rayon	1.54	0.53

[a]All values are the result of one experimental run unless otherwise indicated.

[b]Value is the average of two experimental runs.

[c]Value is the average of four experimental runs.

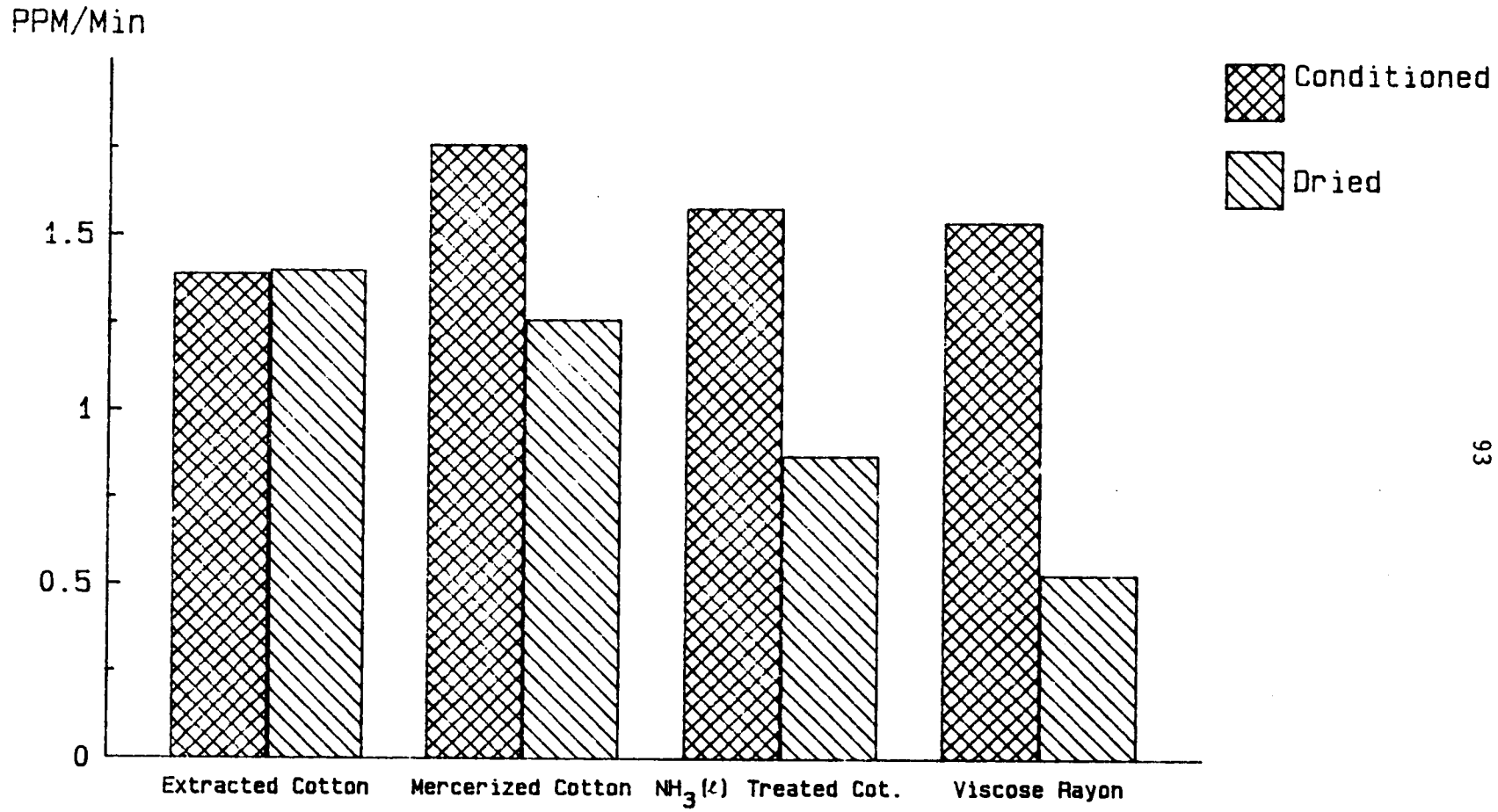


Figure 27. Initial rates of SO_2 removal by conditioned vs. dried fibers at 25°C.

Table 14. Secondary rates of SO_2 sorption by conditioned vs. dried fibers at 25°C (ppm/min).[a]

Fiber type	Conditioned	Dried
Extracted cotton	0.010[b]	0.110[c]
Mercerized cotton	0.001	0.027
$NH_3(\ell)$ treated cotton	0.008	0.046
Viscose rayon	0.038	0.222

[a]All values are the result of one experimental run unless otherwise indicated.

[b]Value is the average of two experimental runs.

[c]Value is the average of four experimental runs.

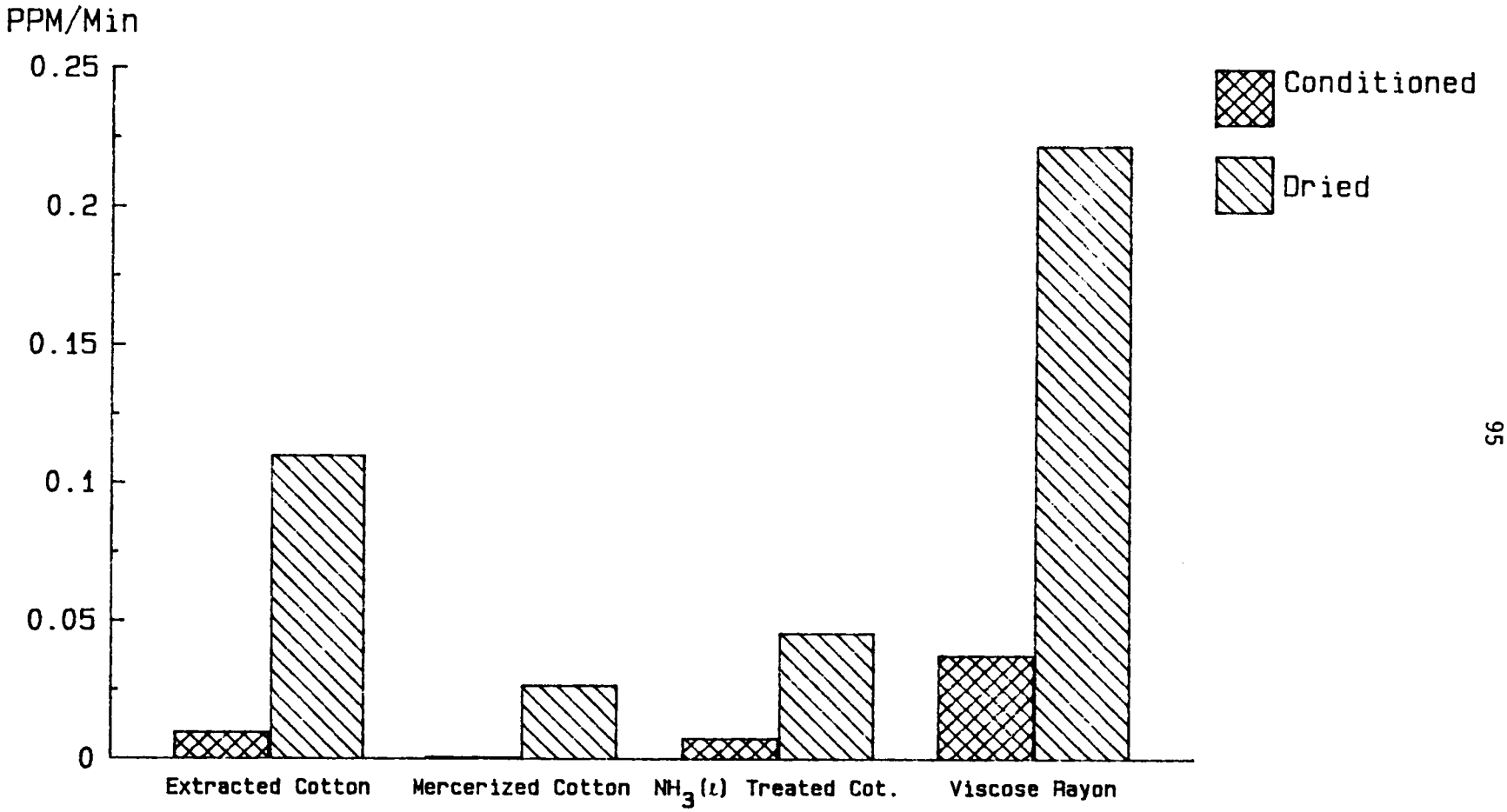


Figure 28. Secondary rates of SO_2 sorption by conditioned vs. dried fibers at 25°C.

Table 15. Time to minimum SO_2 concentration within the exposure chamber for conditioned vs. dried fibers at 25°C (min).[a]

Fiber type	Conditioned	Dried
Extracted cotton	26.54[b]	3.24[c]
Mercerized cotton	14.06	6.50
$NH_3(\ell)$ treated cotton	8.91	7.00
Viscose rayon	4.92	3.28

[a]All values are the result of one experimental run unless otherwise indicated.

[b]Value is the average of two experimental runs.

[c]Value is the average of four experimental runs.

concentration reaching the analyzer. For extracted cotton, it took over 8 times as long for the minimum concentration to be reached.

Total SO_2 sorption shown in Table 16 and Figure 29, illustrate a large increase in SO_2 sorption by conditioned fibers over that exhibited by dried fibers. Because the only difference between the samples used was the fiber moisture content, it can reasonably be concluded that the primary SO_2 removal mechanism for conditioned fibers was dissolution of the gas in the moisture held by the fiber as follows:

$$SO_2 + H_2O \rightarrow H_2SO_3$$

A contributing factor to the overall increased SO_2 sorption by conditioned fibers may well be the slight swelling of the fiber which accompanies moisture sorption. As cellulose absorbs water vapor during conditioning, fiber molecules are pushed apart. Internal fiber voids are filled in addition to the opening of the polymer structure by entering water molecules (51). In a sense, water acts as a carrier for the inward diffusion of SO_2. Thus, it is possible to infer that conditioned cellulose fibers allow easier penetration by SO_2 into the fiber bulk as a result of fiber swelling, and then provide the opportunity for SO_2 to react with the sorbed water.

It is surprising that the amount by which sorption increased for conditioned rayon over dried rayon was so small in view of the fact that rayon has the highest moisture regain of the fibers types examined (found to be 10.38% in the present study). This fact lends further support to the supposition that the orientation of the skin on

Table 16. Comparison of SO_2 sorption by conditioned vs. dried fibers at 25°C (μg SO_2/g fiber).[a]

Fiber type	Conditioned	Dried
Extracted cotton	720.8[b]	92.3[c]
Mercerized cotton	742.7	262.8
$NH_3(\ell)$ treated cotton	630.3	188.9
Viscose rayon	41.9	30.6

[a]All values are the result of one experimental run unless otherwise indicated.

[b]Value is the average of two experimental runs.

[c]Value is the average of four experimental runs.

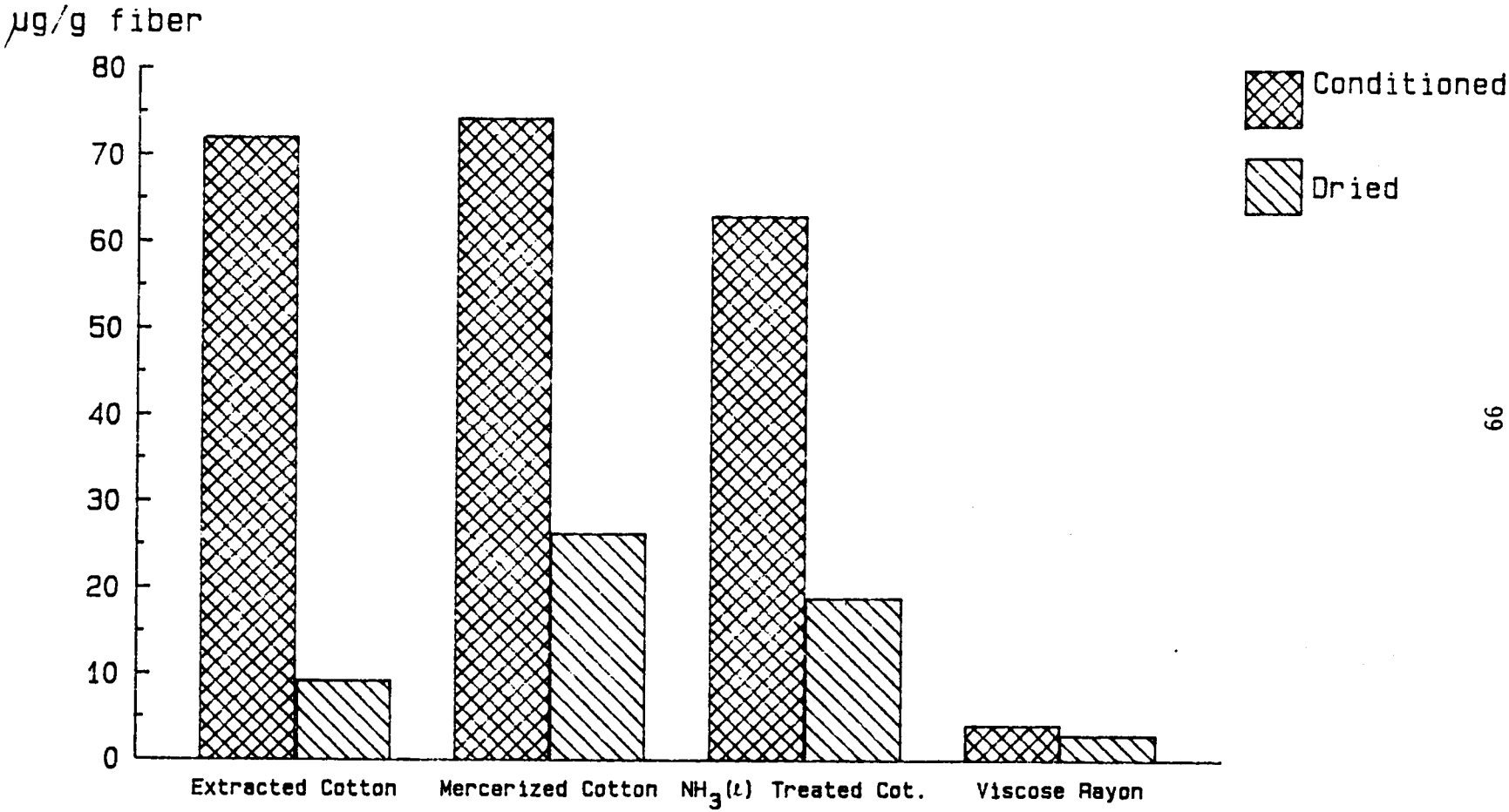


Figure 29. Comparison of SO_2 sorption by conditioned vs. dried fibers at 25°C.

viscose rayon acts to inhibit diffusion of SO_2 into the fiber. Crank (71) states that the rate of penetration by small molecules into a polymeric material is strongly influenced by its degree of orientation. It is well established that the molecules contained in the skin of rayon are more highly oriented than those contained in the core (73).

For each fiber type, the initial rate of SO_2 desorption (Table 17, Figure 30) was greater for dried fibers than for conditioned fibers indicating that the SO_2 was slower to desorb from the conditioned fibers. Moisture loss curves for conditioned fibers exposed to a dry gas stream for 9 hours (Figures 14-17, pp. 61-64) demonstrate that most of the moisture evaporates from the fibers over the course of the exposure period. Therefore, increased fiber moisture content does not seem to be the probable mechanism for the decreased rate of desorption. However, if SO_2 did react chemically within the substrate as outlined above, it could have been released from the fibers without detection by the analyzer which is specific to SO_2. Secondary desorption rates were also determined (Table 18, Figure 31), but as with those rates calculated for dried fibers at four temperatures, there were no noticeable trends.

Post Exposure Analysis

Several instrumental techniques were utilized to examine selected fiber samples following exposure to 3 ppm SO_2. SEM was used to determine the extent of gross surface changes on the fibers. X-ray

Table 17. Initial rates of SO_2 desorption by conditioned vs. dried fibers at 25°C (ppm/min).[a]

Fiber type	Conditioned	Dried
Extracted cotton	0.10	0.15[b]
Mercerized cotton	0.08	0.11
$NH_3(\ell)$ treated cotton	0.07	0.15
Viscose rayon	0.17	0.27

[a]All values are the result of one experimental run unless otherwise indicated.

[b]Value is the average of four experimental runs.

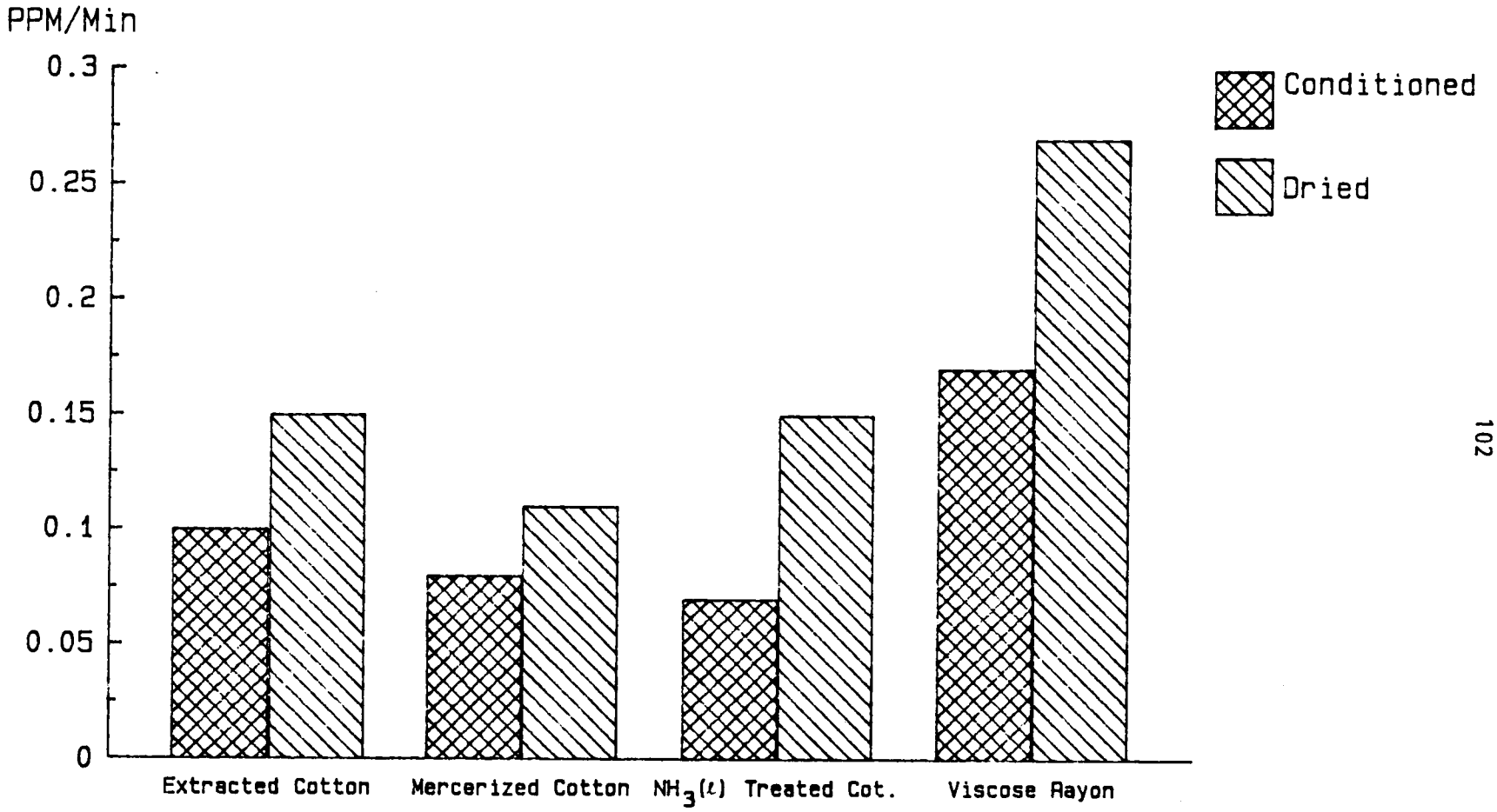


Figure 30. Initial rates of SO_2 desorption by conditioned vs. dried fibers at 25°C.

Table 18. Secondary rates of SO_2 desorption by conditioned vs. dried fibers at 25°C (ppm/min).[a]

Fiber type	Conditioned	Dried
Extracted cotton	0.020	0.006[b]
Mercerized cotton	0.008	0.003
$NH_3(\ell)$ treated cotton	0.004	0.008
Viscose rayon	<0.001	0.006

[a]All values are the result of one experimental run unless otherwise indicated.

[b]Value is the average of four experimental runs.

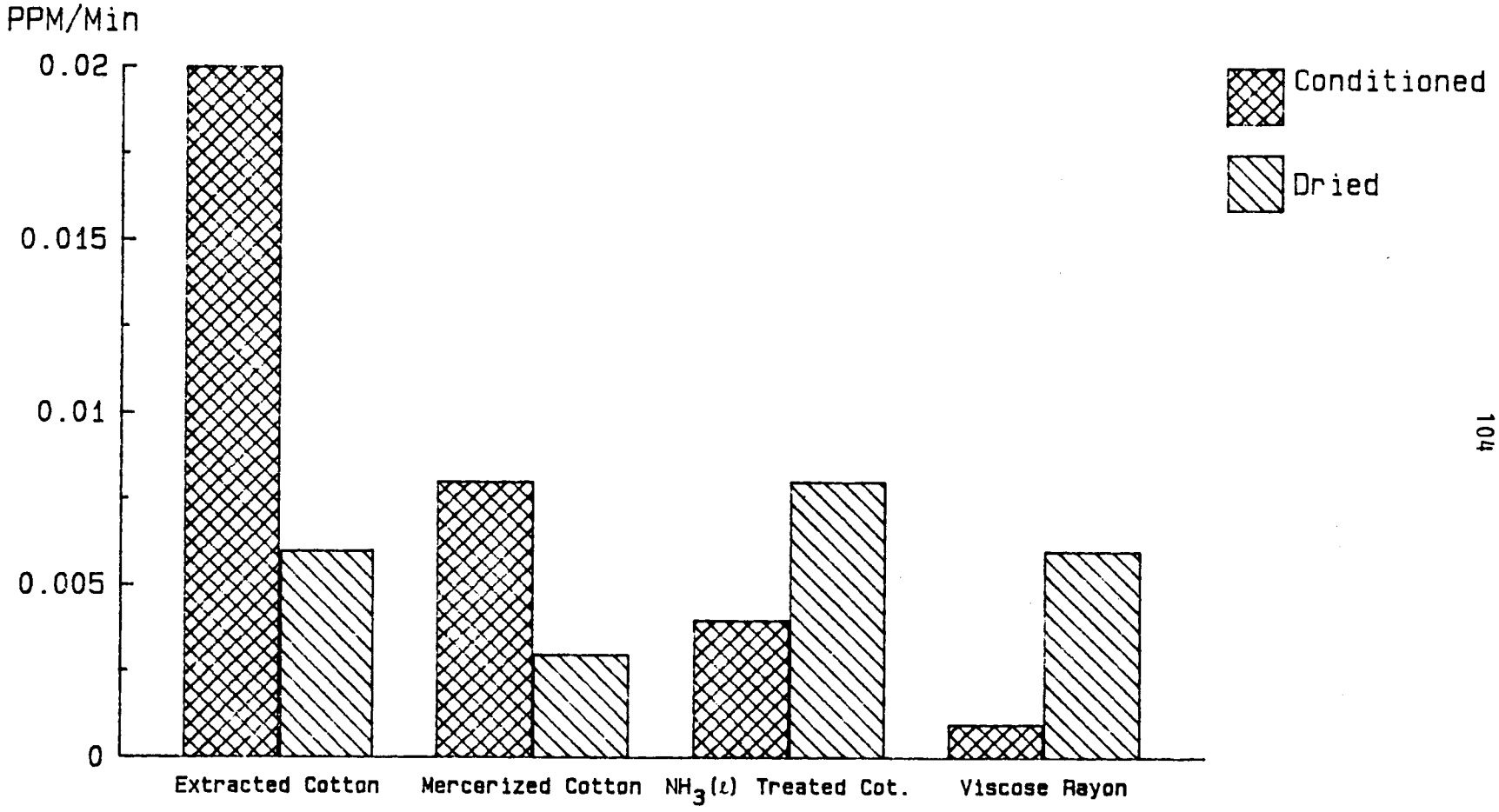


Figure 31. Secondary rates of SO_2 desorption by conditioned vs. dried fibers at 25°C.

spectroscopy, ESCA, FTIR and total sulfur analysis were used to determine the presence of residual sulfur in the samples.

Scanning Electron Microscopy

Photographs of selected exposed and unexposed fibers were taken using SEM. Extracted cotton and viscose rayon are shown before and after exposure in Figures 32 and 33. It can be seen that 3 ppm SO_2 exposure for 5 hours caused no visible changes in the surface of these fibers. Similarly, Zeronian found no gross surface changes in nylon 66 exposed to 0.2 ppm SO_2 (28).

X-Ray Spectroscopy

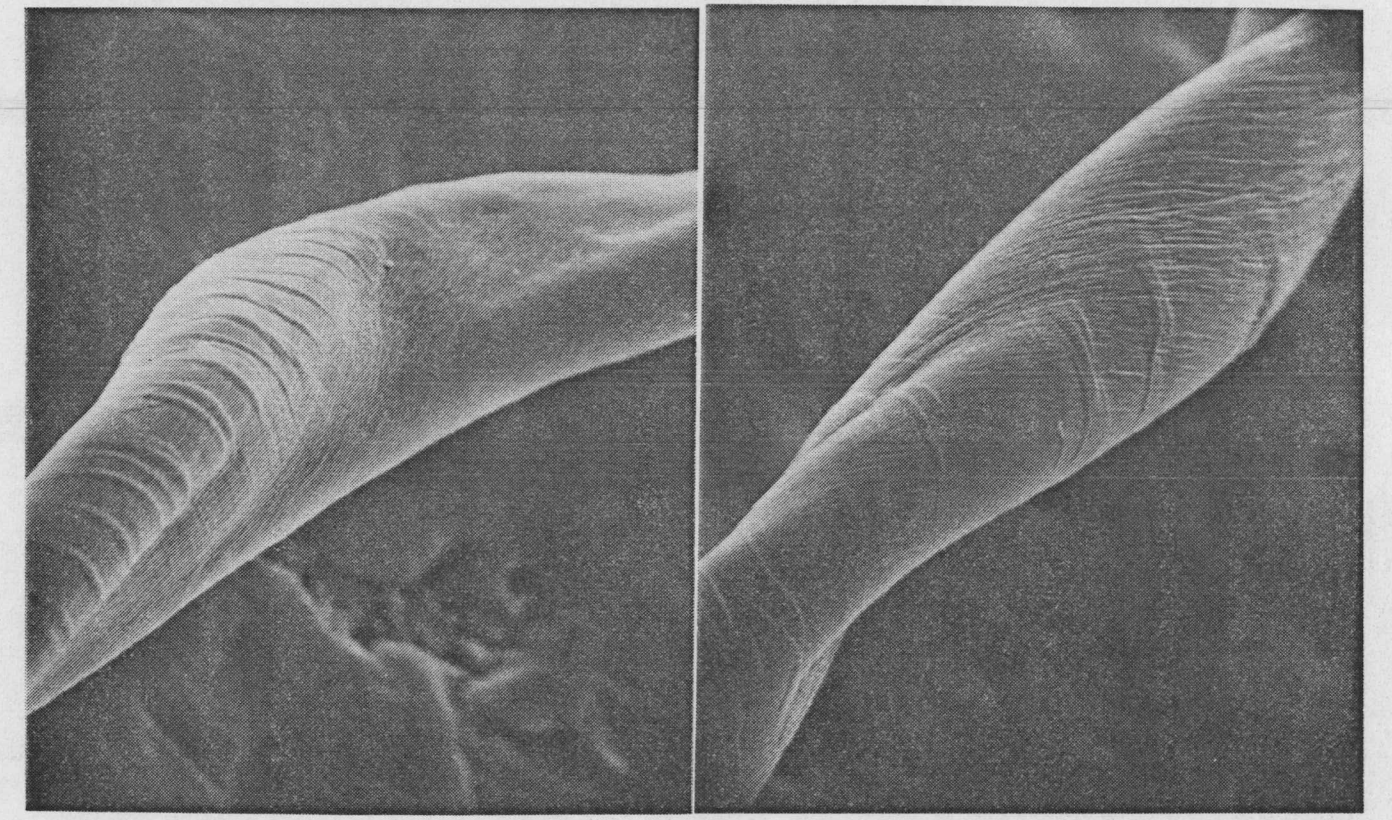
X-ray spectra were obtained for each fiber type previously exposed to SO_2. No sulfur peak was observed on the viscose rayon sample, but small peaks were noted for each of the other samples as shown in Figures 34-36. Confirmation of the presence of residual sulfur within some of the samples and identification of its species was sought using other techniques.

Electron Spectroscopy for Chemical Analysis

Exposed and unexposed extracted cotton fibers were sent to Virginia Tech University for ESCA analysis. The total computer output is contained in Appendix C. No sulfur was detected on the SO_2 exposed sample by this method.

Fourier Transform Infrared Spectroscopy

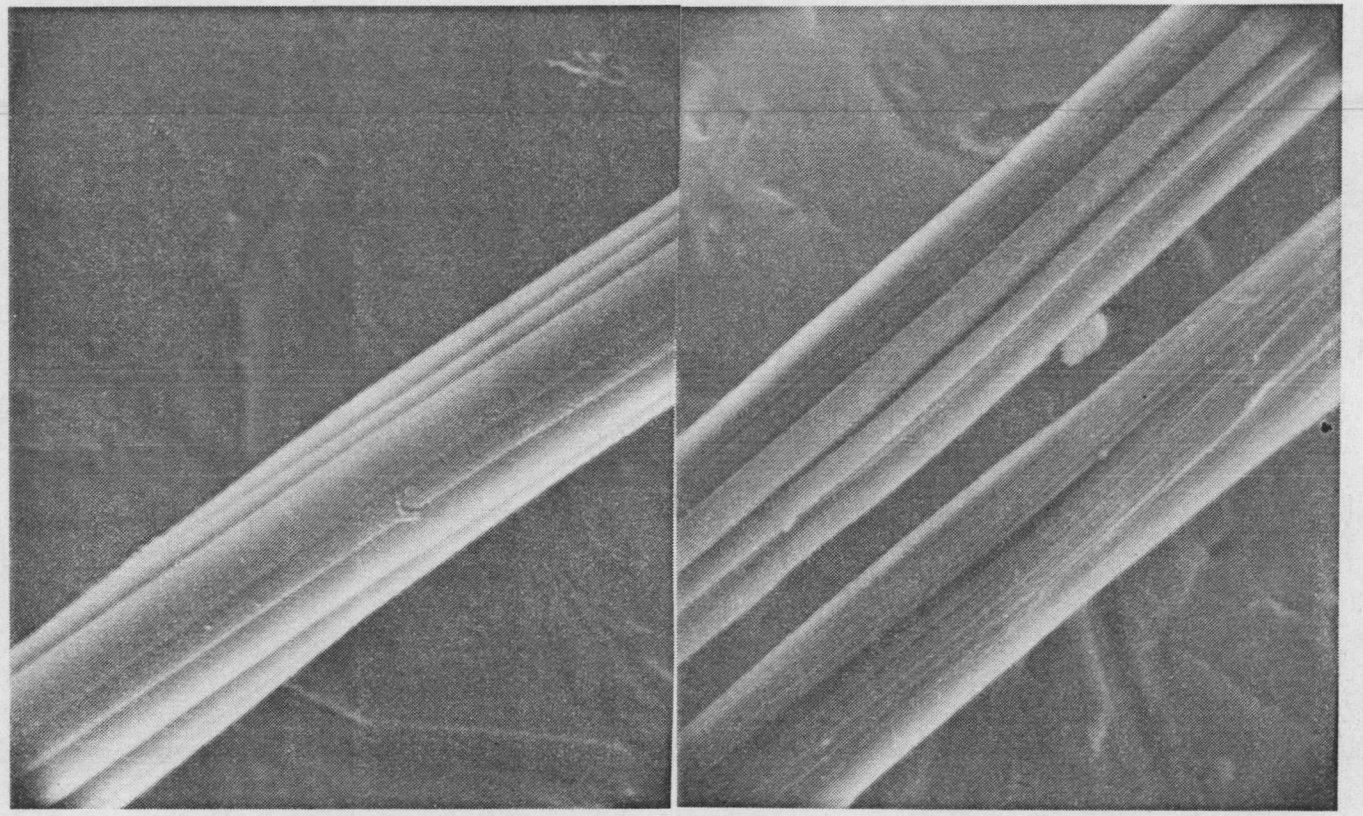
Because the strongest sulfur peaks identified by x-ray spectroscopy were noted on the exposed extracted cotton samples and



(a)
Before Exposure

(b)
After Exposure

Figure 32. Surface of extracted cotton before and after exposure to 3 ppm SO_2 at 25°C (2000x).



(a)
Before Exposure

(b)
After Exposure

Figure 33. Surface of viscose rayon before and after exposure to 3 ppm SO_2 at 25°C (2000x).

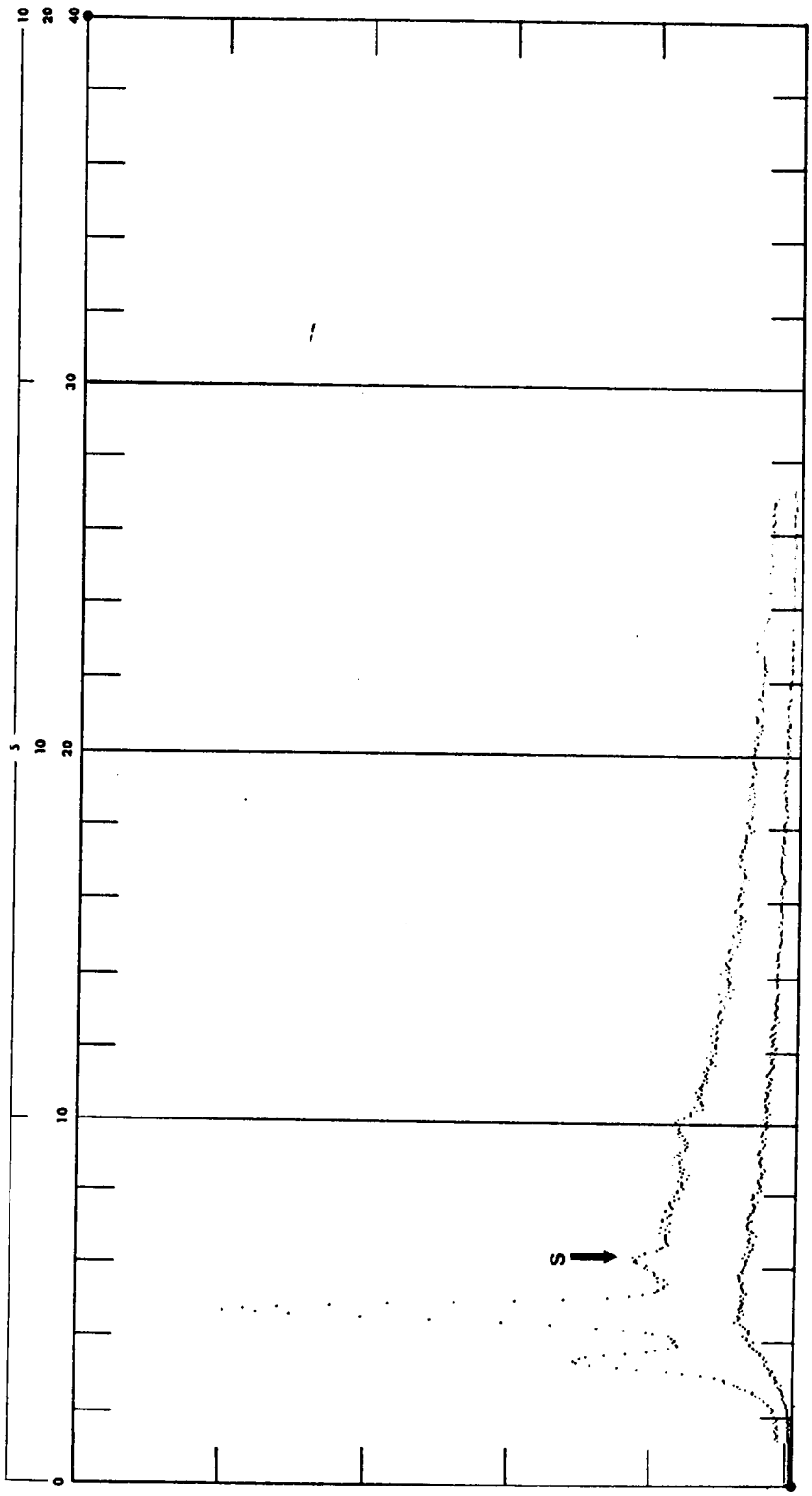


Figure 34. X-ray spectrum for extracted cotton exposed to 3 ppm SO_2.

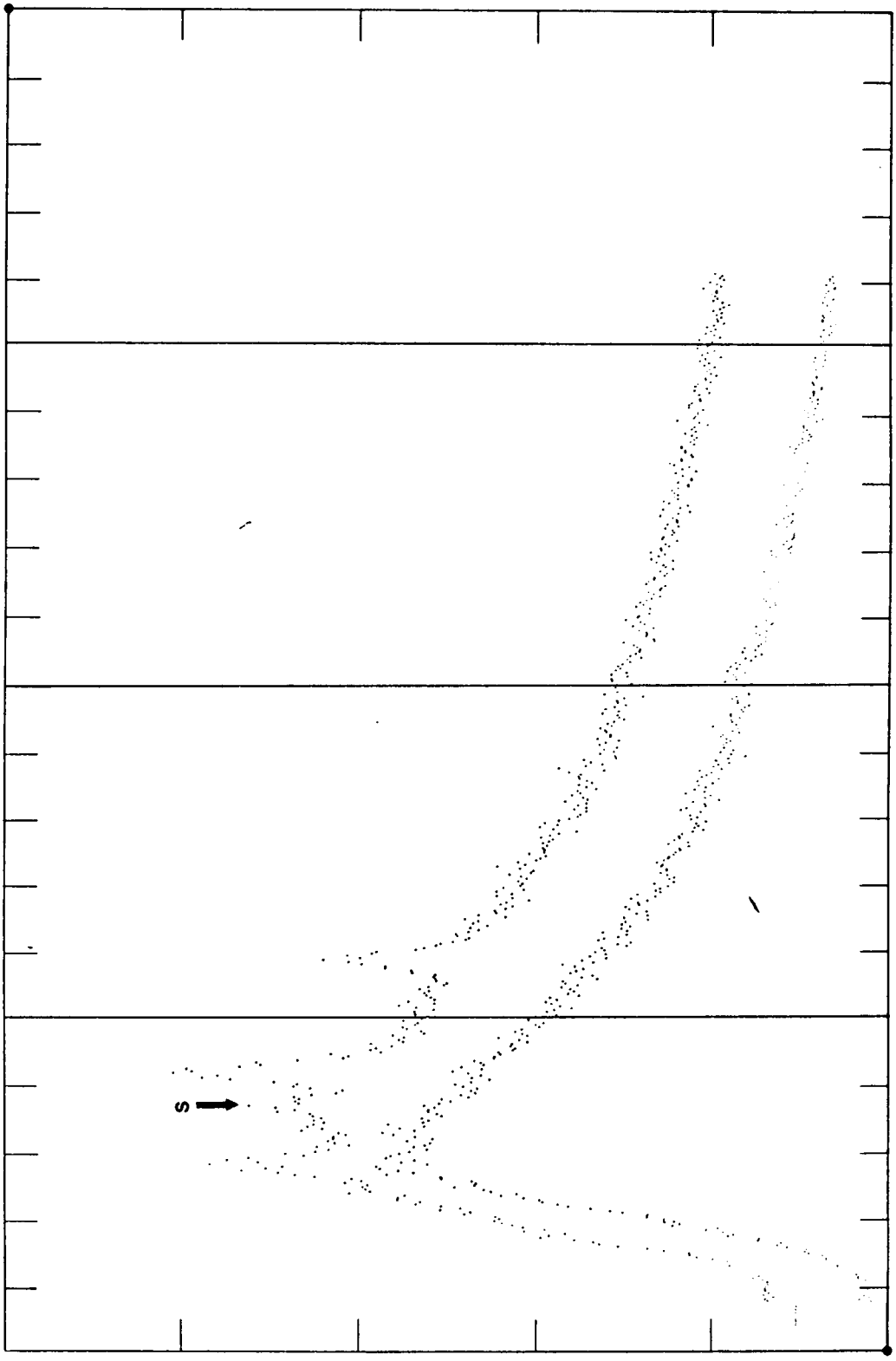


Figure 35. X-ray spectrum for mercerized cotton exposed to 3 ppm SO_2.

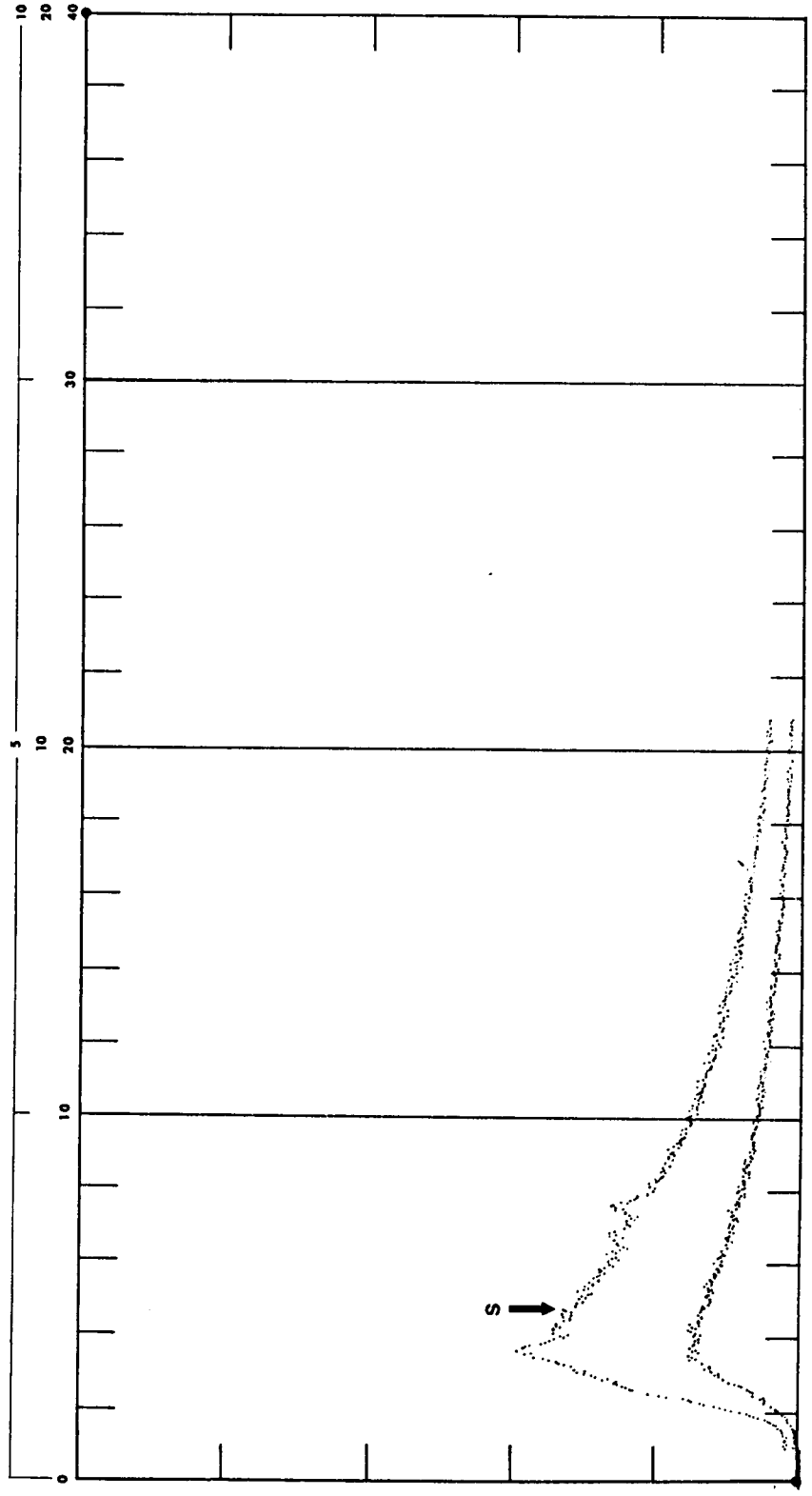


Figure 36. X-ray spectrum for $NH_3(\ell)$ treated cotton exposed to 3 ppm SO_2.

exposed mercerized cotton samples, those samples were analyzed by FTIR in order to identify the species of sulfur present. The resulting spectra are shown in Figures 37-38. The spectra are nearly identical for the exposed and unexposed samples. This technique was unable to confirm the presence of any species of sulfur remaining in the exposed fibers.

Total Sulfur Analysis

Total sulfur analysis was carried out by Galbraith Laboratories, Inc. Using a Leco oxygen combustion sulfur analyzer equipped with an infrared detector, they measured 0.025% sulfur in a sample of unexposed cotton and 0.021% sulfur in a conditioned exposed sample of extracted cotton. Even though the conditioned sample sorbed SO_2, clearly it was all removed during the desorption phase.

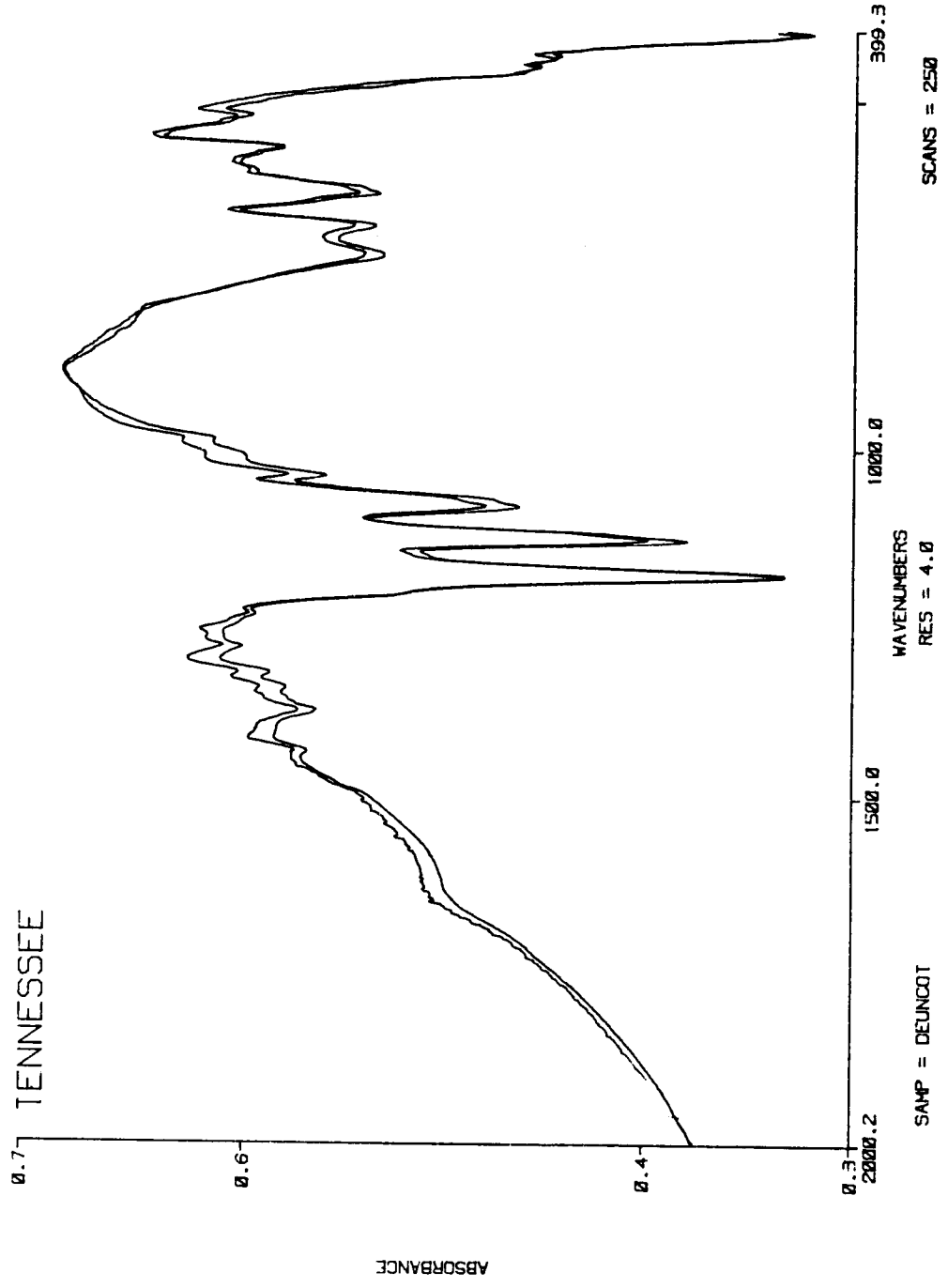


Figure 37. FTIR spectra of exposed and unexposed extracted cotton.

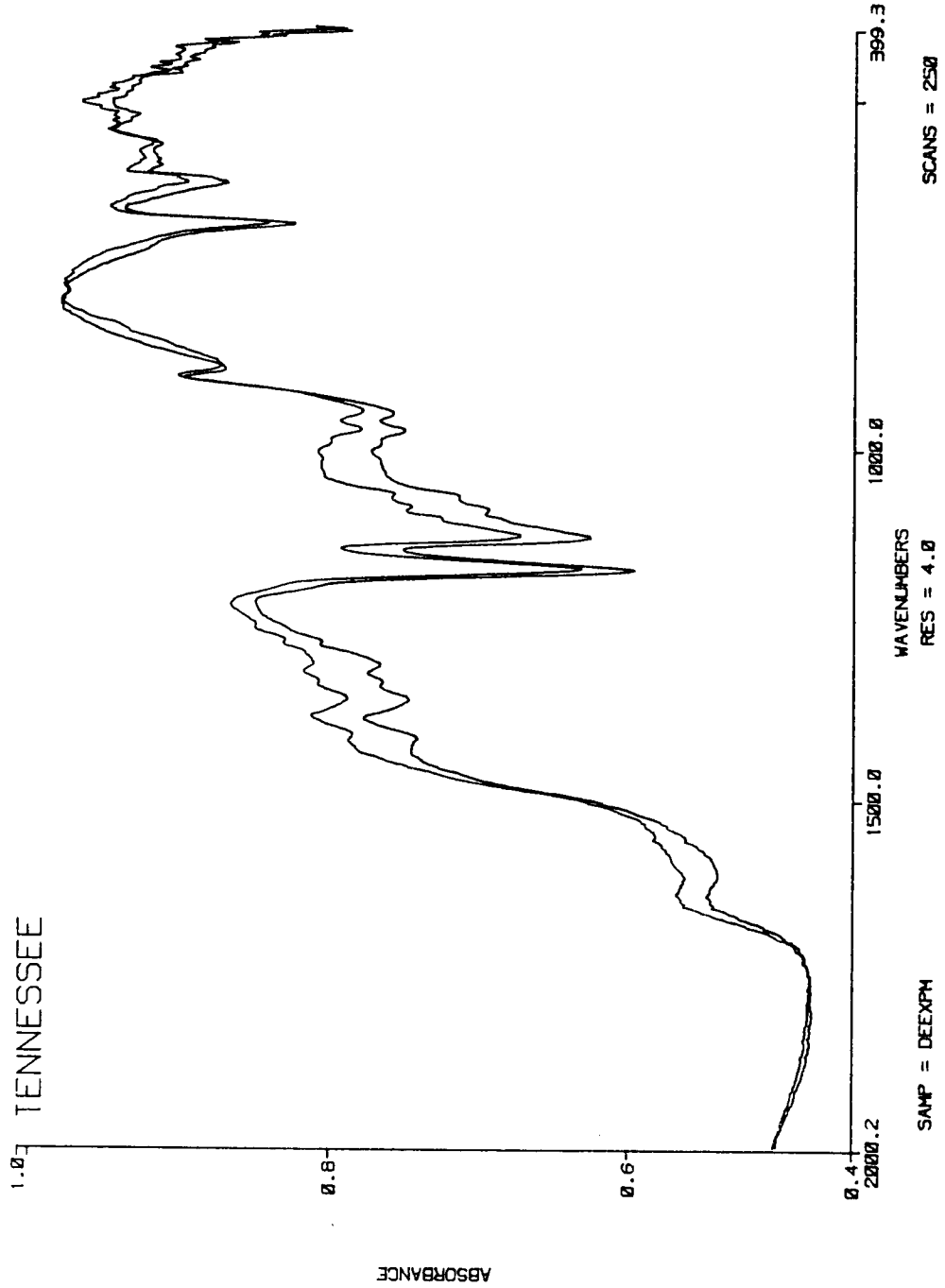


Figure 38. X-ray spectra of exposed and unexposed mercerized cotton.

CHAPTER V

SUMMARY, CONCLUSIONS, AND RECOMMENDATIONS

Summary

The purpose of the present study has been to examine the SO_2 sorption/desorption phenomenon by cellulosic fibers under dynamic conditions. Fiber moisture content and temperature were varied in an attempt to ascertain the mode and extent of sorption. Fiber fine structure was considered as a means to explain the sorptive capabilities of the various fibers.

Native, modified, and regenerated cellulosic fibers were exposed to 3 ppm SO_2 at various temperatures and fiber moisture contents at 170 cc/min for 5 hours. Exposure to SO_2 was followed by exposure to a stream of dry air at the same flow rate for 4 hours. The concentration of SO_2 reaching the analyzer was monitored continuously and compared with the known concentration of SO_2 introduced into the chamber in order to calculate total sorption. Additionally, initial and secondary rates of sorption and desorption were calculated.

Total SO_2 sorption by dried fibers was found to vary inversely with temperature. Each fiber type sorbed less gas as the temperature was increased. Mercerized cotton sorbed the most SO_2 at all temperatures and viscose rayon sorbed the least.

Increased fiber moisture content was found to have a profound effect on the quantity of SO_2 sorbed. All fiber samples conditioned to 69 ± 1% R.H. sorbed more SO_2 than did their dried counterparts.

Examination of the rates of SO_2 desorption showed no discernible differences. No doubt, this was due in part to the dynamics of the process. Some desorption may have been occurring during the sorption phase of the runs. Furthermore, reaction products such as H_2SO_3 could have been released from the fibers without detection by the SO_2 analyzer.

X-ray spectroscopic analysis on fiber samples previously exposed to SO_2 revealed the presence of sulfur in extracted cotton, mercerized cotton, and $NH_3(\ell)$ treated cotton fibers as evidenced by small peaks on each of the spectra. A variety of other techniques was used to identify the species of sulfur present. No sulfur was found using ESCA or FTIR. Total sulfur analysis revealed similar trace amounts of sulfur in exposed and unexposed cotton.

Conclusions

Based on the data it is reasonable to conclude that the overall primary mechanism involved in the interaction of SO_2 with cellulose is physical sorption. The SO_2 bond angle is $119.75 \pm 5°$ (74). Because SO_2 is not a linear molecule it is a permanent dipole and as such can induce dipoles in surrounding molecules. Therefore, sorption of SO_2 by cellulose is probably the result of van der Waals interactions at the fiber surface. Sulfur dioxide sorption by cellulose is temporary. The gas molecules are held weakly and in this case were easily dislodged by a stream of dry air.

It is probable that SO_2 combines with the moisture in fibers. In the present study conditioned fibers sorbed far more SO_2 than did dried fibers. However, all of the SO_2 was desorbed from both the dried and conditioned fibers. It should be noted that during the 9 hour exposure to dried gases, conditioned fibers lost much of their moisture. This dynamic process of simultaneous SO_2 exposure and fiber drying may well have contributed to the total removal of sulfur from the fibers.

Fiber accessibility was also found to affect SO_2 sorption. Mercerized cotton, the most accessible fiber examined, showed a longer sustained sorption and a greater total sorption than the other fibers studied. A possible explanation for the very low degree of SO_2 sorption exhibited by viscose rayon relates to the skin/core structure of the fiber. The finer textured, more highly oriented skin may act as a barrier to penetration of SO_2 molecules.

Liquid ammonia treated cotton demonstrated the greatest drop in SO_2 sorptive capacity with increased temperature. It has been shown that $NH_3(\ell)$ treatment with evaporative removal of NH_3 changes the size and shape of the fiber pores (75). Further evaluation of any internal changes occurring in $NH_3(\ell)$ treated cotton at increased temperatures is warranted.

Recommendations

The dynamic conditions used in the present study have complicated the analysis. It would be advisable to establish the baseline SO_2

sorption of the fibers by means of a static determination. Data generated in this manner could be used to evaluate the effects of the dynamic conditions typically encountered in indoor environments on the overall SO_2 sorption by fibers.

Determination of the breakthrough time, the time required for a stream of gas to traverse a plug of material, is an environmental technique commonly used with soils. Such a measurement would provide more insight into the initial rates of SO_2 sorption without the complicating factor of gas dilution. The apparatus used in the present study could be adapted for these measurements.

Variations in the experimental parameters may also serve to further elucidate the extent and mechanism of SO_2 sorption by fibers. Experimental runs at higher temperatures and lower fiber moisture contents would be interesting. At higher temperatures, it might be possible to identify heat of sorption. There may be a point where chemisorption becomes a factor. The fibers used in the present study were as dry as was reasonably practical. However, further drying with subsequent exposure to SO_2 might further separate out the contribution of fiber moisture to overall sorption of SO_2.

Sample geometry should also be varied. The influence of accessibility could be studied in more detail by examining SO_2 sorption by cellulose powders. Furthermore, rayons of differing skin/core ratios should be examined in order to provide more insight.

Finally, yarns and fabrics should be examined in order to study the effect of these less accessible geometries on SO_2 sorption. Such

measurements would likely produce the most accurate insight into the sorptive capacity of textile structures found within enclosed spaces.

Identification of textile products capable of sorbing gaseous pollutants and thereby modifying the quality of the indoor environment is a worthy goal. Information generated by the present study represents a first step in the process.

LITERATURE CITED

LITERATURE CITED

1. Indoor Air Pollution: An Emerging Health Problem. Comptroller General's Report to the Congress of the United States, CED-80-111, Sept. 24, 1980.

2. Chanlett, E. T. Environmental Protection. McGraw-Hill, New York, 1979.

3. Gold, M. Indoor Air Pollution. Science 80 1980, 1(3), 30.

4. Indoor Air Quality. Residential Energy Conservation. Office of Technology Assessment, U.S. Congress, Washington, D.C., 1980.

5. Indoor Air Quality vs. the Energy Crisis. Tech. Rev. 1979, 81(3), 20.

6. Bogaty, H.; Campbell, K. S.; and Appel, W. D. The Oxidation of Cellulose by Ozone in Small Concentrations. Text. Res. J. 1952, 22, 81.

7. Upham, J. B. and Salvin, V. S. Effects of Air Pollutants on Textile Fibers and Dyes. Environmental Protection Agency Pub. No. 650/3-74-008, 1975.

8. Walters, B. J.; Goswami, B. C.; and Vigo, T. L. Sorption of Pollutants onto Textiles. Text. Res. J. 1983, 53, 354.

9. Gregory, C. J. "Adsorption of Atmospheric Sulfur Dioxide by Natural and Synthetic Textile Fibers." Unpublished Ph.D. dissertaion, Rutgers University, New Brunswick, N.J., 1968.

10. Public Law 88-206. United States Statutes at Large, Vol. 77. United States Government Printing Office, Washington, D.C., 1964, 392.

11. Dudney, C. S. Indoor Air Pollution: Health Effects. Presentation to the Knox Area Home Economics Council. The University of Tennessee, Knoxville, Tennessee. Nov. 3, 1983.

12. Lafavore, M. Warning! This House Cotnains Radon. Reader's Digest. June, 1986, 110.

13. Biersteker, K.; de Graaf, H.; and Nass, Ch. A. G. Indoor Air Quality in Rotterdam Homes. Int. J. Air and Water Poll. 1965, 9, 343.

14. Yocum, J. E.; Clink, W. L.,; and Cote, W. A. Indoor/Outdoor Air Quality Relationships. J. Air Poll. Cont. Assn. 1971, 21(5), 251.

15. Wark, K. and Warner, C. F. Air Pollution: Its Origin and Control. Harper & Row, New York, 1976.

16. Kellog, W. W.; Cadel, R. D.; Allen, E. R.; Lazrus, A. L.; and Martell, E. A. The Sulfur Cycle. Science 1972, 175, 587.

17. Faith, W. L.; Keyes, D. B.; and Clark, R. L. Sulfuric Acid. Industrial Chemicals. John Wiley & Sons, New York, 1950.

18. Panter, R. and Penzhorn, R.-D. Alkyl Sulfonic Acids in the Atmosphere. Atmos. Environ. 1980, 14, 149.

19. Hitchcock, D. R.; Spiller, L. L.; and Wilson, W. E. Sulfuric Acid Aerosols and HCl Release in Costal Atmospheres: Evidence of Rapid Formation of Sulfuric Acid Particulates. Atmos. Environ. 1980, 14, 165.

20. Lipfert, F. W. Sulfur Oxides, Particulates, and Human Mortality: Synopsis of Statistical Correlations. J. Air Poll. Cont. Assn. 1980, 30, 366.

21. Health Consequences of Sulfur Oxides: A Report from CHESS, 1970-1971. Environmental Protection Agency. Research Triangle Park, N.C., 1974.

22. Ember, L. R. Acid Pollutants: Hitchhikers Ride the Wind. Chem. & Engr. News 1981, 59(37), 14.

23. Ember, L. R. Power Plants Cited as Big Acid Rain Source. Chem. & Engr. News 1981, 59(38), 14.

24. Gilardi, E. F. "Absorption of Atmospheric Sulfur Dioxide by Clay Brick and Other Building Mateirals," Unpublished Ph.D. dissertation, Rutgers University, New Brunswick, N.J., 1965.

25. Fye, C.; Flaskerude, K.; and Saville, D. The Effect of an SO_2 Atmosphere on the Breaking Strength of Fabrics of Different Fiber Content. Am. Dyest. Rep. 1968, 58, 16.

26. Long, S. H. and Saville, D. Exposure of Fabrics to a Polluted Atmosphere: Apparatus to Produce High Humidity. Am. Dyest. Rep. 1971, 60, 48.

27. Peters, J. S. and Saville, D. Fabric Deterioration: A Test Chamber for Exposure of Fabrics to a Contaminated Atmosphere. Am. Dyest. Rep. 1967, 56, 340.

28. Zeronian, S. H. The Effect of Light and Air Contaminated with Sulfur Dioxide on the Surface of Nylon 66 Fibers. Text. Res. J. 1971, 41, 184.

29. Zeronian, S. H. Reaction of Cellulosic Fabrics to Air Contaminated with Sulfur Dioxide. Text. Res. J. 1970, 40, 695.

30. Zeronian, S. H.; Alger, K. W.; and Omay, S. T. The Effect of Sulfur Dioxide on the Chemical and Physical Properties of Nylon 66. Text. Res. J. 1973, 43, 228.

31. Hrdlovic, P.; Pavlinec, J.; and Jellinek, H. H. G Degradation of Polymers and Morphology: Photo-Oxidative Degradation of Isotactic Polystyrene in the Presence of Sulfur Dioxide as a Function of Polymer Crystallinity. J. Polym. Sci., A-1 1971, 9, 1235.

32. Jellinek, H. H. G. Reactions of Linear Polymers with Nitrogen Dioxide and Sulfur Dioxide. Text. Res. J. 1973, 43, 557.

33. Jellinek, H. H. G.; Flajsman, F.; and Kryman, F. J. Reaction of SO_2 and NO_2 with Polymers. J. Appl. Polym. Sci. 1969, 13, 107.

34. Jellinek, H. H. G. and Kryman, F. J. Reaction of SO_2 with Polymer. J. Appl. Polym. Sci. 1969, 13, 2504.

35. Mears. P. The Diffusion of Gases Through Polyvinyl Acetate. J. Am. Chem. Soc. 1954, 76, 3415.

36. Michaels, A. S.; Vieth, W. R.; and Barrie, J. A. Solution of Gases in Polyethylene Terephthalate. J. Appl. Phys. 1963, 34, 1.

37. Toi, K. Diffusion and Sorption of Gases in Poly(ethylene Terephthalate). J. Polym. Sci. 1973, 11, 1829.

38. Vieth, W. R.; Tam, P. M.; and Michaels, A. S. Dual Sorption Mechanisms in Glassy Polystyrene. J. Colloid Interface Sci. 1966, 22, 360.

39. Davis, E. G. and Rooney, M. L. Transport of Sulphur Dioxide in Polymers. Kolloid Z. Z. Polym. 1971, 249, 1043.

40. Wohlers, H. C.; Trieff, N. M.; Newstein, H.; and Stevens W. Sulfur Dioxide Adsorption on-and Desorption from Teflon, Tygon, Glass, Stainless Steel, and Aluminum Tubings. Atmos. Environ. 1967, 1, 121.

41. Crawshaw, G. H. The Role of Wool Carpets in Controlling Indoor Air Polution. Text. Inst. Ind. 1978, 16, 12.

42. Spedding, D. J. The Sorption of Sulfur Dioxide by Indoor Surfaces. IV. Flooring Materials. J. Appl. Chem. Biotechnol. 1972, 22, 1.

43. Walsh, M.; Black, A.; Morgan, A.; and Crawshaw, G. H. Sorption of SO_2 by Typical Indoor Surfaces Including Wool Carpets, Wallpaper, and Paint. Atmos. Environ. 1977, 11, 1107.

44. Chamberlain, A. C. Aspects of the Deposition of Radioactive and Other Gases and Particles. Int. J. Air Poll. 1960, 3, 63.

45. Chamberlain, A. C. Experiments on the Deposition of Iodine 131 Vapour Onto Surfaces from an Airstream. Philos. Mag. 1953, 44, 1145.

46. Spedding, D. J. Uptake of Sulphur Dioxide by Barley Leaves at Low Sulphur Dioxide Concentrations. Nature 1969, 224, 1229.

47. Payrissat, M. and Bielke, S. Laboratory Measurements of the Uptake of Sulphur Dioxide by Different European Soils. Atmos. Environ. 1975, 9, 211.

48. Spedding, D. J. Sulphur Dioxide Absorption by Sea Water. Atmos. Environ. 1972, 6, 583.

49. Goswami, B. C.; Martindale, J. G.; and Scardino, F. L. Textile Yarns: Technology, Structure, and Applications. John Wiley & Sons, New York, 1977.

50. Cook, J. G. Handbook of Textile Fibers, I. Natural Fibers. Merrow Pub. Co. Ltd. England. 1968.

51. Morton, W. E. and Hearle, J. W. S. Physical Properties of Textile Fibers. Wm. Heinemann Ltd., London, 1975.

52. Valko, E. I. Mercerization. High Polymers, Vol. V. E. Ott, Ed., Interscience Pub., New York, 1943.

53. Rousselle, M. A. and Nelson, M. L. Reactivity and Fine Structure of Cotton Mercerized in Sodium Hydroxide or Liquid Ammonia. Text. Res. J. 1976, 46, 648.

54. Rousselle, M. A.; Nelson, M. L.; Hassenboehler, C. B.; and Legendre, D. C. Liquid Ammonia and Caustic Mercerization of Cotton Fibers: Changes in Fine Structure and Mechanical Properties. Text. Res. J. 1976, 46, 304.

55. Pandy, S. N. and Nair, P. A Study of the Effect of Anhydrous Liquid Ammonia Treatment on Cotton. Text. Res. J. 1975, 45, 648.

56. Lewin, M. and Roldan, L. G. The effect of Liquid Anhydrous Ammonia on the Structure and Morphology of Cellulose. J. Polym. Sci.: Part C 1971, 36, 213.

57. Calamari, T. A.; Schreiber, S. P.; Cooper, A. S.; and Reeves, W. A. Liquid Ammonia Modification of Cellulose in Cotton and Polyester/Cotton Textiles. Text. Chem. Color. 1971, 3(10), 61.

58. Roldan, L. G. The Effect of Liquid Anhydrous Ammonia on Cellulose II. Modified Cellulosics. R. M. Rowell and R. A. Young, Eds., Academic Press, New York, 1978.

59. Turbak, A. F.; Hammer, R. B.; Davies, R. E.; and Portnoy, N. A. A Critical Review of Cellulose Solvent Systems. Solvent Spun Rayon, Modified Cellulose Fibers and Derivatives. A. F. Turbak, Ed., ACS, Washington, D.C., 1977.

60. Welch, A. F. and Terry, J. P. Developments in the Measurement of Atmospheric Sulfur Dioxide. Am. Ind. Hyg. Assn. J. 1960, 21, 316.

61. Perry, W. H. and Tabor, E. C. National Air Sampling Network Measurement of SO_2 and NO_2. Arch. Envr. Hlth. 1962, 4, 254.

62. Wohlers, H. C.; Newstein, H.; and Daunis, D. Cabon Monoxide and Sulfur Dioxide Adsorption on and Desorption from Glass, Plastic, and Metal Tubings. J. Air Poll. Cont. Assn. 1967, 17, 753.

63. Rogers, H. H.; Jefferies, H. E.; Stahel, E. P.; Heck, W. W.; Ripperton, L. A.; and Witherspoon, A. M. Measuring Air Pollution Uptake by Plants: A Direct Kinetic Technique. J. Air Poll. Cont. Assn. 1977. 27, 1192.

64. Model 906A Sulfur Dioxide Analyzer Manual. Beckman Instructions 82043-A, Beckman Instruments, Fullerton, California, 1970.

65. Mikhail, R. S. and Robens, E. Microstructure and Thermal Analysis of Solid Surfaces. John Wiley & Sons, New York, 1983.

66. Needles, H. L. Handbook of Textile Fibers, Dyes, and Finishes. Garland STPM Press, London, 1981.

67. Carter, M. E. Essential Fiber Chemistry. Marcel Dekker, New York, 1971.

68. Howsman, J. A. and Sisson, W. A. Structures and Properties of Cellulose Fibers, B. Submicroscopic Structure. High Polymers, Vol. V. E. Ott, Ed. Interscience Publishers, New York, 1954.

69. Phillip, H. J.; Nelson, M. L.; and Ziifle, H. M. Crystallinity of Cellulose Fibers as Determined by Acid Hydrolysis. Text. Res. J. 1947, 17, 585.

70. Nickerson, R. F. Accessibility of Cellulose by Formic Acid Esterification. Text. Res. J. 1951, 21, 195.

71. Crank, J. Diffusion in Fibre-Forming Substances. Moisture in Textiles. J. W. S. Hearle and R. H. Peters, Eds. Textile Book Publishers, New York, 1960.

72. Nickerson, R. F. Strength of Native Fibers and Yarns. High Polymers, Vol. V. E. Ott, Ed. Interscience Publishers, New York, 1943.

73. Hindeleh, A. M. X-ray Characterization of Viscose Rayon and the Significance of Crystallinity on Tensile Properties. Text. Res. J. 1980, 50, 581.

74. Handbook of Chemistry and Physics. R. C. Weast, Ed. The Chemical Rubber Co., Cleveland, Ohio, 1970.

75. Bertoniere, N. R.; King, W. D.; and Rowland, S. P. Effect of Mode of Agent Removal on Pore Structure of Liquid Ammonia Treated Cotton Cellulose. J. Appl. Polym. Sci. 1986, 31, 2769.

APPENDICES

APPENDIX A

X-RAY DIFFRACTOGRAMS

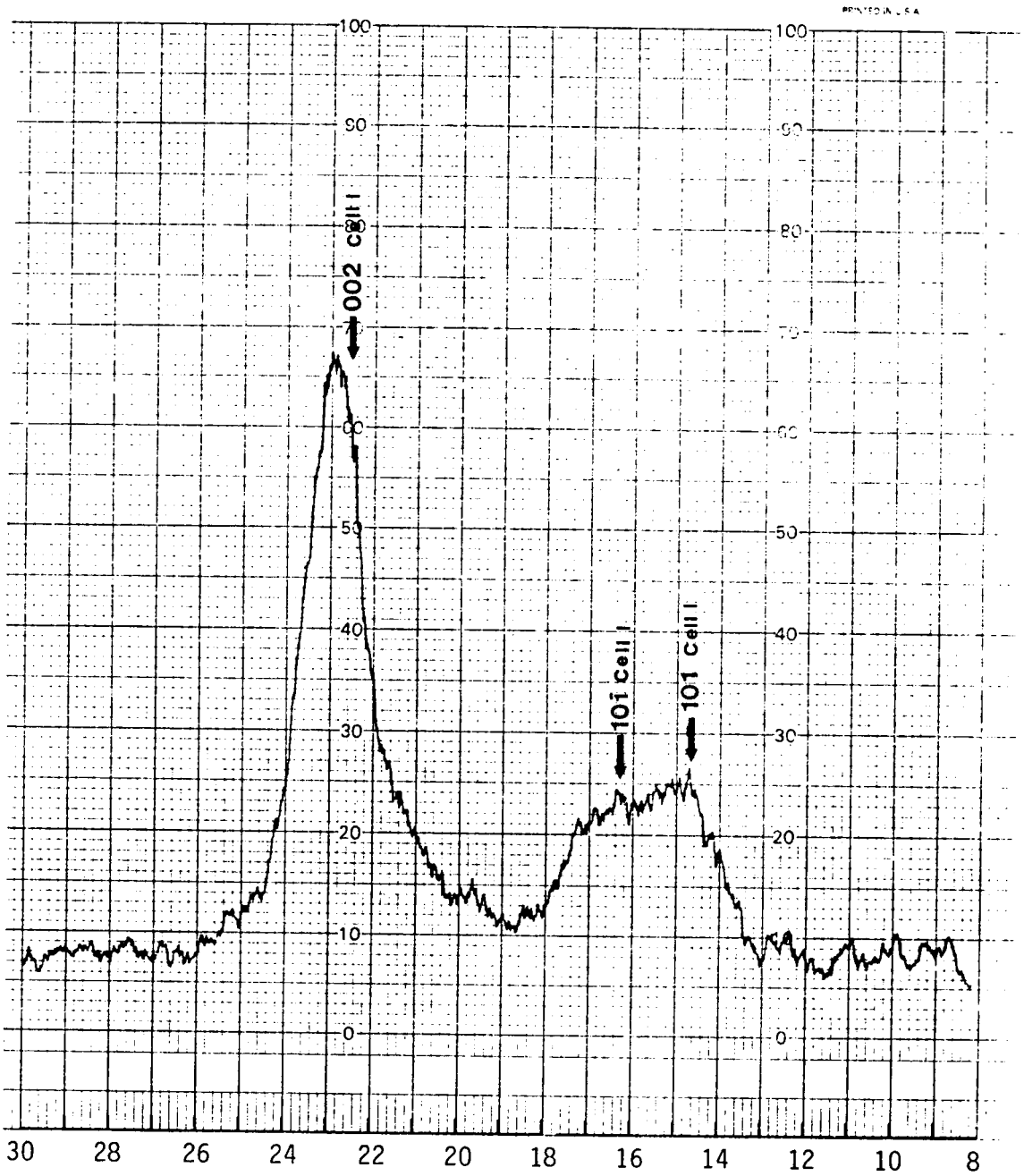


Figure A-1. X-ray diffractogram of dried extracted cotton exposed to 3 ppm SO_2 at 25°C.

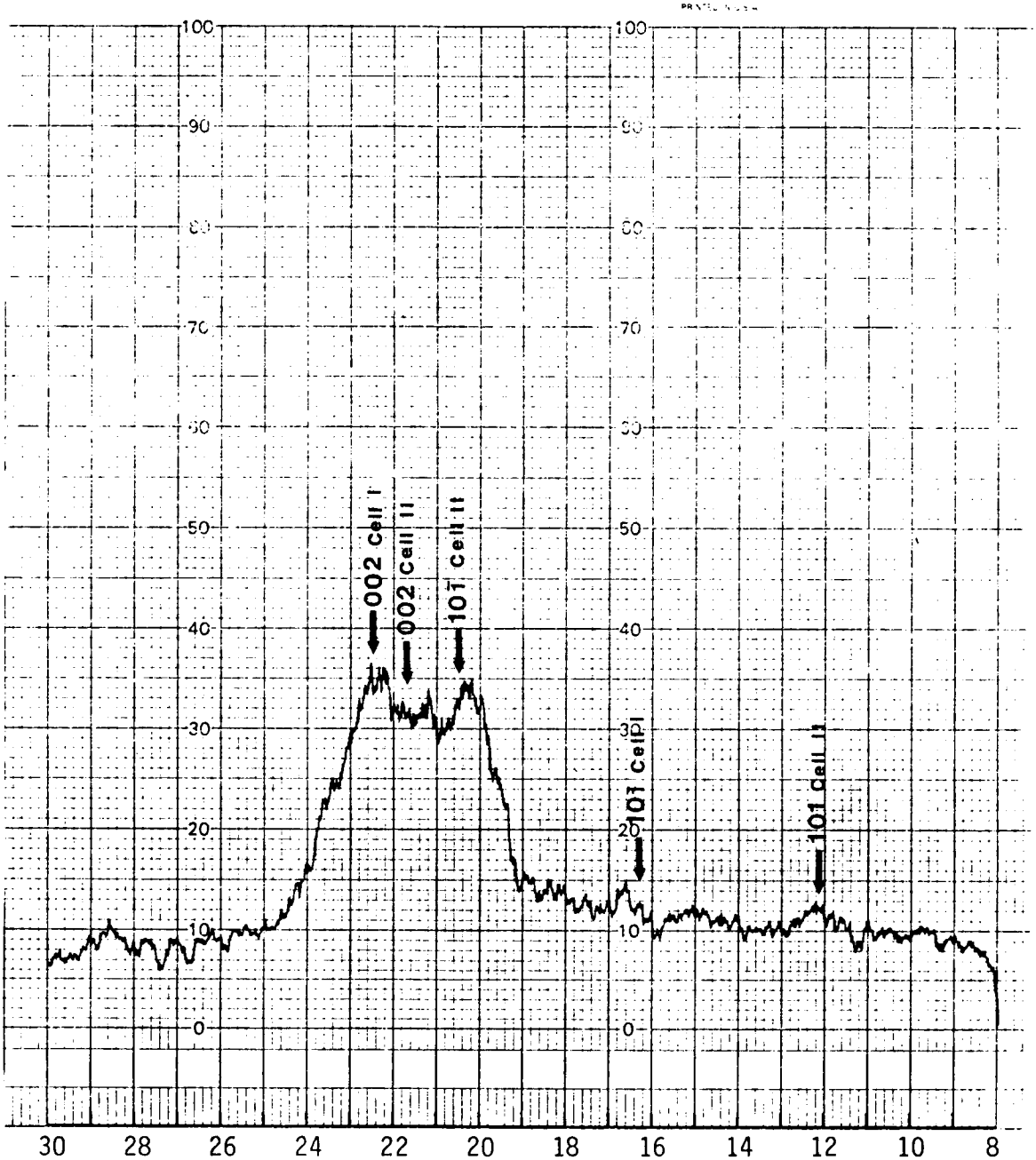


Figure A-2. X-ray diffractogram of dried mercerized cotton exposed to 3 ppm SO_2 at 25°C.

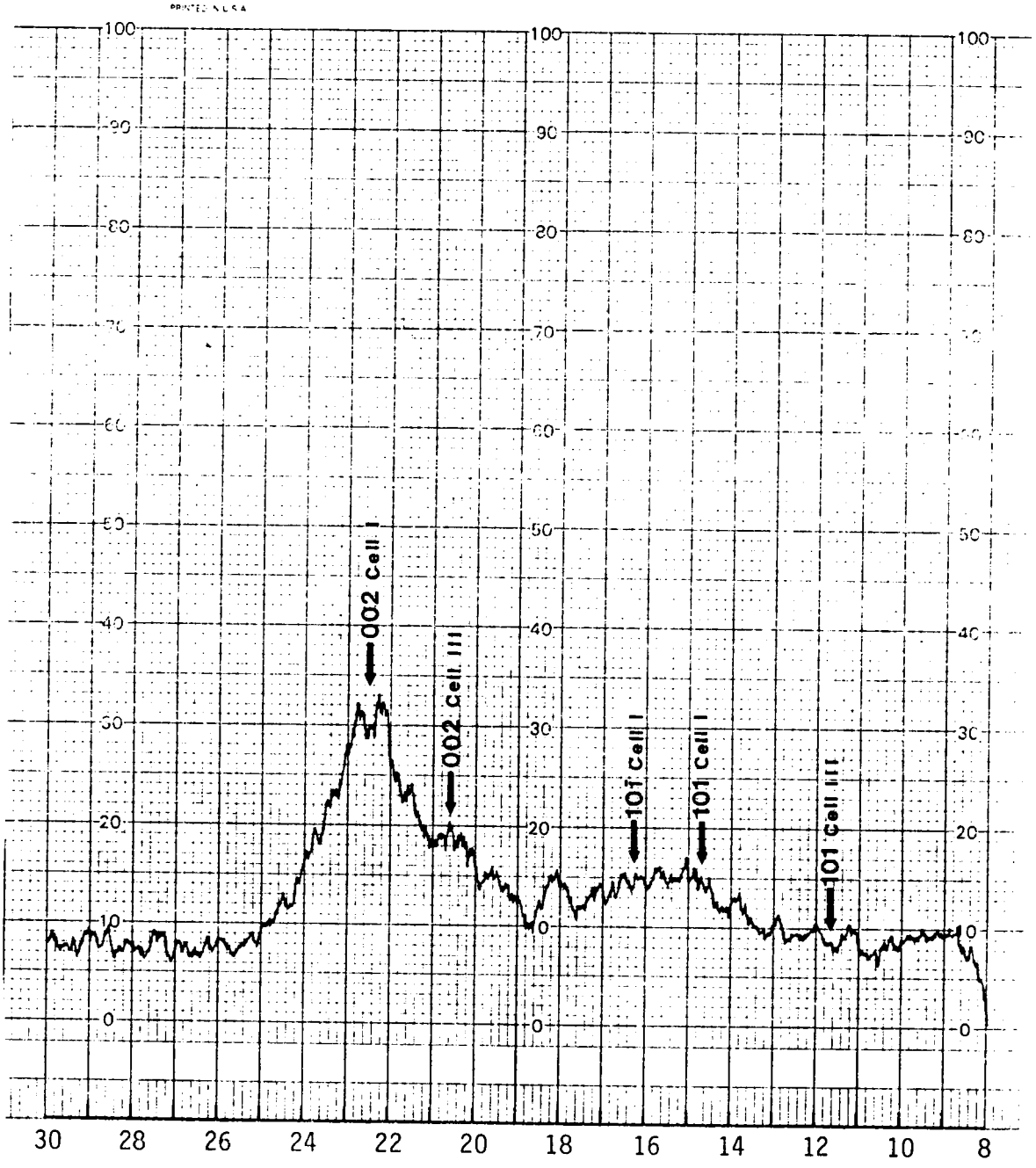


Figure A-3. X-ray diffractogram of dried $NH_3(\ell)$ treated cotton exposed to 3 ppm SO_2 at 25°C.

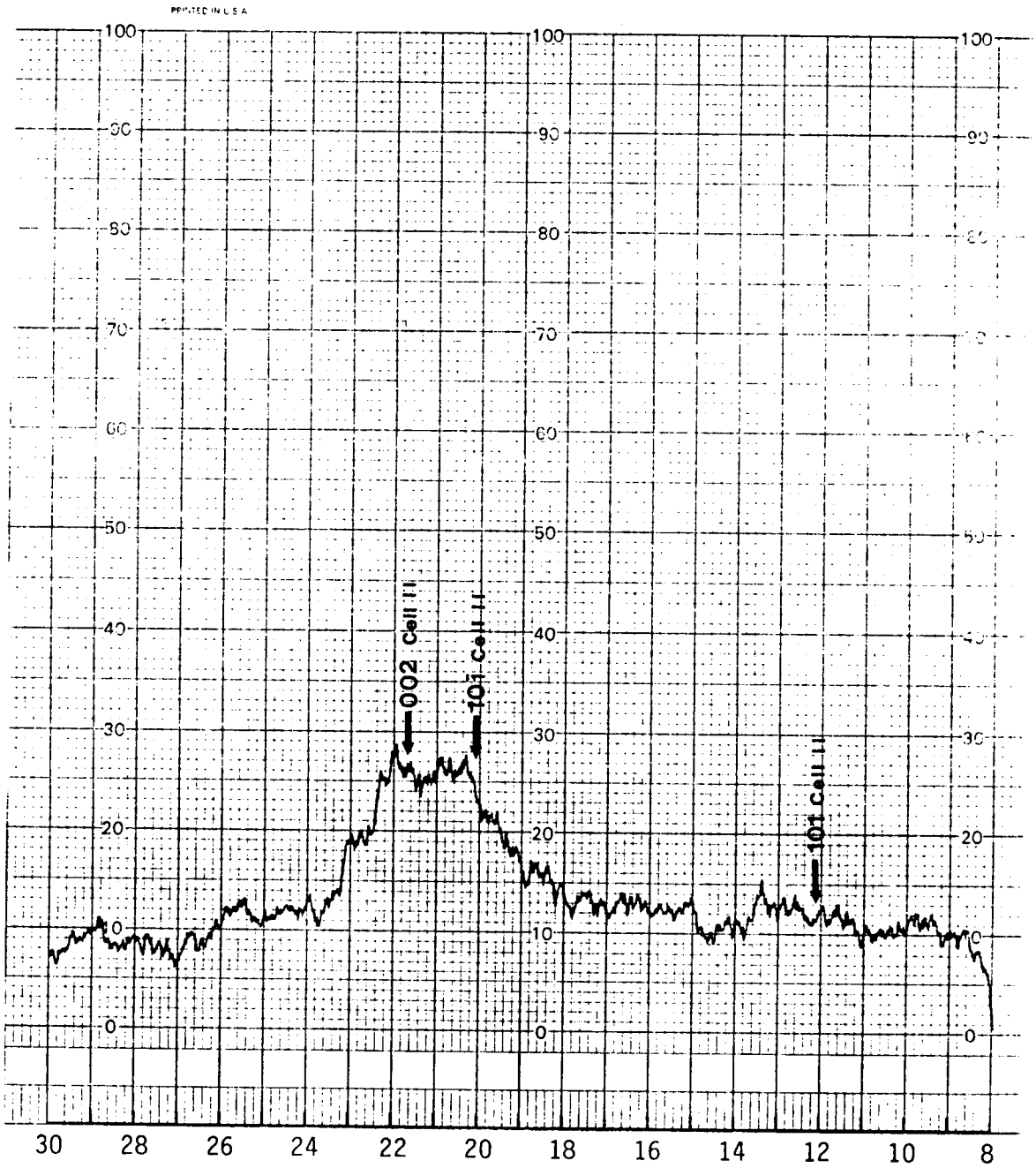


Figure A-4. X-ray diffractogram of dried viscose rayon exposed to 3 ppm SO_2 at 25°C.

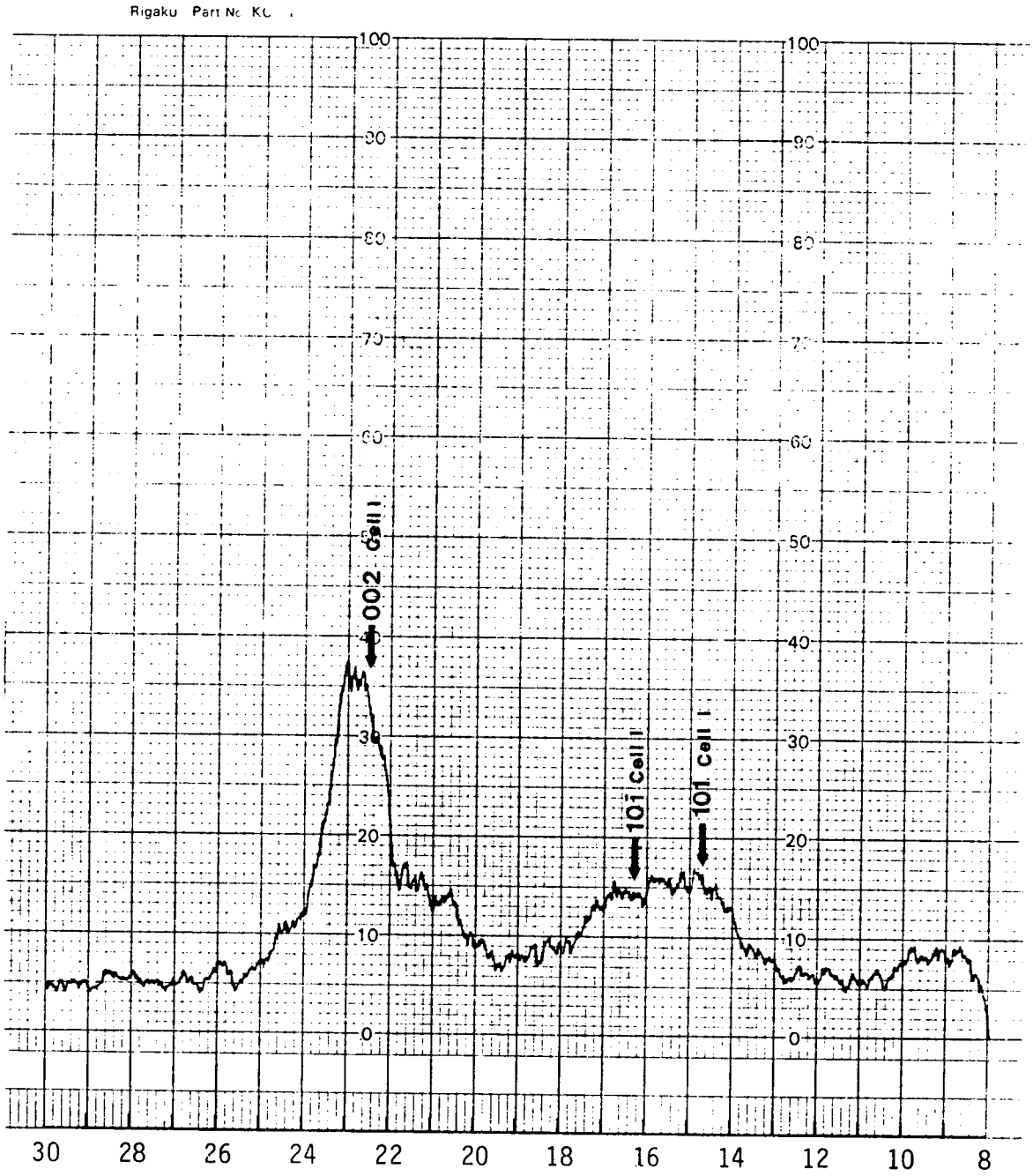


Figure A-5. X-ray diffractogram of dried extracted cotton exposed to 3 ppm SO_2 at 50°C.

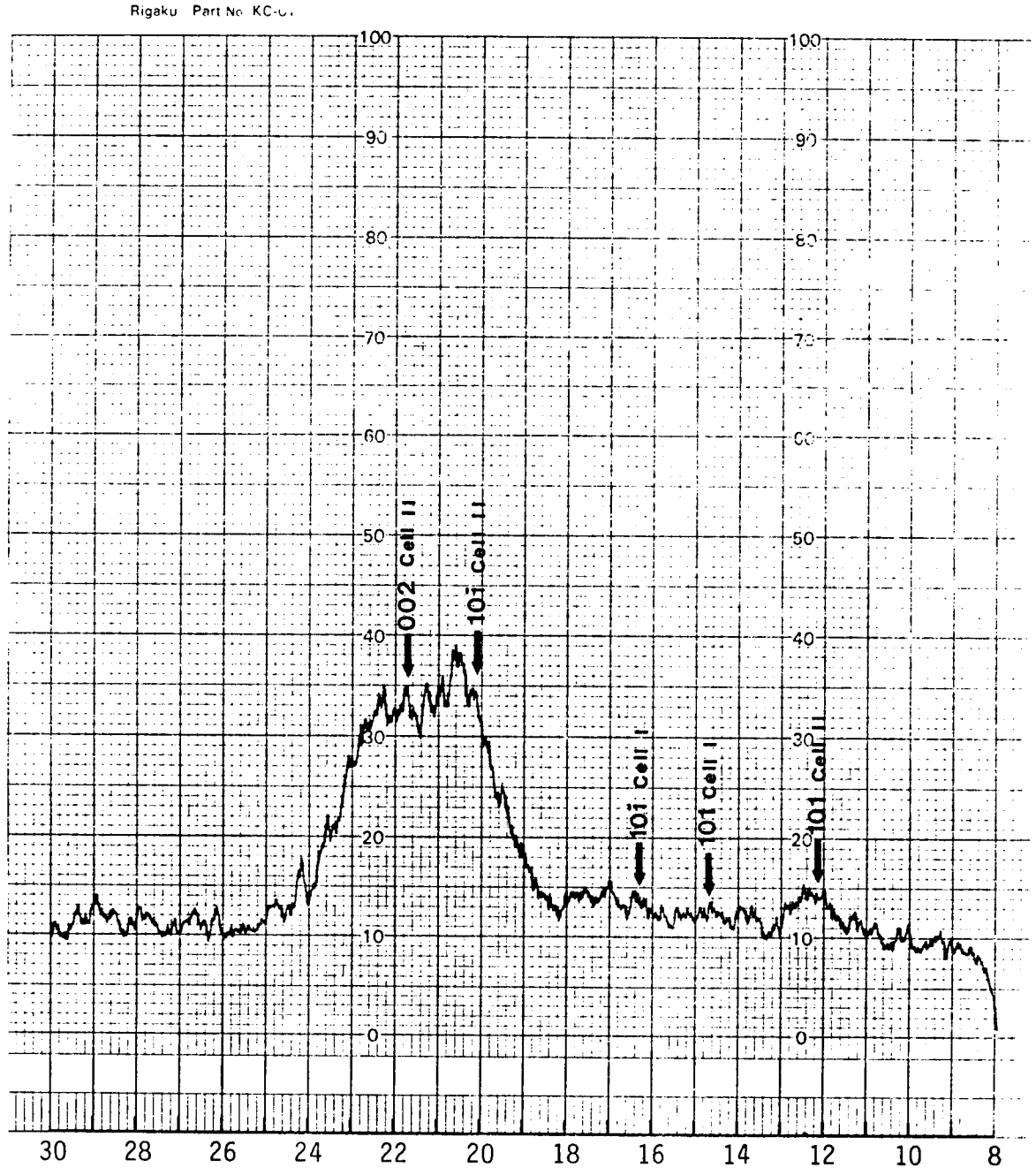


Figure A-6. X-ray diffractogram of dried mercerized cotton exposed to 3 ppm SO_2 at 50°C.

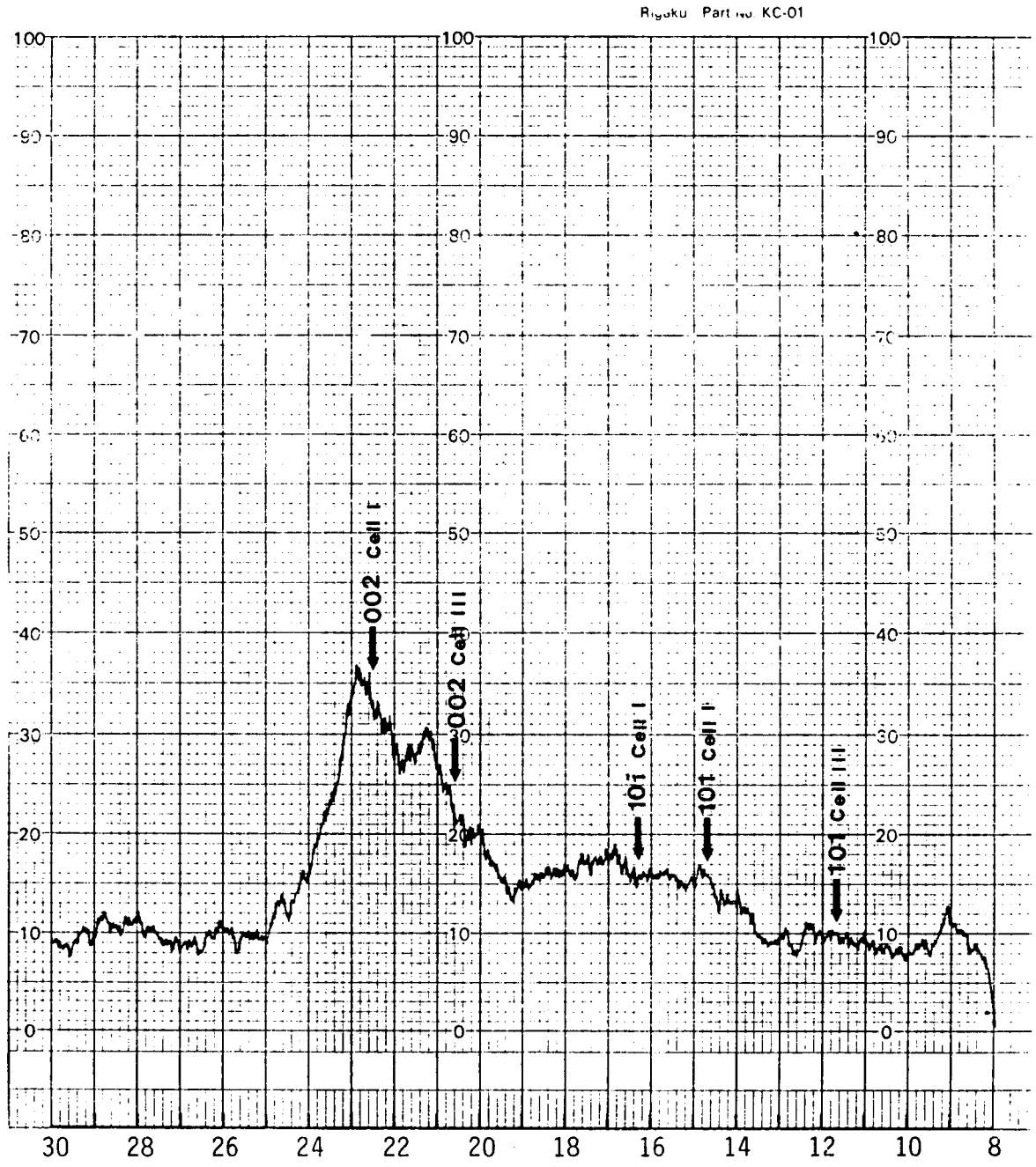


Figure A-7. X-ray diffractogram of dried $NH_3(\ell)$ treated cotton exposed to 3 ppm SO_2 at 50°C.

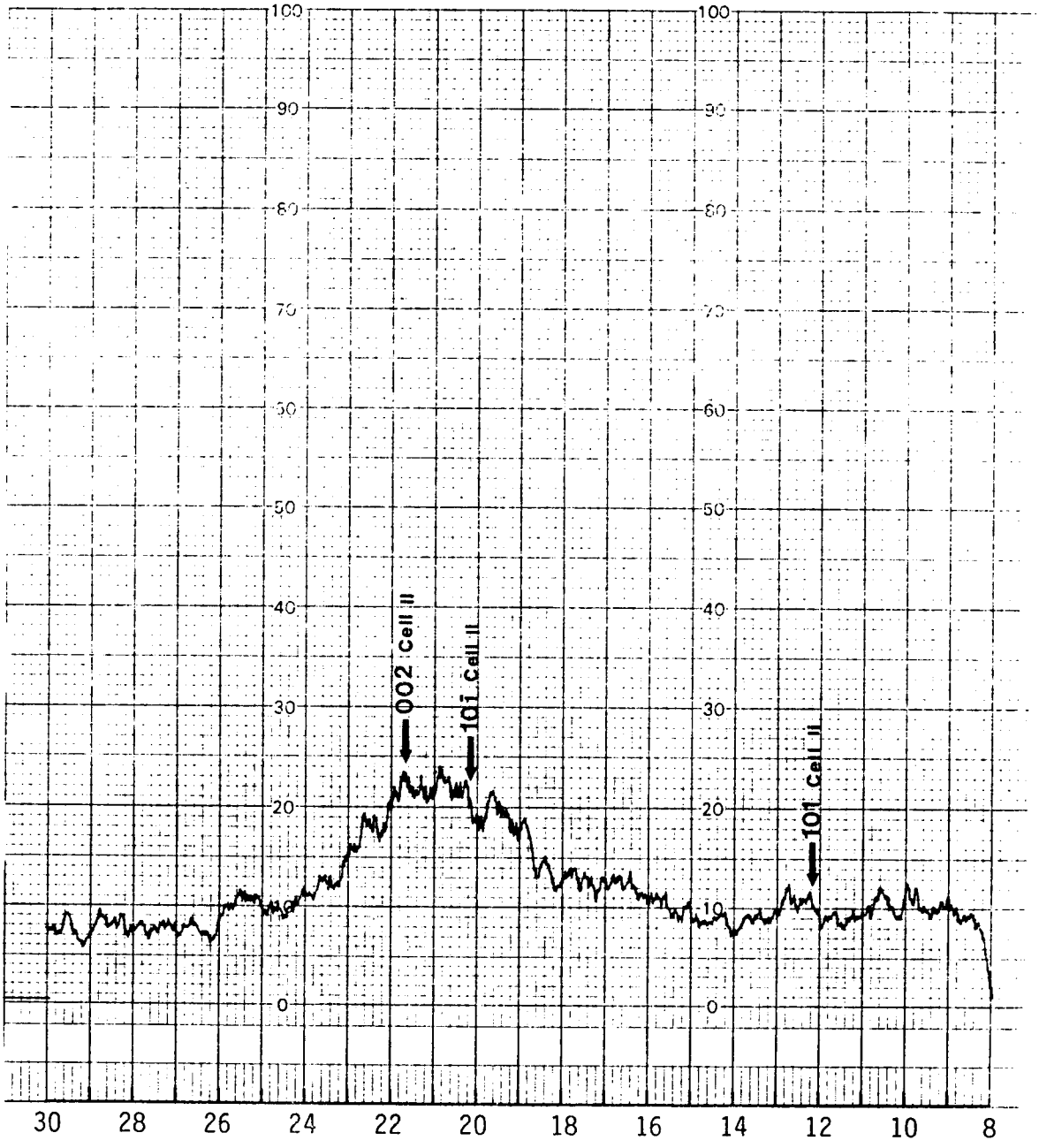


Figure A-8. X-ray diffractogram of dried viscose rayon exposed to 3 ppm SO_2 at 50°C.

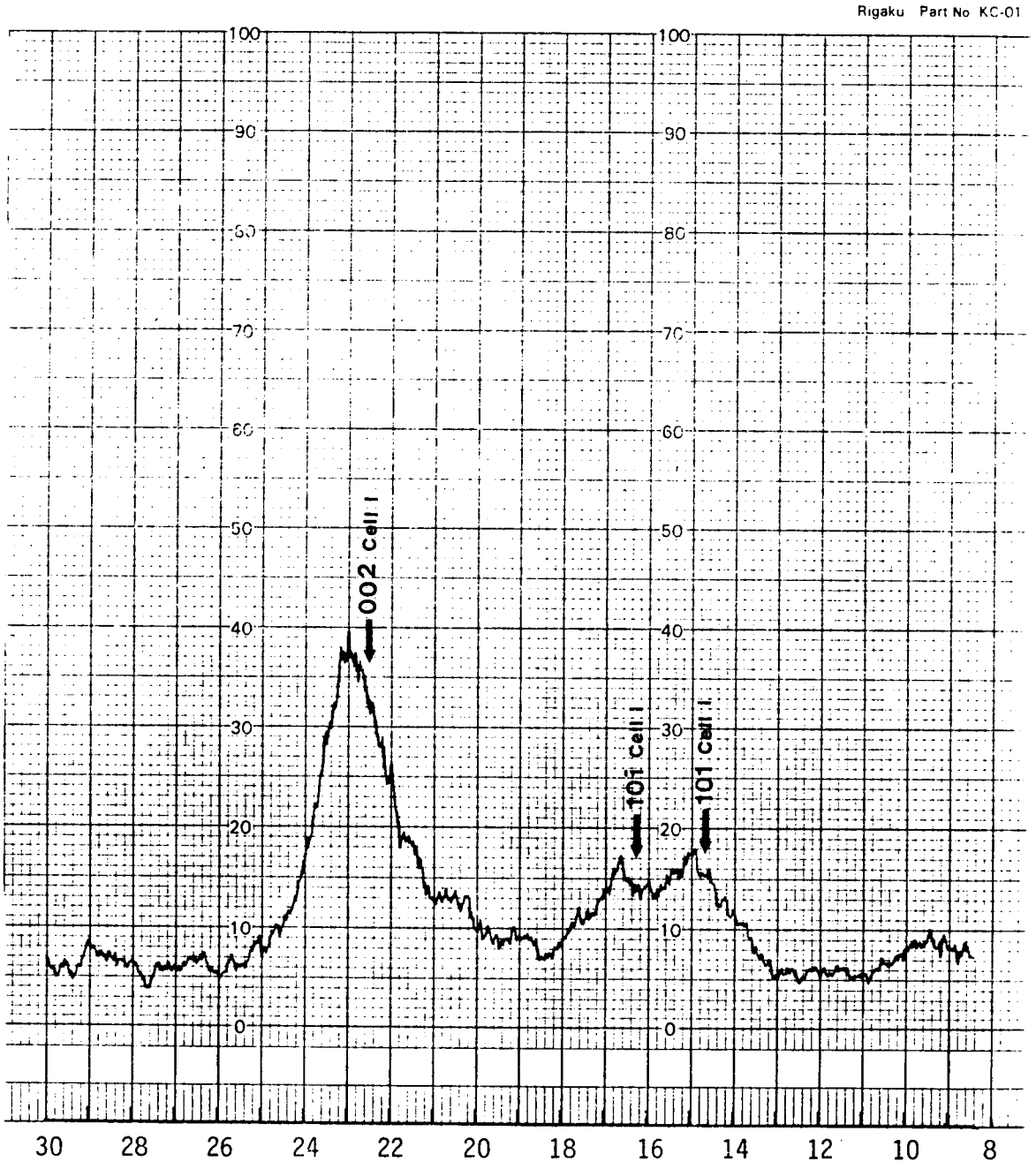


Figure A-9. X-ray diffractogram of conditioned extracted cotton exposed to 3 ppm SO_2 at 25°C.

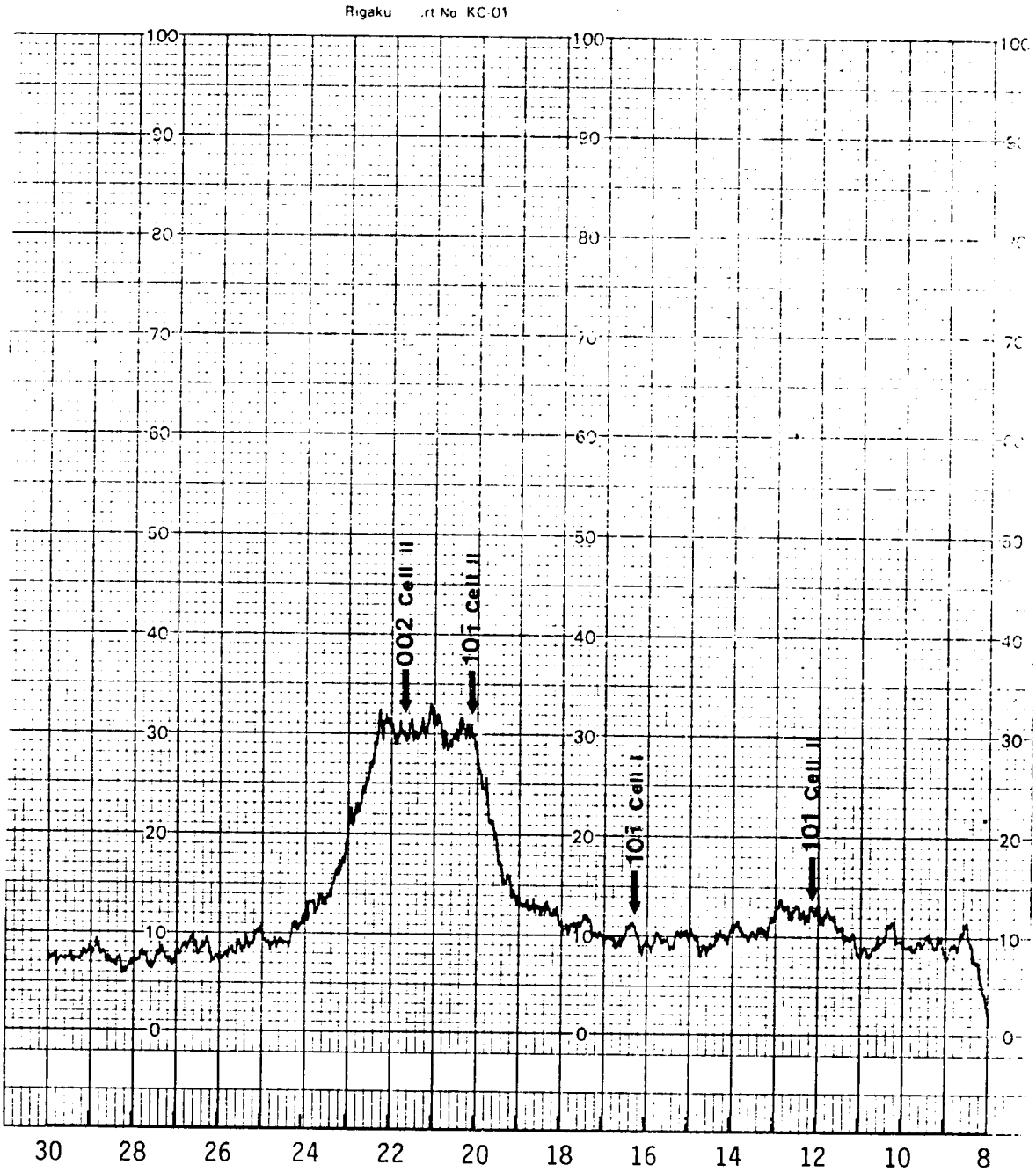


Figure A-10. X-ray diffractogram of conditioned mercerized cotton exposed to 3 ppm SO_2 at 25°C.

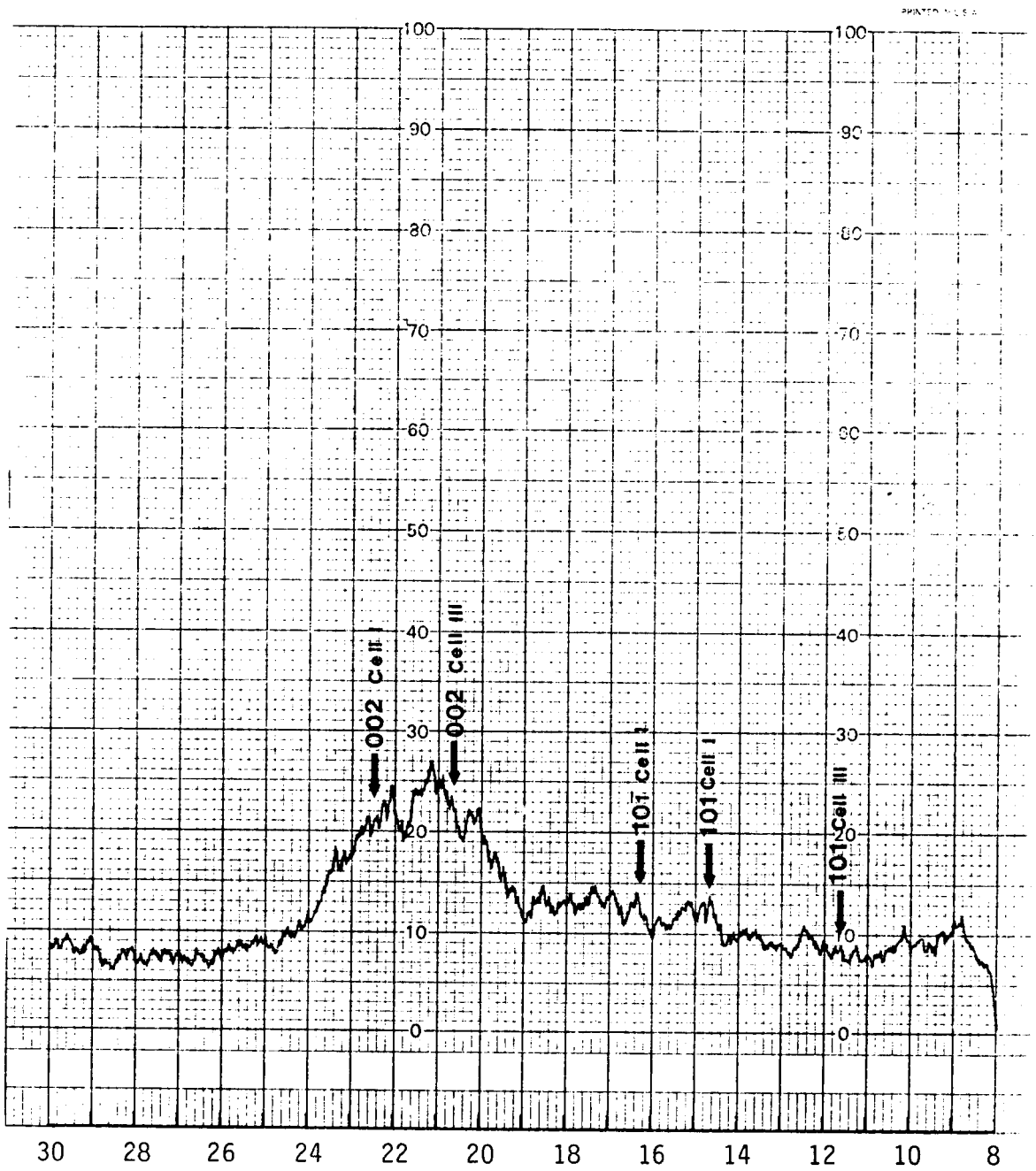
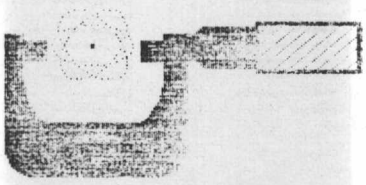


Figure A-11. X-ray diffractogram of conditioned $NH_3(\ell)$ treated cotton exposed to 3 ppm SO_2 at 25°C.

APPENDIX B

MERCURY POROSIMETRY DATA



QUANTACHROME

Extracted Cotton

FA .5CC
SAMPLE WEIGHT = .0326 GRAMS
WETTING ANGLE = 140.0000 DEGREES
SURFACE TENSION = 480.0000 ERGS/SQ CM
PRINTING EVERY 3 POINTS

PRESSURE PSIA	RADIUS ANGSTROMS	VOLUME C.C.	%V %	DV/DP C.C./PSIA	DV(R) C.C./A	DS(R) SQ M/A	AREA SQ METER
1.14	.9363E+06	0.0000	0.00	.7700E-02	.9150E-08	.1955E-09	.0000E+01
1.22	.8755E+06	0.0000	0.00	.1047E+00	.1422E-06	.3243E-08	.0000E+01
1.36	.7868E+06	.0180	.26	.3230E+00	.5312E-06	.1350E-07	.4500E-03
1.62	.6602E+06	.1753	2.54	.6221E+00	.1429E-05	.4330E-07	.4951E-02
1.94	.5502E+06	.4562	6.61	.1101E+01	.3663E-05	.1331E-06	.1463E-01
2.26	.4726E+06	.8584	12.43	.1869E+01	.9509E-05	.3601E-06	.3102E-01
2.56	.4162E+06	1.6787	24.31	.2568E+01	.1519E-04	.7301E-06	.6901E-01
2.88	.3708E+06	2.6270	38.04	.2743E+01	.2048E-04	.1105E-05	.1183E+00
3.69	.2891E+06	5.0563	73.22	.2276E+01	.2833E-04	.1960E-05	.2786E+00
3.95	.2699E+06	5.5372	80.18	.1607E+01	.2301E-04	.1705E-05	.3133E+00
4.21	.2531E+06	5.8361	84.51	.1093E+01	.1782E-04	.1408E-05	.3364E+00
4.47	.2386E+06	6.0428	87.50	.7457E+00	.1371E-04	.1149E-05	.3534E+00
4.73	.2257E+06	6.1889	89.62	.5346E+00	.1100E-04	.9748E-06	.3661E+00
4.98	.2142E+06	6.2945	91.15	.3806E+00	.8697E-05	.8121E-06	.3758E+00
5.47	.1951E+06	6.4361	93.20	.2638E+00	.7175E-05	.7356E-06	.3898E+00
5.95	.1794E+06	6.5237	94.47	.1774E+00	.5727E-05	.6380E-06	.3993E+00
6.41	.1663E+06	6.5867	95.38	.1241E+00	.4673E-05	.5620E-06	.4067E+00
6.87	.1553E+06	6.6316	96.03	.9307E-01	.4023E-05	.5180E-06	.4124E+00
7.31	.1460E+06	6.6653	96.52	.7356E-01	.3610E-05	.4947E-06	.4169E+00
7.73	.1379E+06	6.6900	96.88	.5810E-01	.3197E-05	.4635E-06	.4204E+00
8.15	.1309E+06	6.7103	97.17	.4703E-01	.2879E-05	.4400E-06	.4234E+00
8.55	.1247E+06	6.7282	97.43	.3922E-01	.2649E-05	.4250E-06	.4263E+00
8.95	.1192E+06	6.7417	97.62	.3454E-01	.2554E-05	.4283E-06	.4285E+00
9.33	.1144E+06	6.7552	97.82	.3153E-01	.2536E-05	.4435E-06	.4308E+00
9.70	.1100E+06	6.7642	97.95	.2799E-01	.2437E-05	.4433E-06	.4324E+00
10.07	.1059E+06	6.7754	98.11	.2415E-01	.2269E-05	.4286E-06	.4345E+00
10.44	.1022E+06	6.7822	98.21	.2031E-01	.2057E-05	.4017E-06	.4358E+00
10.81	.9869E+05	6.7889	98.31	.2048E-01	.2217E-05	.4495E-06	.4372E+00
11.17	.9547E+05	6.7979	98.44	.2065E-01	.2390E-05	.5007E-06	.4390E+00
11.54	.9246E+05	6.8046	98.54	.2076E-01	.2563E-05	.5544E-06	.4405E+00
11.89	.8969E+05	6.8114	98.63	.2082E-01	.2733E-05	.6095E-06	.4420E+00
12.25	.8707E+05	6.8181	98.73	.1870E-01	.2606E-05	.5985E-06	.4435E+00
12.61	.8456E+05	6.8249	98.83	.1642E-01	.2425E-05	.5737E-06	.4451E+00
12.98	.8217E+05	6.8294	98.89	.1213E-01	.1898E-05	.4620E-06	.4462E+00
13.36	.7987E+05	6.8339	98.96	.9967E-02	.1650E-05	.4133E-06	.4473E+00
13.73	.7769E+05	6.8361	98.99	.1186E-01	.2077E-05	.5346E-06	.4478E+00
14.11	.7559E+05	6.8429	99.09	.1175E-01	.2175E-05	.5753E-06	.4496E+00
14.49	.7359E+05	6.8473	99.15	.1371E-01	.2675E-05	.7271E-06	.4508E+00
14.88	.7169E+05	6.8518	99.22	.5851E-02	.1204E-05	.3358E-06	.4521E+00
15.27	.6987E+05	6.8541	99.25	.1950E-02	.4225E-06	.1209E-06	.4527E+00
15.63	.6814E+05	6.8473	99.15	.1900E-02	.4329E-06	.1271E-06	.4527E+00

Extracted Cotton (con.)

16.04	.6648E+05	6.8563	99.28	.5801E-02	.1389E-05	.4177E-06	.4554E+00
16.43	.6490E+05	6.8586	99.32	.7701E-02	.1935E-05	.5961E-06	.4561E+00
16.82	.6341E+05	6.8608	99.35	.7752E-02	.2041E-05	.6427E-06	.4568E+00
17.21	.6197E+05	6.8631	99.38	.7751E-02	.2127E-05	.6896E-06	.4575E+00
17.60	.6061E+05	6.8653	99.41	.7802E-02	.2248E-05	.7419E-06	.4582E+00
17.98	.5932E+05	6.8676	99.48	.7854E-02	.2364E-05	.7969E-06	.4589E+00
18.37	.5808E+05	6.8721	99.51	.7907E-02	.2483E-05	.8550E-06	.4605E+00
18.74	.5692E+05	6.8766	99.58	.1007E-01	.3594E-05	.1158E-05	.4621E+00
19.11	.5582E+05	6.8788	99.61	.2179E-02	.4782E-05	.9960E-06	.4629E+00
19.48	.5476E+05	6.8833	99.67	.1033E-01	.3659E-05	.1336E-05	.4645E+00
19.84	.5377E+05	6.8878	99.74	.8603E-02	.3067E-05	.1179E-05	.4662E+00
20.19	.5284E+05	6.8900	99.77	.6093E-02	.2291E-05	.9051E-06	.4670E+00
20.52	.5194E+05	6.8900	99.77	.4434E-02	.1743E-05	.6711E-06	.4670E+00
20.87	.5110E+05	6.8923	99.80	.2317E-02	.9412E-06	.3694E-06	.4679E+00
21.20	.5031E+05	6.8923	99.80	.2242E-02	.9399E-06	.3736E-06	.4677E+00
21.52	.4956E+05	6.8923	99.80	.0000E+01	.0000E+01	.0000E+01	.4689E+00
21.83	.4886E+05	6.8923	99.80	.2395E-02	.1065E-05	.4259E-06	.4689E+00
22.13	.4819E+05	6.8945	99.84	.5117E-02	.2339E-05	.9707E-06	.4697E+00
22.42	.4757E+05	6.8968	99.87	.1041E-01	.4826E-05	.2054E-05	.4707E+00
22.70	.4698E+05	6.9013	99.93	.7941E-02	.3822E-05	.1627E-05	.4726E+00
22.97	.4643E+05	6.9013	99.93	.8144E-02	.4014E-05	.1729E-05	.4726E+00
23.23	.4591E+05	6.9035	99.97	.4905E-02	.2431E-05	.1078E-05	.4735E+00
23.60	.4520E+05	6.7038	100.00	.4709E-02	.2550E-05	.1128E-05	.4745E+00
23.92	.4459E+05	6.9058	100.00	.2050E-02	.1110E-05	.4934E-06	.4745E+00

INTRUSION DISTRIBUTIONS

VOLUME
MODE = .2937E-04 C.C. / ANGSTROM AT A RADIUS OF .2964E+06 ANGSTROMS
MEAN PORE RADIUS = .3546E+06 ANGSTROMS
MEDIAN PORE RADIUS = .3853E+06 ANGSTROMS

SURFACE AREA
MODE = .2054E-05 Sq. M. / ANGSTROM AT A RADIUS OF .4757E+05 ANGSTROMS
MEAN PORE RADIUS = .2914E+06 ANGSTROMS
MEDIAN PORE RADIUS = .3570E+06 ANGSTROMS

PORE POPULATION
MODE = .1987E-02 % NUMBER / ANGSTROM AT A RADIUS OF .4757E+05 ANGSTROMS
MEAN PORE RADIUS = .2194E+06 ANGSTROMS
MEDIAN PORE RADIUS = .2432E+06 ANGSTROMS



QUANTACHROME

Mercerized Cotton

FA .5CC
SAMPLE WEIGHT = .0639 GRAMS
WETTING ANGLE = 140.0000 DEGREES
SURFACE TENSION = 480.0000 ERGS/SQ CM
PRINTING EVERY 3 POINTS

PRESSURE PSIA	RADIUS ANGSTROMS	VOLUME C.C.	%V %	DV/DP C.C./PSIA	DV(R) C.C./A	DS(R) SQ M/A	AREA SQ METER
1.65	.6459E+06	0.0000	0.00	.0000E+01	.0000E+01	.0000E+01	.0000E+01
1.73	.6162E+06	0.0000	0.00	.1130E+00	.3117E-06	.1012E-07	.0000E+01
1.88	.5643E+06	.0355	.74	.3783E+00	.1213E-05	.4284E-07	.1248E-02
2.20	.4828E+06	.2316	4.83	.9956E+00	.4225E-05	.1739E-06	.8986E-02
2.63	.4062E+06	.8567	17.91	.1516E+01	.9274E-05	.4566E-06	.3852E-01
3.71	.2875E+06	3.1620	65.93	.1677E+01	.2069E-04	.1460E-05	.1882E+00
4.04	.2640E+06	3.6332	75.76	.1351E+01	.2009E-04	.1522E-05	.2229E+00
4.36	.2445E+06	3.9519	82.40	.9077E+00	.1581E-04	.1294E-05	.2482E+00
4.67	.2282E+06	4.1629	86.80	.6213E+00	.1244E-04	.1090E-05	.2662E+00
4.98	.2141E+06	4.3027	89.72	.4242E+00	.9676E-05	.9040E-06	.2790E+00
5.29	.2016E+06	4.3990	91.73	.2975E+00	.7655E-05	.7592E-06	.2884E+00
5.59	.1908E+06	4.4690	93.19	.2190E+00	.6299E-05	.6602E-06	.2956E+00
5.88	.1813E+06	4.5206	94.26	.1689E+00	.5387E-05	.5942E-06	.3012E+00
6.17	.1729E+06	4.5607	95.10	.1304E+00	.4581E-05	.5298E-06	.3057E+00
6.45	.1657E+06	4.5917	95.74	.1033E+00	.3972E-05	.4805E-06	.3094E+00
6.73	.1585E+06	4.6157	96.25	.8387E-01	.3515E-05	.4437E-06	.3124E+00
7.00	.1523E+06	4.6364	96.68	.7037E-01	.3195E-05	.4196E-06	.3151E+00
7.27	.1467E+06	4.6524	97.01	.5871E-01	.2874E-05	.3919E-06	.3172E+00
7.53	.1416E+06	4.6662	97.30	.4979E-01	.2619E-05	.3699E-06	.3190E+00
7.79	.1369E+06	4.6776	97.54	.4299E-01	.2421E-05	.3538E-06	.3208E+00
8.05	.1326E+06	4.6868	97.73	.3758E-01	.2257E-05	.3404E-06	.3222E+00
8.30	.1285E+06	4.6960	97.92	.3188E-01	.2037E-05	.3170E-06	.3236E+00
8.67	.1236E+06	4.7052	98.11	.2755E-01	.1906E-05	.3084E-06	.3251E+00
9.13	.1169E+06	4.7178	98.37	.2389E-01	.1832E-05	.3136E-06	.3272E+00
9.54	.1118E+06	4.7258	98.54	.1936E-01	.1623E-05	.2902E-06	.3286E+00
9.95	.1072E+06	4.7327	98.69	.1626E-01	.1483E-05	.2766E-06	.3299E+00
10.35	.1030E+06	4.7384	98.80	.1409E-01	.1393E-05	.2705E-06	.3310E+00
10.84	.9844E+05	4.7453	98.95	.1345E-01	.1458E-05	.2962E-06	.3323E+00
11.31	.9428E+05	4.7510	99.07	.1121E-01	.1327E-05	.2814E-06	.3335E+00
11.79	.9048E+05	4.7556	99.16	.8097E-02	.1041E-05	.2301E-06	.3345E+00
12.26	.8702E+05	4.7579	99.21	.6559E-02	.9121E-06	.2096E-06	.3350E+00
12.72	.8384E+05	4.7613	99.28	.6650E-02	.9967E-06	.2378E-06	.3359E+00
13.18	.8095E+05	4.7648	99.35	.6686E-02	.1076E-05	.2659E-06	.3367E+00
13.63	.7825E+05	4.7671	99.40	.5883E-02	.1013E-05	.2590E-06	.3373E+00
14.09	.7572E+05	4.7694	99.45	.5005E-02	.9210E-06	.2433E-06	.3379E+00
14.55	.7332E+05	4.7716	99.50	.5809E-02	.1140E-05	.3111E-06	.3385E+00
15.01	.7106E+05	4.7751	99.57	.4950E-02	.1035E-05	.2912E-06	.3395E+00
15.47	.6893E+05	4.7774	99.62	.4950E-02	.1100E-05	.3192E-06	.3401E+00
15.94	.6692E+05	4.7797	99.67	.4110E-02	.9694E-06	.2897E-06	.3408E+00
16.40	.6502E+05	4.7820	99.71	.4931E-02	.1232E-05	.3791E-06	.3415E+00
16.87	.6323E+05	4.7831	99.74	.4110E-02	.1086E-05	.3436E-06	.3419E+00

Mercerized Cotton (con.)

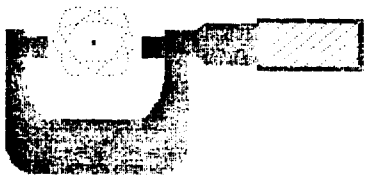
17.33	.6133E+05	4.7954	99.78	.1644E-02	.4585E-06	.1492E-06	.2426E+00
17.80	.5994E+05	4.7954	99.76	.3280E-02	.9951E-06	.3320E-06	.2426E+00
18.25	.5844E+05	4.7877	99.83	.3298E-02	.1053E-05	.3602E-06	.2438E+00
18.70	.5703E+05	4.7900	99.88	.5079E-02	.1652E-05	.5754E-06	.2446E+00
19.15	.5571E+05	4.7911	99.90	.2579E-02	.8795E-06	.3157E-06	.2450E+00
19.58	.5447E+05	4.7911	99.90	.1739E-02	.6204E-06	.2278E-06	.2450E+00
20.01	.5331E+05	4.7922	99.93	.1802E-02	.6715E-06	.2519E-06	.2454E+00
20.43	.5222E+05	4.7934	99.95	.9221E-03	.3583E-06	.1372E-06	.2458E+00
20.83	.5120E+05	4.7934	99.95	.9221E-03	.3727E-06	.1436E-06	.2458E+00
21.23	.5025E+05	4.7934	99.95	.1022E-02	.4291E-06	.1708E-06	.2458E+00
21.61	.4936E+05	4.7946	99.98	.1022E-02	.4447E-06	.1905E-06	.2463E+00
21.98	.4850E+05	4.7946	99.98	.1022E-02	.4605E-06	.1998E-06	.2463E+00
22.33	.4776E+05	4.7946	99.98	.1112E-02	.5173E-06	.2166E-06	.2463E+00
22.69	.4703E+05	4.7957	100.00	.1112E-02	.5374E-06	.2248E-06	.2468E+00
23.04	.4637E+05	4.7957	100.00	.1112E-02	.5489E-06	.2367E-06	.2468E+00
23.31	.4575E+05	4.7957	100.00	.0000E+01	.0000E+01	.0000E+01	.2468E+00
23.61	.4517E+05	4.7957	100.00	.0000E+01	.0000E+01	.0000E+01	.2468E+00
23.90	.4463E+05	4.7957	100.00	.0000E+01	.0000E+01	.0000E+01	.2468E+00

INTRUSION DISTRIBUTIONS

VOLUME
MODE = .2154E+04 C.C. / ANGSTROM AT A RADIUS OF .2791E+06 ANGSTROMS
MEAN PORE RADIUS = .3159E+06 ANGSTROMS
MEDIAN PORE RADIUS = .3658E+06 ANGSTROMS

SURFACE AREA
MODE = .1562E+05 SQ. M. / ANGSTROM AT A RADIUS OF .2715E+06 ANGSTROMS
MEAN PORE RADIUS = .2766E+06 ANGSTROMS
MEDIAN PORE RADIUS = .3652E+06 ANGSTROMS

PORE POPULATION
MODE = .6817E+03 % NUMBER / ANGSTROM AT A RADIUS OF .5702E+05 ANGSTROMS
MEAN PORE RADIUS = .2027E+06 ANGSTROMS
MEDIAN PORE RADIUS = .2570E+06 ANGSTROMS



QUANTACHROME

$NH_3(\ell)$ Treated Cotton

FA .SCD
SAMPLE WEIGHT = .0865 GRAMS
WETTING ANGLE = 140.0000 DEGREES
SURFACE TENSION = 480.0000 ERGS/SQ CM
PRINTING EVERY 3 POINTS

PRESSURE PSIA	RADIUS ANGSTROMS	VOLUME C.C.	%V %	DV/DP C.C./PSIA	DV(R) C.C./A	DS(R) SQ M/A	AREA SQ METER
2.49	.4279E+06	0.0000	0.00	.8097E-01	.4665E-06	.2161E-07	.0000E+01
2.63	.4052E+06	.0136	.39	.5796E+00	.3670E-05	.1811E-06	.6640E-03
2.92	.3658E+06	.2973	8.60	.1159E+01	.8508E-05	.4871E-06	.1586E-01
3.69	.2891E+06	1.9048	55.08	.1496E+01	.1866E-04	.1291E-05	.1223E+00
3.94	.2706E+06	2.2512	65.10	.1242E+01	.1770E-04	.1309E-05	.1473E+00
4.43	.2409E+06	2.6992	78.06	.7985E+00	.1414E-04	.1173E-05	.1829E+00
4.90	.2179E+06	2.9255	84.89	.4691E+00	.1021E-04	.9369E-06	.2038E+00
5.35	.1992E+06	3.0668	88.68	.2713E+00	.7085E-05	.7112E-06	.2166E+00
5.80	.1838E+06	3.1481	91.04	.1719E+00	.5286E-05	.5750E-06	.2252E+00
6.24	.1709E+06	3.2031	92.63	.1183E+00	.4219E-05	.4776E-06	.2315E+00
6.67	.1600E+06	3.2421	93.75	.8758E-01	.3573E-05	.4467E-06	.2362E+00
7.07	.1505E+06	3.2717	94.61	.6644E-01	.3067E-05	.4075E-06	.2401E+00
7.49	.1424E+06	3.2946	95.27	.5384E-01	.2780E-05	.3905E-06	.2432E+00
7.89	.1352E+06	3.3132	95.81	.4375E-01	.2509E-05	.3711E-06	.2459E+00
8.27	.1290E+06	3.3276	96.23	.3619E-01	.2286E-05	.3545E-06	.2481E+00
8.65	.1234E+06	3.3395	96.57	.3107E-01	.2146E-05	.3478E-06	.2500E+00
9.01	.1184E+06	3.3496	96.87	.2619E-01	.1966E-05	.3321E-06	.2517E+00
9.37	.1138E+06	3.3581	97.11	.2412E-01	.1961E-05	.3446E-06	.2532E+00
9.74	.1095E+06	3.3666	97.35	.2029E-01	.1780E-05	.3251E-06	.2547E+00
10.10	.1056E+06	3.3734	97.55	.1882E-01	.1777E-05	.3365E-06	.2560E+00
10.45	.1020E+06	3.3793	97.72	.1654E-01	.1675E-05	.3284E-06	.2571E+00
10.81	.9866E+05	3.3852	97.89	.1585E-01	.1717E-05	.3482E-06	.2583E+00
11.17	.9553E+05	3.3903	98.04	.1432E-01	.1656E-05	.3467E-06	.2594E+00
11.52	.9260E+05	3.3945	98.16	.1277E-01	.1571E-05	.3396E-06	.2603E+00
11.87	.8984E+05	3.3980	98.29	.1124E-01	.1471E-05	.3275E-06	.2612E+00
12.22	.8726E+05	3.4021	98.38	.1052E-01	.1459E-05	.3343E-06	.2620E+00
12.57	.8488E+05	3.4064	98.51	.8990E-02	.1319E-05	.3108E-06	.2630E+00
12.91	.8260E+05	3.4089	98.58	.8943E-02	.1386E-05	.3356E-06	.2636E+00
13.26	.8043E+05	3.4123	98.68	.8872E-02	.1450E-05	.3606E-06	.2644E+00
13.61	.7834E+05	3.4157	98.78	.8780E-02	.1513E-05	.3861E-06	.2652E+00
13.97	.7634E+05	3.4182	98.85	.7914E-02	.1426E-05	.3761E-06	.2659E+00
14.33	.7444E+05	3.4208	98.92	.6896E-02	.1202E-05	.3229E-06	.2666E+00
14.69	.7261E+05	3.4233	99.00	.6251E-02	.1254E-05	.3455E-06	.2672E+00
15.05	.7086E+05	3.4250	99.04	.6229E-02	.1313E-05	.3705E-06	.2678E+00
15.42	.6918E+05	3.4276	99.12	.6186E-02	.1360E-05	.3954E-06	.2685E+00
15.78	.6759E+05	3.4292	99.17	.5389E-02	.1249E-05	.3695E-06	.2690E+00
16.15	.6604E+05	3.4318	99.24	.4613E-02	.1120E-05	.3291E-06	.2698E+00
16.52	.6457E+05	3.4326	99.27	.4634E-02	.1177E-05	.3644E-06	.2700E+00
16.88	.6318E+05	3.4352	99.34	.4655E-02	.1235E-05	.3910E-06	.2708E+00
17.25	.6183E+05	3.4369	99.39	.4655E-02	.1290E-05	.4171E-06	.2714E+00
17.62	.6054E+05	3.4386	99.44	.4655E-02	.1345E-05	.4444E-06	.2719E+00

$NH_3(\ell)$ Treated Cotton

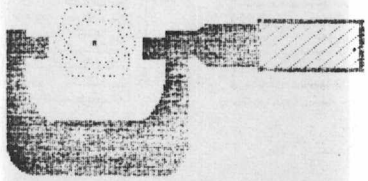
17.98	.5932E+05	3.4403	99.49	.4677E-02	.1408E-05	.4748E-06	.2725E+00
18.34	.5815E+05	3.4420	99.53	.3924E-02	.1130E-05	.4229E-06	.2731E+00
18.70	.5704E+05	3.4428	99.56	.3292E-02	.1300E-05	.4599E-06	.2734E+00
19.05	.5599E+05	3.4436	99.58	.2829E-02	.1096E-05	.3914E-06	.2737E+00
19.40	.5498E+05	3.4450	99.63	.4084E-02	.1432E-05	.5211E-06	.2743E+00
19.75	.5402E+05	3.4470	99.69	.3311E-02	.1201E-05	.4455E-06	.2749E+00
20.09	.5310E+05	3.4479	99.71	.3336E-02	.1255E-05	.4726E-06	.2752E+00
20.42	.5223E+05	3.4487	99.73	.2566E-02	.9976E-06	.3820E-06	.2755E+00
20.75	.5141E+05	3.4496	99.76	.3493E-02	.1402E-05	.5453E-06	.2759E+00
21.07	.5063E+05	3.4504	99.78	.2578E-02	.1481E-05	.5852E-06	.2762E+00
21.38	.4989E+05	3.4513	99.80	.2705E-02	.1154E-05	.4625E-06	.2765E+00
21.69	.4919E+05	3.4521	99.83	.1894E-02	.8710E-06	.3479E-06	.2769E+00
21.98	.4853E+05	3.4530	99.85	.1961E-02	.8841E-06	.3644E-06	.2772E+00
22.27	.4790E+05	3.4538	99.88	.2958E-02	.1369E-05	.5716E-06	.2776E+00
22.55	.4730E+05	3.4547	99.90	.3070E-02	.1457E-05	.6162E-06	.2779E+00
22.82	.4674E+05	3.4555	99.93	.3148E-02	.1530E-05	.6546E-06	.2783E+00
23.08	.4621E+05	3.4564	99.95	.2925E-02	.1455E-05	.6279E-06	.2787E+00
23.37	.4564E+05	3.4572	99.98	.2648E-02	.1349E-05	.5912E-06	.2790E+00
23.73	.4494E+05	3.4580	100.00	.1574E-02	.8269E-06	.3680E-06	.2794E+00

INTRUSION DISTRIBUTIONS

VOLUME
MODE = .1950E-04 C.C. / ANGSTROM AT A RADIUS OF .2827E+06 ANGSTROMS
MEAN PORE RADIUS = .2648E+06 ANGSTROMS
MEDIAN PORE RADIUS = .2765E+06 ANGSTROMS

SURFACE AREA
MODE = .1390E-05 SQ. M. / ANGSTROM AT A RADIUS OF .2765E+06 ANGSTROMS
MEAN PORE RADIUS = .2475E+06 ANGSTROMS
MEDIAN PORE RADIUS = .2827E+06 ANGSTROMS

PORE POPULATION
MODE = .1008E-02 % NUMBER / ANGSTROM AT A RADIUS OF .4674E+05 ANGSTROMS
MEAN PORE RADIUS = .2012E+06 ANGSTROMS
MEDIAN PORE RADIUS = .2250E+06 ANGSTROMS



QUANTACHROME

Viscose Rayon

FA .5CC
SAMPLE WEIGHT = .0694 GRAMS
WETTING ANGLE = 140.0000 DEGREES
SURFACE TENSION = 480.0000 ERGS/SQ CM
PRINTING EVERY 3 POINTS

PRESSURE PSIA	RADIUS ANGSTROMS	VOLUME C.C.	%V %	DV/DP C.C./PSIA	DV(R) C.C./A	DS(R) SQ M/A	AREA SQ METER
1.78	.5987E+06	.0063	.26	.2023E+00	.5944E-06	.1985E-07	.1410E-03
1.86	.5721E+06	.0232	.94	.2924E+00	.9363E-06	.3273E-07	.7230E-03
1.96	.5454E+06	.0538	2.17	.5041E+00	.1776E-05	.6514E-07	.1832E-02
2.06	.5170E+06	.1341	5.41	.9010E+00	.3533E-05	.1367E-06	.4886E-02
2.18	.4897E+06	.2692	10.86	.1342E+01	.5859E-05	.2393E-06	.1032E-01
2.30	.4634E+06	.4845	19.56	.1562E+01	.7617E-05	.3288E-06	.1946E-01
2.43	.4398E+06	.6840	27.61	.1652E+01	.8962E-05	.4076E-06	.2837E-01
2.54	.4191E+06	.8667	34.98	.1632E+01	.9753E-05	.4654E-06	.3695E-01
2.67	.3997E+06	1.0936	44.14	.1543E+01	.1014E-04	.5075E-06	.4813E-01
2.80	.3814E+06	1.2657	51.09	.1344E+01	.9706E-05	.5090E-06	.5700E-01
2.93	.3638E+06	1.4209	57.35	.1037E+01	.8224E-05	.4521E-06	.6540E-01
3.31	.3221E+06	1.7523	70.73	.7952E+00	.7911E-05	.4913E-06	.8543E-01
3.64	.2931E+06	1.9413	78.36	.5510E+00	.6637E-05	.4528E-06	.9792E-01
3.96	.2694E+06	2.0680	83.47	.3649E+00	.5220E-05	.3875E-06	.1070E+00
4.28	.2495E+06	2.1535	86.92	.2520E+00	.4213E-05	.3377E-06	.1137E+00
4.59	.2324E+06	2.2126	89.31	.1762E+00	.3399E-05	.2925E-06	.1187E+00
4.90	.2179E+06	2.2548	91.01	.1255E+00	.2762E-05	.2535E-06	.1225E+00
5.20	.2050E+06	2.2823	92.12	.9285E-01	.2310E-05	.2253E-06	.1251E+00
5.50	.1940E+06	2.3065	93.10	.7720E-01	.2149E-05	.2216E-06	.1275E+00
5.79	.1842E+06	2.3276	93.95	.6317E-01	.1953E-05	.2121E-06	.1298E+00
6.08	.1755E+06	2.3424	94.55	.5163E-01	.1760E-05	.2006E-06	.1314E+00
6.36	.1678E+06	2.3540	95.01	.4141E-01	.1546E-05	.1843E-06	.1328E+00
6.63	.1608E+06	2.3646	95.44	.3560E-01	.1449E-05	.1802E-06	.1341E+00
6.91	.1544E+06	2.3741	95.82	.2966E-01	.1309E-05	.1695E-06	.1353E+00
7.18	.1486E+06	2.3804	96.08	.2837E-01	.1353E-05	.1822E-06	.1362E+00
7.45	.1431E+06	2.3878	96.38	.2470E-01	.1270E-05	.1775E-06	.1372E+00
7.72	.1381E+06	2.3941	96.63	.2088E-01	.1153E-05	.1670E-06	.1381E+00
7.99	.1335E+06	2.3984	96.80	.1582E-01	.9360E-06	.1402E-06	.1387E+00
8.25	.1292E+06	2.4015	96.93	.1577E-01	.9967E-06	.1543E-06	.1392E+00
8.52	.1252E+06	2.4068	97.15	.1453E-01	.9788E-06	.1564E-06	.1400E+00
8.79	.1214E+06	2.4110	97.32	.1329E-01	.9524E-06	.1569E-06	.1407E+00
9.05	.1179E+06	2.4131	97.40	.9373E-02	.7127E-06	.1209E-06	.1411E+00
9.31	.1145E+06	2.4163	97.53	.9373E-02	.7549E-06	.1318E-06	.1416E+00
9.57	.1114E+06	2.4174	97.57	.9427E-02	.8023E-06	.1440E-06	.1418E+00
9.83	.1085E+06	2.4205	97.70	.8088E-02	.7266E-06	.1339E-06	.1424E+00
10.09	.1057E+06	2.4226	97.78	.8141E-02	.7704E-06	.1458E-06	.1428E+00
10.35	.1031E+06	2.4248	97.87	.4070E-02	.4052E-06	.7861E-07	.1432E+00
10.60	.1006E+06	2.4248	97.87	.2731E-02	.2855E-06	.5675E-07	.1432E+00
10.88	.9802E+05	2.4248	97.87	.0000E+01	.0000E+01	.0000E+01	.1432E+00
11.16	.9556E+05	2.4248	97.87	.3536E-02	.4089E-06	.8558E-07	.1432E+00
11.47	.9303E+05	2.4269	97.95	.4624E-02	.5644E-06	.1213E-06	.1436E+00

Viscose Rayon (con.)

11.77	.9064E+05	2.4290	98.04	.6739E-02	.8748E-06	.1930E-06	.1441E+00
12.07	.8838E+05	2.4311	98.13	.9791E-02	.1325E-05	.2998E-06	.1446E+00
12.37	.8624E+05	2.4330	98.30	.1088E-01	.1547E-05	.3587E-06	.1456E+00
12.69	.8404E+05	2.4390	98.47	.1091E-01	.1604E-05	.3869E-06	.1466E+00
13.01	.8200E+05	2.4417	98.55	.6633E-02	.1044E-05	.2546E-06	.1471E+00
13.32	.8007E+05	2.4427	98.59	.4457E-02	.7358E-06	.1838E-06	.1473E+00
13.63	.7825E+05	2.4438	98.64	.2246E-02	.3884E-06	.9529E-07	.1476E+00
13.94	.7653E+05	2.4438	98.64	.1160E-02	.2096E-06	.5483E-07	.1476E+00
14.24	.7490E+05	2.4438	98.64	.5842E-02	.1103E-05	.2945E-06	.1476E+00
14.54	.7335E+05	2.4480	98.81	.1048E-01	.2044E-05	.5628E-06	.1487E+00
14.84	.7185E+05	2.4512	98.93	.1080E-01	.2627E-05	.7213E-06	.1496E+00
15.15	.7041E+05	2.4542	99.06	.1215E-01	.2728E-05	.7747E-06	.1505E+00
15.45	.6903E+05	2.4596	99.28	.8173E-02	.1806E-05	.5233E-06	.1520E+00
15.75	.6770E+05	2.4607	99.32	.3481E-02	.8049E-06	.2378E-06	.1523E+00
16.06	.6643E+05	2.4596	99.28	.0000E+01	.0000E+01	.0000E+01	.1523E+00
16.36	.6520E+05	2.4596	99.28	.0000E+01	.0000E+01	.0000E+01	.1523E+00
16.66	.6402E+05	2.4585	99.23	.0000E+01	.0000E+01	.0000E+01	.1523E+00
16.96	.6288E+05	2.4585	99.23	.0000E+01	.0000E+01	.0000E+01	.1523E+00
17.26	.6179E+05	2.4575	99.19	.0000E+01	.0000E+01	.0000E+01	.1523E+00
17.56	.6074E+05	2.4564	99.15	.1203E-02	.2459E-06	.1179E-06	.1523E+00
17.85	.5974E+05	2.4575	99.19	.2404E-02	.7144E-06	.2391E-06	.1527E+00
18.15	.5877E+05	2.4575	99.19	.4807E-02	.1476E-05	.5023E-06	.1530E+00
18.44	.5785E+05	2.4585	99.23	.4808E-02	.1552E-05	.5353E-06	.1534E+00
18.73	.5696E+05	2.4620	99.40	.6131E-02	.2035E-05	.7041E-06	.1549E+00
19.01	.5610E+05	2.4628	99.40	.6217E-02	.2096E-05	.7473E-06	.1552E+00
19.30	.5528E+05	2.4670	99.57	.1197E-02	.4156E-06	.1504E-06	.1569E+00
19.58	.5448E+05	2.4649	99.49	.0000E+01	.0000E+01	.0000E+01	.1569E+00
19.86	.5374E+05	2.4607	99.32	.0000E+01	.0000E+01	.0000E+01	.1569E+00
20.13	.5301E+05	2.4585	99.23	.0000E+01	.0000E+01	.0000E+01	.1569E+00
20.39	.5233E+05	2.4575	99.19	.0000E+01	.0000E+01	.0000E+01	.1569E+00
20.64	.5169E+05	2.4575	99.19	.1123E-02	.4467E-06	.1729E-06	.1569E+00
20.90	.5106E+05	2.4596	99.28	.7376E-02	.2937E-05	.1135E-05	.1576E+00
21.19	.5040E+05	2.4617	99.36	.8718E-02	.3486E-05	.1370E-05	.1584E+00
21.49	.4976E+05	2.4649	99.49	.1478E-01	.6152E-05	.2479E-05	.1597E+00
21.79	.4890E+05	2.4723	99.79	.9404E-02	.4167E-05	.1702E-05	.1627E+00
22.07	.4903E+05	2.4712	99.74	.9661E-02	.4392E-05	.1818E-05	.1627E+00
22.34	.4774E+05	2.4744	99.87	.2529E-02	.1179E-05	.4940E-06	.1640E+00
22.61	.4717E+05	2.4744	99.87	.3975E-02	.1898E-05	.8047E-06	.1645E+00
22.87	.4665E+05	2.4754	99.91	.4003E-02	.1967E-05	.8444E-06	.1654E+00
23.12	.4614E+05	2.4765	99.96	.7812E-02	.3903E-05	.1691E-05	.1658E+00

INTRUSION DISTRIBUTIONS

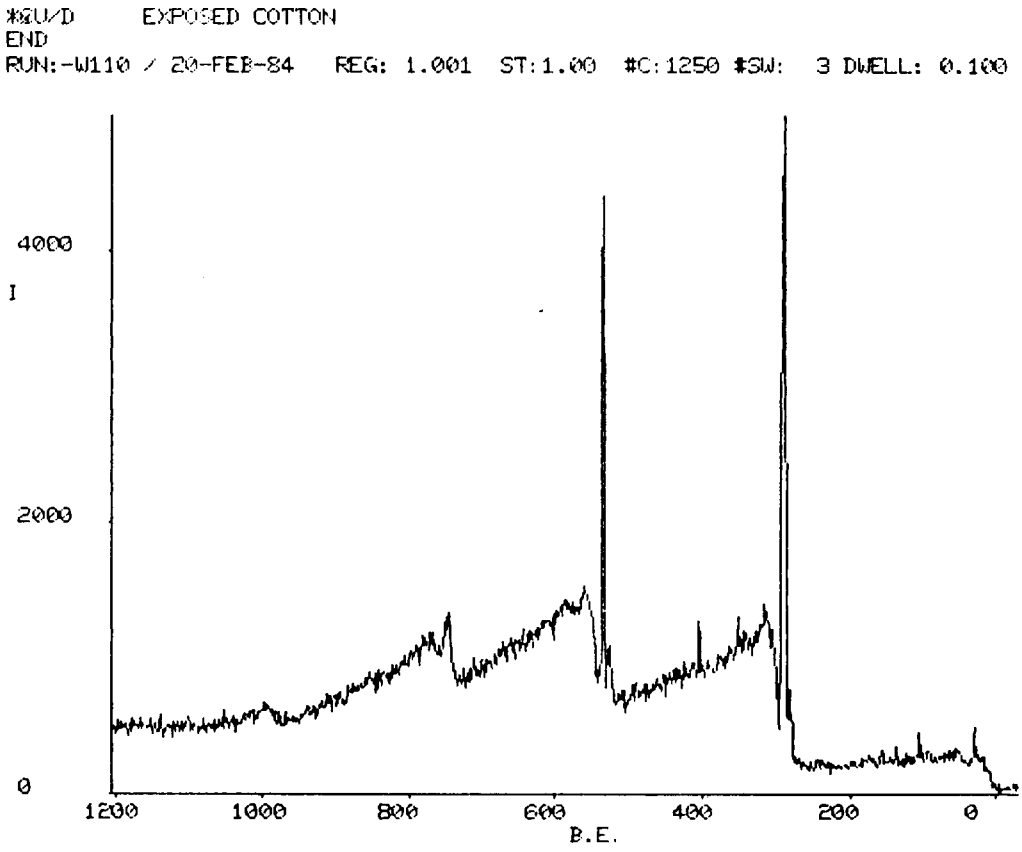
VOLUME
MODE = .1005E+04 C.C. / ANGSTROM AT A RADIUS OF .3525E+06 ANGSTROMS
MEAN PORE RADIUS = .3451E+06 ANGSTROMS
MEDIAN PORE RADIUS = .2935E+06 ANGSTROMS

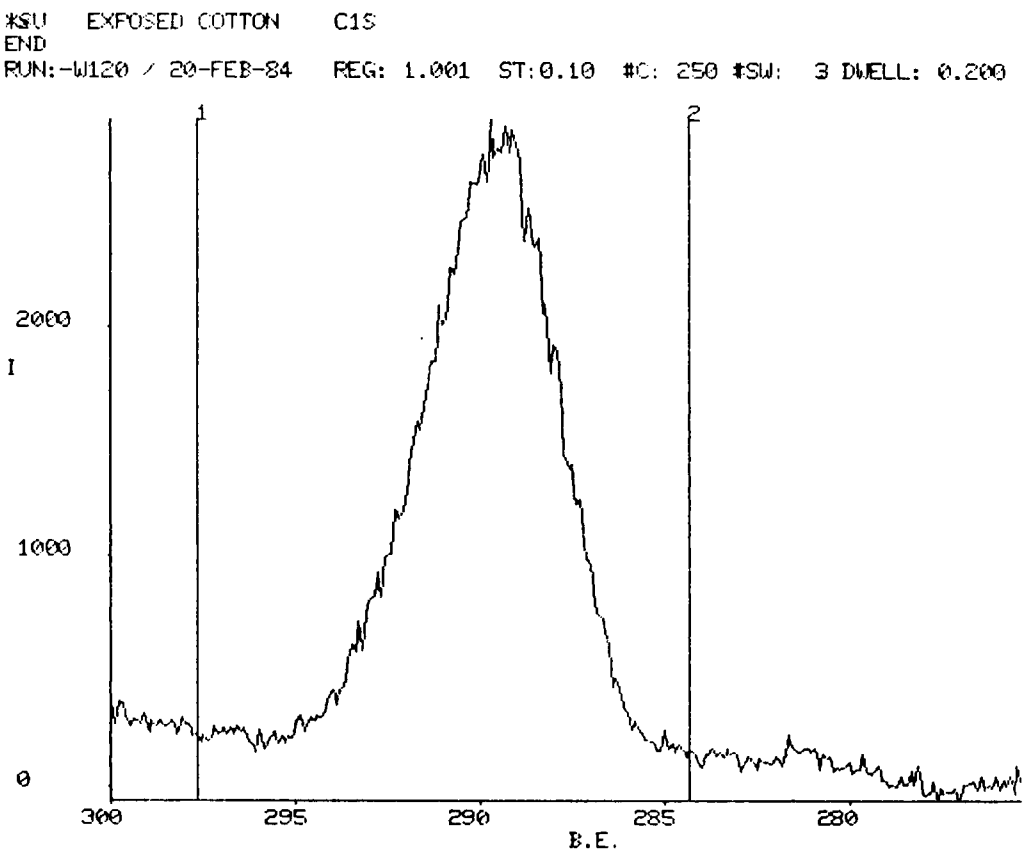
SURFACE AREA
MODE = .2479E-05 SQ. M. / ANGSTROM AT A RADIUS OF .4964E+05 ANGSTROMS
MEAN PORE RADIUS = .2998E+06 ANGSTROMS
MEDIAN PORE RADIUS = .3525E+06 ANGSTROMS

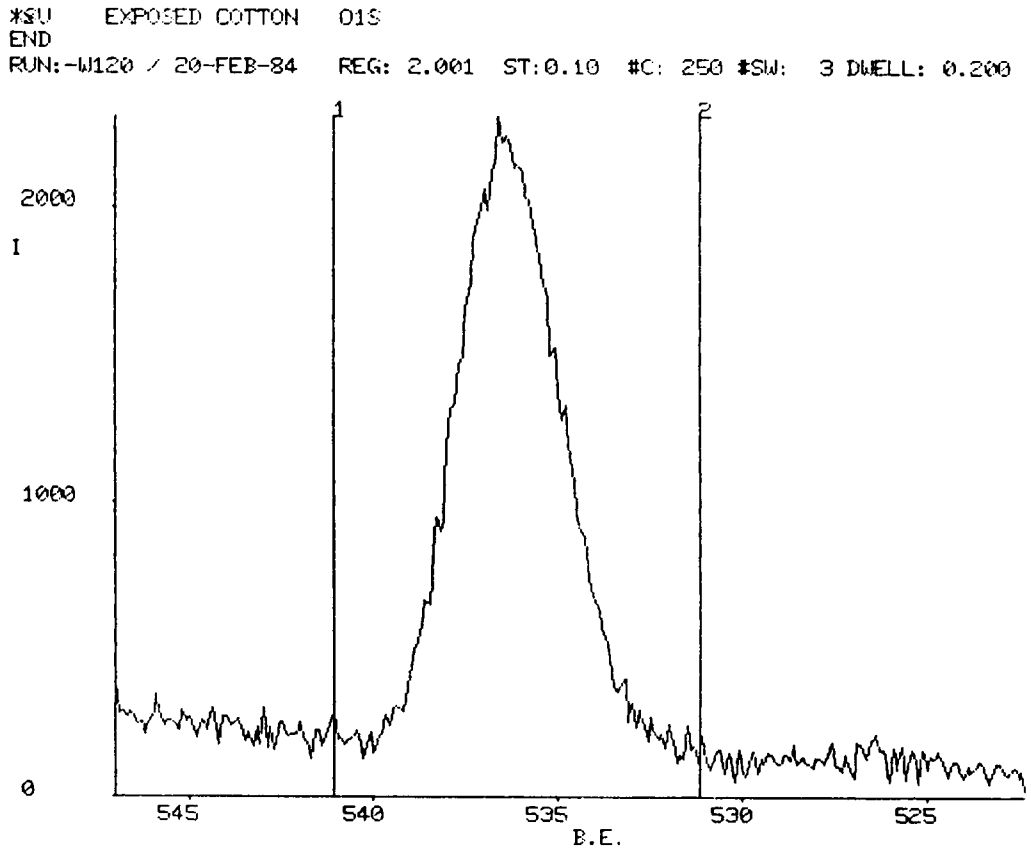
PORE POPULATION
MODE = .5716E-02 % NUMBER / ANGSTROM AT A RADIUS OF .4964E+05 ANGSTROMS
MEAN PORE RADIUS = .1902E+06 ANGSTROMS
MEDIAN PORE RADIUS = .1431E+06 ANGSTROMS

APPENDIX C

ESCA OUTPUT


*&U/D EXPOSED COTTON
END
RUN:-W110 / 20-FEB-84 REG: 1.001 ST:1.00 #C:1250 #SW: 3 DWELL: 0.100
4000
I
2000
0
1200
1000
800
600
400
200
0
B.E.


*KSU EXPOSED COTTON C1S
END
RUN:-W120 / 20-FEB-84 REG: 1.001 ST:0.10 #C: 250 #SW: 3 DWELL: 0.200
1
2
2000
I
1000
0
300
295
290
285
280
B.E.


*SU EXPOSED COTTON O1S
END
RUN:-W120 / 20-FEB-84 REG: 2.001 ST:0.10 #C: 250 #SW: 3 DWELL: 0.200
1
2
2000
I
1000
0
545
540
535
530
525
B.E.

RUN : W120 / 20-FEB-84
SAMPLE: 1
NAME : EXPOSED COTTON
TITLE : DR. WIGHTMAN
13KV 20MA SLIT=2 CUR=8.5

EXCITATION : MG ANALYSER MODE: FRR
SCAN MODE : T FACTOR : 0

MAGNIFICATION: L RESOLUTION: M

BASELINE THRESHOLD: 0 MIN. PEAK WIDTH: 1.00

REGION: 1 - WITH MARKERS

ELMT	K.E.	STEP	DWELL	#CHAN	#AVG
XC1	968.60	0.10	0.200	250	3

SCAN: 1

START E.V. : 953.60 END E.V. : 978.50

PEAK	K.E.	B.E.	MAX	AREA	FWHH
1	964.40	289.20	2668	116687	4.10

RUN : W120 / 20-FEB-84
SAMPLE: 1
NAME : EXPOSED COTTON
TITLE : DR. WIGHTMAN
13KV 20MA SLIT=2 CUR=8.5

EXCITATION : MG ANALYSER MODE: FRR
SCAN MODE : T FACTOR : 0

MAGNIFICATION: L RESOLUTION: M

BASELINE THRESHOLD: 0 MIN. PEAK WIDTH: 1.00

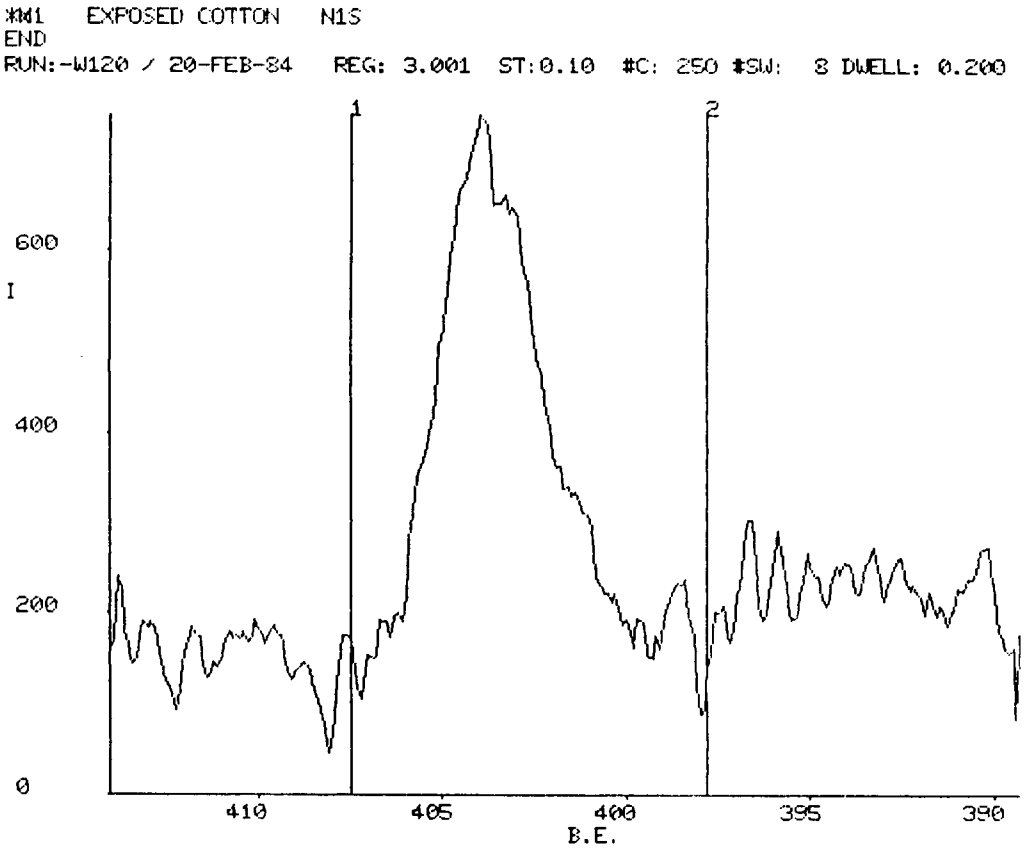
REGION: 2 - WITH MARKERS

ELMT	K.E.	STEP	DWELL	#CHAN	#AVG
X01	721.60	0.10	0.200	250	3

SCAN: 1

START E.V. : 706.60 END E.V. : 731.50

PEAK	K.E.	B.E.	MAX	AREA	FWHH
1	717.10	536.50	2093	70551	3.20


%%1 EXPOSED COTTON N1S
END
RUN:-W120 / 20-FEB-84 REG: 3.001 ST:0.10 #C: 250 #SW: 8 DWELL: 0.200
1
2
600
I
400
200
0
410
405
400
395
390
B.E.

```
RUN    : W120 / 20-FEB-84
SAMPLE:      1
NAME   : EXPOSED COTTON
TITLE  : DR. WIGHTMAN
         13KV 20MA SLIT=2 CUR=8.5

EXCITATION : MG          ANALYSER MODE: FRR
SCAN MODE  : T           FACTOR       :  0

MAGNIFICATION: L          RESOLUTION: M

BASELINE THRESHOLD:   0     MIN. PEAK WIDTH:  1.00

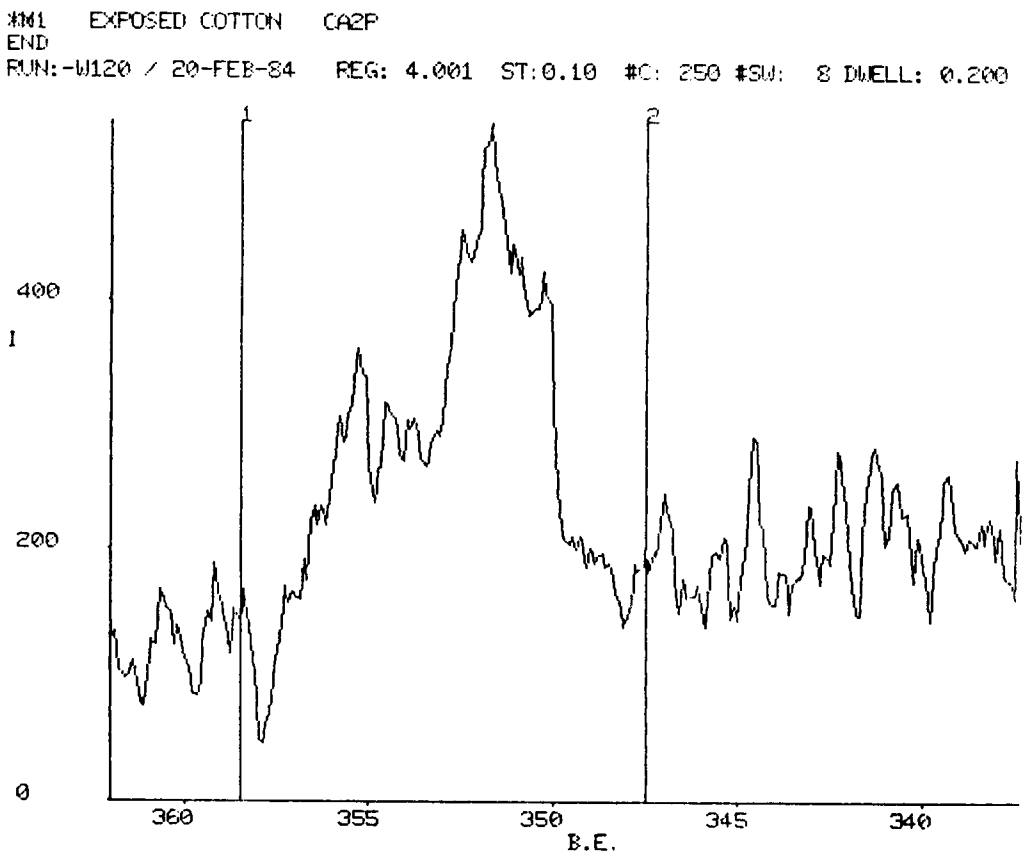

REGION:  3  -  WITH MARKERS
 ELMT     K.E.        STEP      DWELL     #CHAN    #AVG
 XN1     854.60       0.10      0.200      250       8

SCAN:  1


            START E.V. :  839.60 END E.V. :  864.50
  PEAK     K.E.        B.E.            MAX       AREA        FWHH

    1     849.60     404.00           629      23277        3.10

051460
@
```


*M1 EXPOSED COTTON CA2P
END
RUN:-W120 / 20-FEB-84 REG: 4.001 ST:0.10 #C: 250 #SW: 8 DWELL: 0.200
1
2
400
I
200
0
360
355
350
345
340
B.E.

RUN : W120 / 20-FEB-84
SAMPLE: 1
NAME : EXPOSED COTTON
TITLE : DR. WIGHTMAN
13KV 20MA SLIT=2 CUR=8.5

EXCITATION : MG ANALYSER MODE: FRR
SCAN MODE : T FACTOR : 0

MAGNIFICATION: L RESOLUTION: M

BASELINE THRESHOLD: 0 MIN. PEAK WIDTH: 1.00

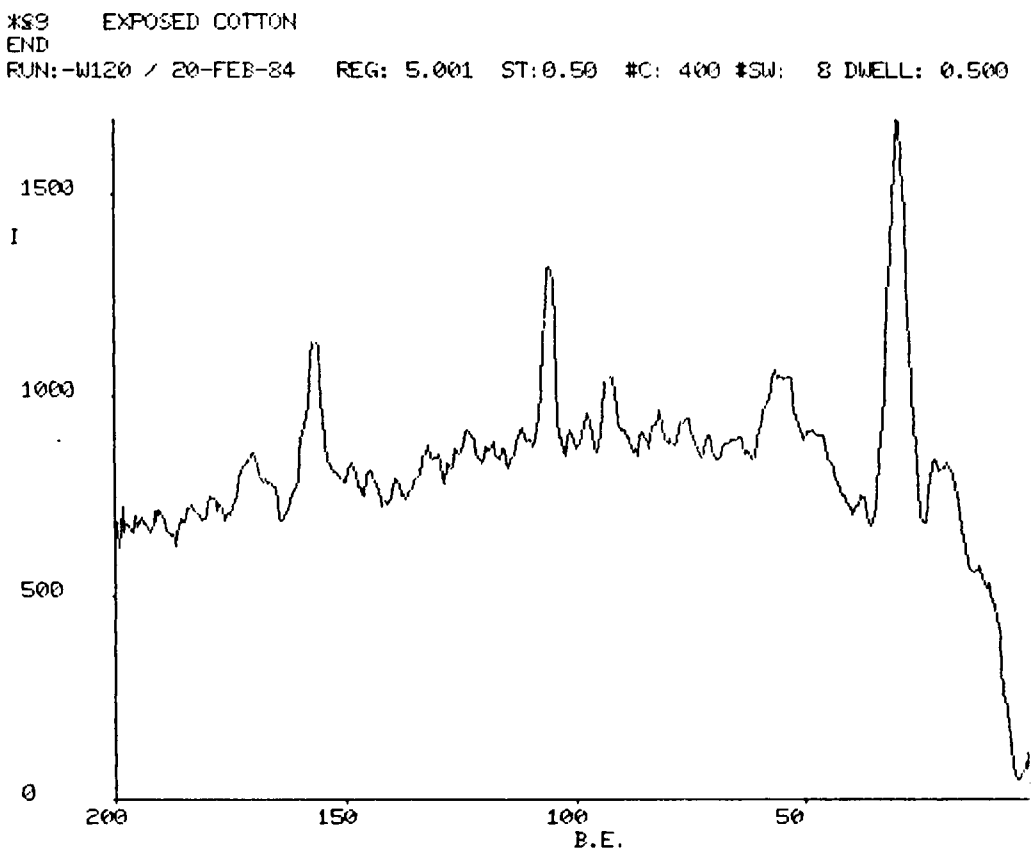
REGION: 4 - WITH MARKERS

ELMT	K.E.	STEP	DWELL	#CHAN	#AVG
XCA	906.60	0.10	0.200	250	8

SCAN: 1

START E.V. : 891.60 END E.V. : 916.50

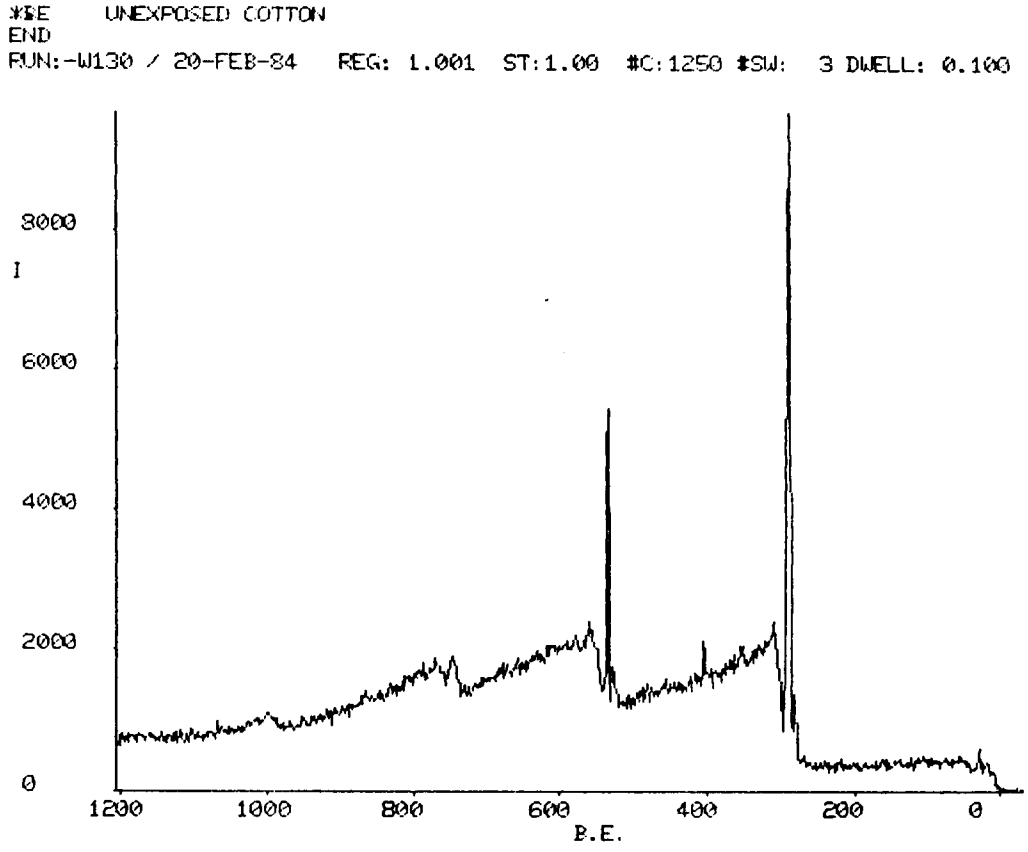
PEAK	K.E.	B.E.	MAX	AREA	FWHH
1	901.90	351.70	419	19365	5.90

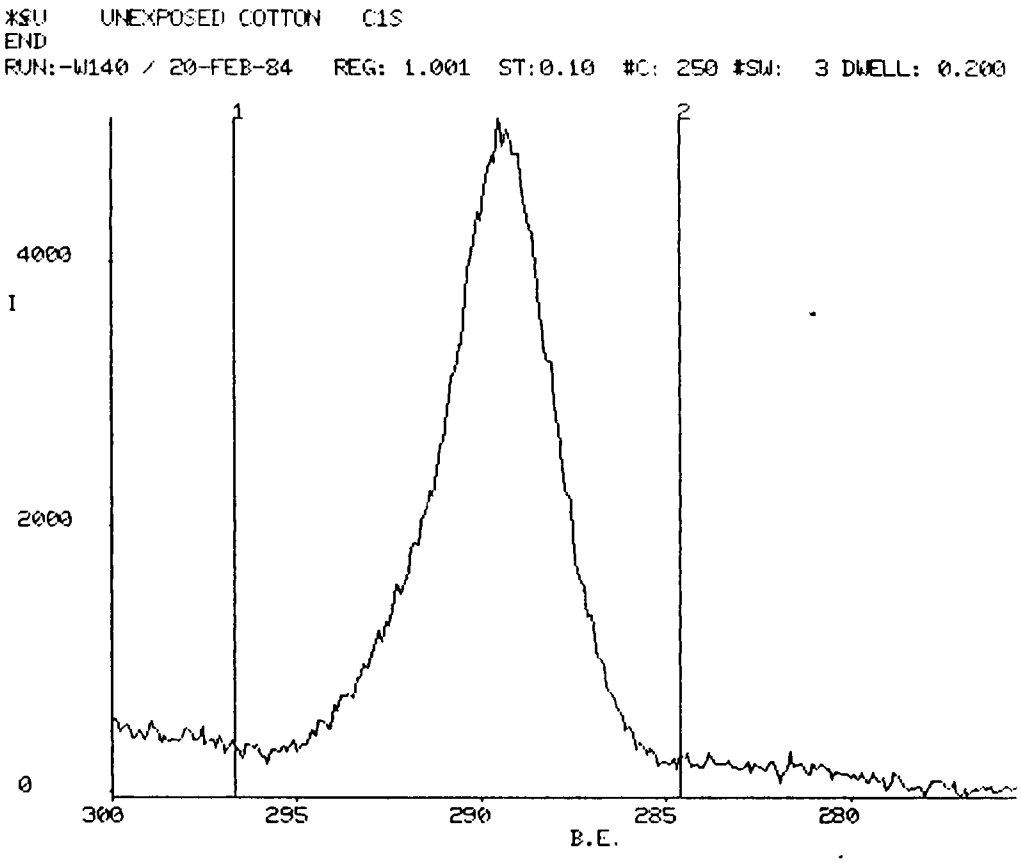

*S9 EXPOSED COTTON
END
RUN:-W120 / 20-FEB-84 REG: 5.001 ST:0.50 #C: 400 #SW: 8 DWELL: 0.500
1500
I
1000
500
0
200
150
100
50
B.E.

X-sec	Area/SW*TF/ (MFP*X-sec)	Sum	Atomic Fraction
22.2	96.41467178	136.976	0.703882429
63.27	34.16397115		0.249416593
39.294	5.083377574		0.037111573
113.886	1.313513793		0.009589404

Treatment	Element	Correction	B.E.	Corrected B.E.
Cotton Exposed	Carbon	-4.2	289.2	285
	Oxygen	-4.2	536.5	532.3
	Nitrogen	-4.2	404	399.8
	Calcium	-4.2	351.7	347.5

Transmission Function	Area	Sweeps	Area/ Sweep	Mean Free Path
1	116687	3	38895.66667	18.1721
1.342853182	70551	3	23517	14.6098
1.134457718	23277	8	2909.625	16.5252
1.068976934	19365	8	2420.625	17.2978


*$E UNEXPOSED COTTON
END
RUN:-W130 / 20-FEB-84 REG: 1.001 ST:1.00 #C:1250 #SW: 3 DWELL: 0.100
8000
I
6000
4000
2000
0
1200
1000
800
600
400
200
0
B.E.


*SU UNEXPOSED COTTON C1S
END
RUN:-W140 / 20-FEB-84 REG: 1.001 ST:0.10 #C: 250 #SW: 3 DWELL: 0.200
1
2
4000
I
2000
0
300
295
290
285
280
B.E.

RUN : W140 / 20-FEB-84
SAMPLE: 1
NAME : UNEXPOSED COTTON
TITLE : DR. WIGHTMAN
13KV 20MA SLIT=2 CUR=8.5

EXCITATION : MG ANALYSER MODE: FRR
SCAN MODE : T FACTOR : 0

MAGNIFICATION: L RESOLUTION: M

BASELINE THRESHOLD: 0 MIN. PEAK WIDTH: 1.00

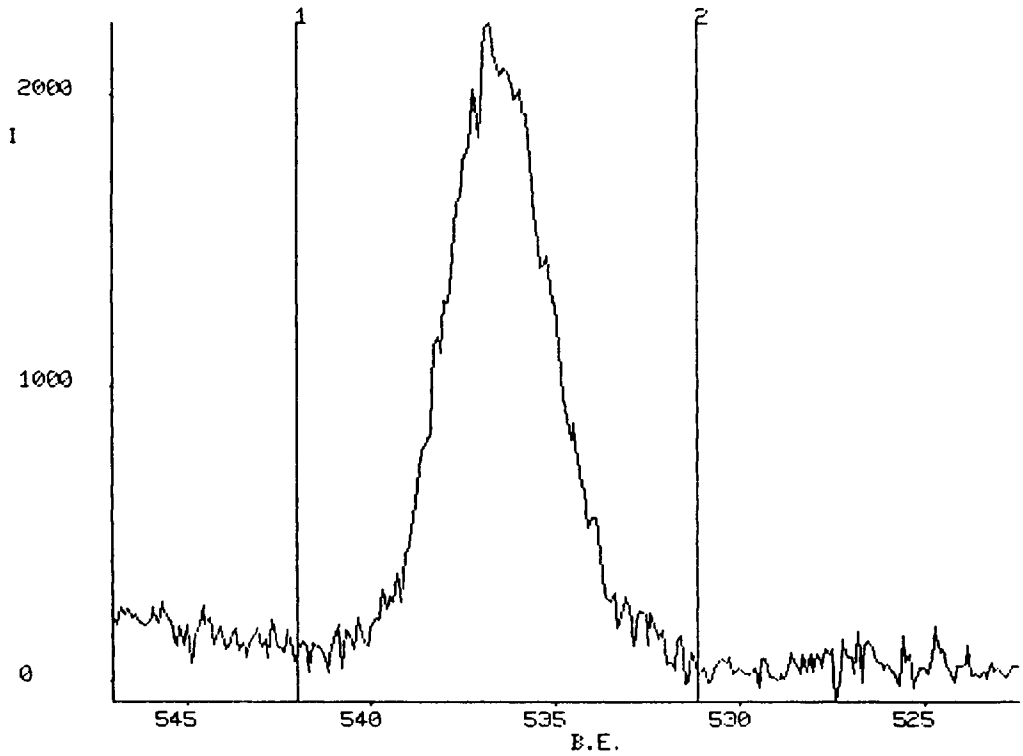
REGION: 1 - WITH MARKERS

ELMT	K.E.	STEP	DWELL	#CHAN	#AVG
XC1	968.60	0.10	0.200	250	3

SCAN: 1

START E.V. : 953.60 END E.V. : 978.50

PEAK	K.E.	B.E.	MAX	AREA	FWHH
1	964.30	289.30	4742	177076	3.20


*SU UNEXPOSED COTTON O1S
END
RUN:-W150 / 20-FEB-84 REG: 1.001 ST:0.10 #C: 250 #SW: 3 DWELL: 0.200
1
2
2000
I
1000
0
545
540
535
530
525
B.E.

RUN : W150 / 20-FEB-84
SAMPLE: 1
NAME : UNEXPOSED COTTON
TITLE : DR. WIGHTMAN
13KV 20MA SLIT=2 CUR=8.5

EXCITATION : MG ANALYSER MODE: FRR
SCAN MODE : T FACTOR : 0

MAGNIFICATION: L RESOLUTION: M

BASELINE THRESHOLD: 0 MIN. PEAK WIDTH: 1.00

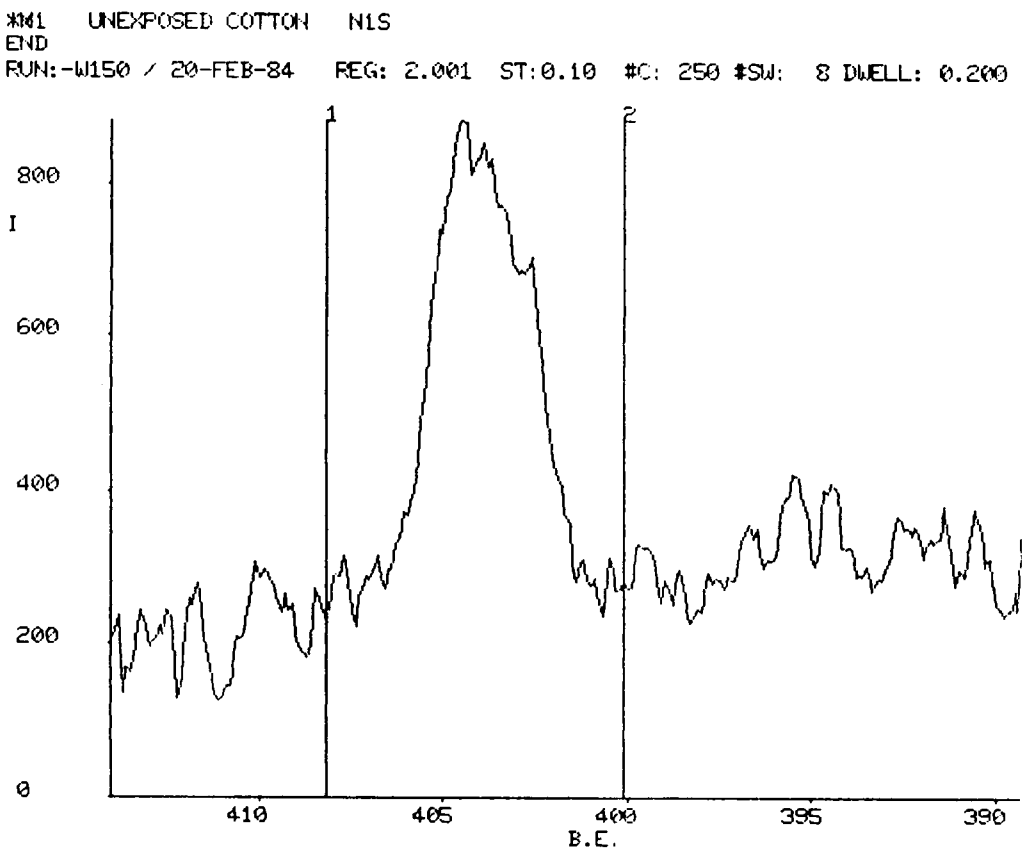
REGION: 1 - WITH MARKERS

ELMT	K.E.	STEP	DWELL	#CHAN	#AVG
X01	721.60	0.10	0.200	250	3

SCAN: 1

START E.V. : 706.60 END E.V. : 731.50

PEAK	K.E.	B.E.	MAX	AREA	FWHH
1	716.80	536.80	2121	74948	3.40


%%1 UNEXPOSED COTTON N1S
END
RUN:-W150 / 20-FEB-84 REG: 2.001 ST:0.10 #C: 250 #SW: 8 DWELL: 0.200
1
2
800
I
600
400
200
0
410
405
400
395
390
B.E.

RUN : W150 / 20-FEB-84
SAMPLE: 1
NAME : UNEXPOSED COTTON
TITLE : DR. WIGHTMAN
13KV 20MA SLIT=2 CUR=8.5

EXCITATION : MG ANALYSER MODE: FRR
SCAN MODE : T FACTOR : 0

MAGNIFICATION: L RESOLUTION: M

BASELINE THRESHOLD: 0 MIN. PEAK WIDTH: 1.00

REGION: 2 - WITH MARKERS

ELMT	K.E.	STEP	DWELL	#CHAN	#AVG
XN1	854.60	0.10	0.200	250	8

SCAN: 1

START E.V. : 839.60 END E.V. : 864.50

PEAK	K.E.	B.E.	MAX	AREA	FWHH
1	849.10	404.50	622	19036	3.10

Treatment	Element	Correction	B.E.	Corrected B.E.
Cotton Unexposed	Carbon	-4.3	289.3	285
	Oxygen	-4.3	536.8	532.5
	Nitrogen	-4.3	404.5	400.2

Transmission Function	Area	Sweeps	Area/ Sweep	Mean Free Path
1	177076	3	59025.33333	18.1721
1.343225628	74948	3	24982.66667	14.6098
1.134989454	19036	8	2379.5	16.5252

X-sec	Area/SW*TF/ (MFP*X-sec)	Sum	Atomic Fraction
22.2	146.3121378	186.775	0.783362281
63.27	36.30326262		0.194369429
39.294	4.159149872		0.02226829

VITA

Geraldine Mahany Eaton was born in Hamilton, Ohio on April 8, 1949. She attended McGuffey Laboratory School of Miami University and was graduated from Talawanda High School, Oxford, Ohio in 1967.

She received her B.S. in Clothing & Textiles from Auburn University, Auburn, Alabama in 1971 and her M.Ed. from Miami University, Oxford, Ohio in 1973. Following completion of her Master's degree, Ms. Eaton taught vocational home economics at West Carrollton Senior High, West Carrollton, Ohio for two years. Later she taught chemistry at Colegio La Piedad, San Juan, Puerto Rico for two years.

In 1980, Ms. Eaton entered the interdisciplinary doctoral program in the department of Textiles, Merchandising & Design at the University of Tennessee, Knoxville. While at UT she served as a graduate teaching assistant and a graduate research assistant. Her doctoral research was funded through an extra-mural grant from the U.S. Department of Agriculture, Agricultural Research Service. Additionally, she received an AATCC Student Research Grant.

Ms. Eaton was awarded a Chancellor's Citation for Extraordinary Professional Promise in 1983. That year she was also named as the Outstanding Graduate Student in the College of Human Ecology and was recognized by the UT Commission for Women for Exceptional Performance as a Graduate Student. She is a member of the American Association of Textile Chemists and Colorists, the Association of College Professors of Textiles and Clothing, Phi Kappa Phi, Omicron Nu, and Phi Upsilon Omicron.